Hippocampal Circuits

Pyramidal Cell Diversity During Hippocampal Oscillations and Serotonergic Modulation of O-LM Interneurons

Dissertation

zur Erlangung des akademischen Grades
Doctor rerum naturalium (Dr. rer. nat.)

eingereicht an der
Lebenswissenschaftlichen Fakultät der Humboldt-Universität zu Berlin

von

Dipl. Biol. Claudia Böhm

Präsidentin der Humboldt-Universität zu Berlin: Prof. Dr. Sabine Kunst
Dekan der Lebenswissenschaftlichen Fakultät: Prof. Dr. Richard Lucius

Gutachter:

1. Prof. Dr. Andreas Draguhn

2. Prof. Dr. Dietmar Schmitz

3. Prof. Dr. Richard Kempter

Tag der mündlichen Prüfung: 13.09.2016

Erklärung

Hiermit erkäre ich, Claudia Böhm,

- die Dissertation selbstständig und nur unter Verwendung der angegebenen Hilfen und Hilfsmittel angefertigt zu haben.
- Ich habe mich anderwärts nicht um einen Doktorgrad beworben und besitze keinen entsprechenden Doktorgrad.
- Ich erkläre, dass ich die Dissertation oder Teile davon nicht bereits bei einer anderen wissenschaftlichen Einrichtung eingereicht habe und dass sie dort weder angenommen noch abgelehnt wurde.
- Ich erkläre die Kenntnisnahme der dem Verfahren zugrunde liegenden Promotionsordnung der Lebenswissenschaftlichen Fakultät der Humboldt-Universität zu Berlin vom 5. März 2015.
- Weiterhin erkläre ich, dass keine Zusammenarbeit mit gewerblichen Promotionsberaterinnen/Promotionsberatern stattgefunden hat und dass die Grundsätze der Humboldt-Universität zu Berlin zur Sicherung guter wissenschaftlicher Praxis eingehalten wurden.

Unterschrift:_____

Abstract

The hippocampus plays an important role in the acquisition, consolidation and retrieval of memory. These processes are carried out in a brain-state dependent manner. Different brain states are accompanied by hippocampal oscillations, which reflect synchronized neuronal activity and have behavioral correlates. One part of this thesis focuses on ripples, a fast oscillatory activity with a peak frequency around 120 – 200 Hz which is involved in the consolidation of memory. During consolidation, information is transferred from the hippocampus to the neocortex for more permanent storage. The subiculum is located at the interface between hippocampus and neocortex and is thereby ideally suited to mediate information transfer to a variety of cortical and subcortical targets. Here I investigated the properties of subicular pyramidal cells and their modulation during ripples in awake animals. I found that subicular pyramidal cells exhibit different types of modulation during ripples: by juxtacellular recordings I could show that a subset of pyramidal cells increases its firing rate during ripples whereas another subset decreases its firing rate. Whole-cell current clamp recordings allowed me to identify a correlate between modulation and cell subtype: burst firing cells, i. e. cells, whose output mode consists of a series of closely timed action potentials, increased their firing rate, and regular firing cells decreased their firing rate on average. The modulation in firing rate was accompanied by a depolarization or a hyperpolarization, respectively. In order to illuminate the mechanism of this differential modulation, we employed voltage clamp recordings in acute slices. These recordings showed that regular firing cells exhibit a higher ratio of inhibition to excitation as compared to burst firing cells. In accordance with this finding, multiple-cell patch-clamp recordings in vitro revealed that the number of inhibitory synaptic connections onto regular firing cells was higher than onto burst firing cells. Furthermore we found excitatory connections both among regular and burst firing cells, but connections between subtypes were unilateral, only regular firing cells were connected to burst firing cells but not vice versa. We conclude that the local network topology contributes to the different modulation of burst and regular firing cells during ripples. Concerning the output of the subiculum it has been shown that the two pyramidal cell subtypes of the subiculum have in part different preferential target areas. Therefore information transferred during ripples is likely to be routed preferentially to target regions of the burst firing subtype, e. g. the medial entorhinal cortex.

Besides the differential employment of pyramidal cell subtypes during network oscillations, the hippocampus hosts a variety of interneuron types to achieve functionality. In addition, neuromodulatory inputs allow for a temporally flexible, widespread and cell-type specific control of activity in the hippocampus. Among these interneuron types are GABAergic O-LM interneurons. They play an important role in controlling the input to the hippocampus from the entorhinal cortex. Their somata reside in area CA1 in stratum oriens and their axons project to stratum lacunosum-moleculare. The excitatory input onto

those cells arises primarily from local pyramidal cells. We could show that this synapse is modulated by serotonin, a neuromodulator released from the midbrain raphe nuclei in a state-dependent manner. Excitatory transmission onto O-LM interneurons is decreased upon release of serotonin. This modulation is mediated by a presynaptic mechanism and is likely to involve a decrease in calcium influx into presynaptic terminals. Accordingly, O-LM interneurons elicit less action potentials in the presence of serotonin. We conclude that serotonin, by decreasing O-LM output, might release fibers from entorhinal cortex impinging onto CA1 pyramidal cell dendrites from inhibition. This mechanism of input control might play a role in switching between a state of prevailing intrahippocampal processing and a state in which external input from entorhinal cortex is integrated into local computation.

Zusammenfassung

Der Hippokampus spielt eine wichtige Rolle bei der Erfassung, der Konsolidierung und dem Wiederabrufen von Gedächtnisinhalten. Diese Prozesse laufen in Abhängigkeit des jeweiligen Verarbeitungszustands des Gehirns ab. Verschiedene Zustände werden von hippokampalen Oszillationen begleitet, welche synchronisierte neuronale Aktivität widerspiegeln und mit bestimmten Verhaltenszuständen korrelieren. Der erste Teil dieser Arbeit konzentriert sich auf 'ripples', eine schnell schwingende Netzwerkaktivität mit Hauptfrequenzen zwischen 120 – 220 Hz, die an der Festigung von Gedächtnisinhalten beteiligt ist. Während der Gedächtnis-Konsolidierung wird Information vom Hippokampus zum Neokortex zur langfristigeren Speicherung weitergegeben. Das Subikulum liegt zwischen Hippokampus und Neokortex und ist somit hervorragend geeignet die Weiterleitung und Verteilung zu einer Vielzzahl kortikaler und subkortikaler Zielregionen zu vermitteln. In dieser Studie untersuchte ich in wachen Mäusen die Eigenschaften von subikulären Pyramidenzellen und deren Regulierung während ripples. Es zeigte sich, dass Pyramidenzellen des Subikulums auf verschiedene Art reguliert werden: durch juxta-zelluläre Ableitungen konnte ich zeigen, dass eine Untergruppe von Pyramidenzellen ihre Aktivität während ripples erhöht, eine zweite Gruppe hingegen ihre Aktivität während ripples vermindert. Intrazelluläre Ableitungen ermöglichten es uns einen Zusammenhang zwischen Regulierung und Zelluntertyp aufzudecken: Zellen, die mit einer dichten Abfolge von Aktionspotentialen auf Depolarisierung reagieren ('burst feuende Zellen', in etwa: in Salven feuernde Zellen) erhöhen ihre Aktivität und regulär feuernde Zellen vermindern im Mittel ihre Aktivität. Die Regulierung der Feuerrate geht mit einer Depolarisierung, bzw. Hyperpolarisierung des Membranpotentials einher. Um den Mechanismus dieser verschiedenen Regulierung aufzudecken, verwendeten wir Aufnahmen mit Spannungsklemme in frischen Hirnschnittpräparaten. Diese Aufnahmen zeigten, dass bei regulär feuernden Zellen das Verhältnis zwischen Inhibition und Exzitation kleiner ist als bei burst feuernden Zellen. In Übereinstimmung mit diesen Erkenntnissen, haben wir mit Hilfe von multiplen simultanen in vitro Intrazellulärableitungen herausgefunden, dass die Anzahl inhibitorischer synaptischer Verbindungen auf regulär feuernde Zellen höher ist als die auf burst feuernden Zellen. Desweiteren haben wir exzitatorische Verbindungen zwischen regulär und burst feuernden Zellen gefunden; Verbindungen zwischen den Subtypen waren jedoch einseitig, regulär feuernde Zellen hatten Verbindungen mit burst feuernden Zellen, aber nicht umgekehrt. Wir schließen daraus, dass die lokale Netzwerktopologie zur unterschiedlichen Regulierung von burst und regulär feuernden Zellen beiträgt. In Bezug auf ausgehende Verbindungen wurde in früheren Studien gezeigt, dass die beiden verschiedenen Subtypen des Subikulums teilweise verschiedene bevorzugte Zielstrukturen haben. Hieraus folgt, dass Informationen

die während ripples übertragen werden aller Wahrscheinlichkeit nach bevorzugt zu Zielregionen der burst feuernden Zellen geleitet werden, wie zum Beispiel zum medialen entorhinalen Kortex.

Neben der Zell-Subtyp spezifischen Regulierung von Pyramidenzellen während Netzwerkoszillationen, beherbergt der Hippokampus auch eine Vielzahl von Interneuron-Typen um Funktionalität zu erreichen. Zusätzlich ermöglichen neuromodulatorische Eingänge eine zeitlich flexible, weit reichende und Zelltyp-spezifische Kontrolle der Aktivität im Hippokampus. Unter diesen Interneurontypen finden sich die GABAergen O-LM Interneurone. Sie spielen eine wichtige Rolle bei der Kontrolle von Eingängen aus dem entorhinalen Kortex in den Hippokampus. Ihre Somata befinden sich im Areal CA1 im stratum oriens und ihre axonalen Fortsätze ragen in die stratum lacunosum-moleculare-Schicht. Sie erhalten ihre exzitatorischen Eingänge hauptsächlich von lokalen Pyramidenzellen. Wir konnten zeigen, dass diese Synapse durch Serotonin reguliert wird. Serotonin ist ein Neuromodulator der von den Raphekernen des Mittelhirns zustandsabhängig ausgeschüttet wird. Exzitatorische Übertragung auf O-LM Interneurone wird durch die Ausschüttung von Serotonin vermindert. Diese Regulierung wird durch einen präsynaptischen Mechanismus vermittelt und beinhaltet wahrscheinlich eine Verminderung des Kalziumeinstroms in die präsynaptischen Endigungen. Dementsprechend werden weniger Aktionspotentiale unter Serotonineinfluss ausgelöst. Wir folgern hieraus, dass durch die verminderte O-LM Interneuron Aktivität in Gegenwart von Serotonin die Hemmung entorhinaler Kortex Fasern, welche auf CA1 Pyramidenzelldendriten zielen, aufgehoben wird. Beim Wechsel zwischen einem Zustand der durch Hippokampus-interne Berechnungen geprägt ist und einem komplementären Zustand in welchem externe Eingänge des entorhinalen Kortex in lokale Berechnungen miteinbezogen werden, könnte dieser Mechanismus eine Rolle spielen.

Acknowledgements

I would like to take this opportunity to thank all the people that have supported me during my thesis projects. First of all, I would like to thank Dietmar, he has been very supportive all the way. I enjoyed our scientific discussions during which I learned a lot. I appreciate the freedom I had to pursue my interests and ideas, and the great supervision of my thesis projects. I have greatly benefited from his openness to collaborate with other research groups and his support in these collaborations. Through this, I had the opportunity to collaborate with James Poulet, who helped me to get started with the intracellular in vivo recordings. James' positive attitude has been very motivating and he and his whole lab were very welcoming during the time I did experiments in his lab, for which I would like to thank them. I also had the opportunity to work with Jörg Geiger, his creativity in science was very helpful, any scientific discussion, on the subiculum project or any other topic, were always a lot of fun.

I am very glad I met Richard during my work for my doctoral thesis, his enthusiasm for science is very inspiring, I always enjoyed discussions with him and his presence in our lab meetings was very enriching. His questions often revealed another side of a problem that I hadn't thought of before.

Furthermore, I am grateful to the people who contributed to my projects with their experimental expertise: Yangfan & Jochen – the multipatch wonders, Maria – she kept spirits high while we tried to solve the riddle of the serotonin receptor, and Nikolaus, the oscillation enthusiast of the lab.

Additional thanks go to Jochen, he was involved in my thesis work almost right from the beginning and I highly appreciate his contributions and advice, and our discussions.

I also would like to thank all other people in Dietmar's lab, they have made my time in the lab very enjoyable, especially Nutabi, John, Prateep, Vanessa, Anne-Kathrin, Anke, Susanne, the other two Claudias and Sonja.

Finally, I feel very lucky for having continuous support from great people outside the lab, especially Anja, Schokofeh, Karo, Meike, Robert and Julia, from my family and from Hauke.

Contents

Abbreviations

AMPA	α-**A**mino-3-hydroxy-5-**M**ethyl-4-isoxazole**P**ropionic **A**cid
CA	**C**ornu **A**mmonis
CB	**C**al**B**indin
5-HT	**5-H**ydroxy **T**ryptamine
DNMS	**D**elayed **N**on-**M**atch-to-**S**ample
EEG	**E**lectro**E**ncephalo**G**ram
GABA	**G**amma-**A**mino**B**utyric **A**cid
IEI	**I**nter-**E**vent **I**nterval
LEC	**L**ateral **E**ntorhinal **C**ortex
LFP	**L**ocal **F**ield **P**otential
LTD	**L**ong-**T**erm **D**epression
LTP	**L**ong-**T**erm **P**otentiation
MEC	**M**edial **E**ntorhinal **C**ortex
O-LM interneuron	**O**riens-**L**acunosum **M**oleculare interneuron
PSD	**P**ower **S**pectral **D**ensity
REM	**R**apid **E**ye **M**ovement
SERT	**S**ERotonin **T**ransporter
SEM	**S**tandard **E**rror of the **M**ean
STDP	**S**pike-**T**iming **D**ependent **P**lasticity
SWRs	**S**harp **W**ave-**R**ipples

Chapter 1

Introduction

1.1 The hippocampal formation

Anatomy and connectivity

The hippocampus has long been an area of intense research. Its popularity can be attributed to its clearly structured layering as well as its function in the formation and consolidation of memory and in spatial navigation. Alterations in hippocampal function have also been implicated in a number of neurodegenerative and neuropsychiatric diseases. In addition, a unique correlation of behavior and neuronal activity, i.e. an animal's position can be decoded from hippocampal action potential patterns, makes the hippocampus an attractive research area. It is evolutionary conserved across all vertebrates, and many of the anatomical details of the hippocampal formation are similar across mammalian species. Both the hippocampus and the neocortex arise from the dorsal telencephalon but become anatomically distinct parts during development. The hippocampus is located deep in the brain, within the temporal lobe. The hippocampal formation consists of two interlocked C–shaped structures and comprises the dentate gyrus, the Cornu ammonis (CA) areas CA3, CA2, CA1 and the subiculum (Figure 1.1).

Classically, connections between the hippocampal subareas and the entorhinal cortex are viewed as a feed-forward excitatory circuit, including entorhinal cortex, dentate gyrus, area CA3 and area CA1. The granule cells of the dentate gyrus receive excitatory input from the entorhinal cortex via the perforant path, which is conventionally considered the first synapse in the circuit. This synapse gained early attention by the seminal work of Lømo and Bliss, demonstrating long-term potentiation at this synapse (Bliss and Lømo, 1973). The granule cells form the second synapse: their axons, termed mossy fibers, connect to pyramidal cells of area CA3. CA3 pyramidal cells, in turn project onto CA1 pyramidal cells via the Schaffer collateral pathway. The circuit is completed by projections from CA1 pyramidal cells to the entorhinal cortex .

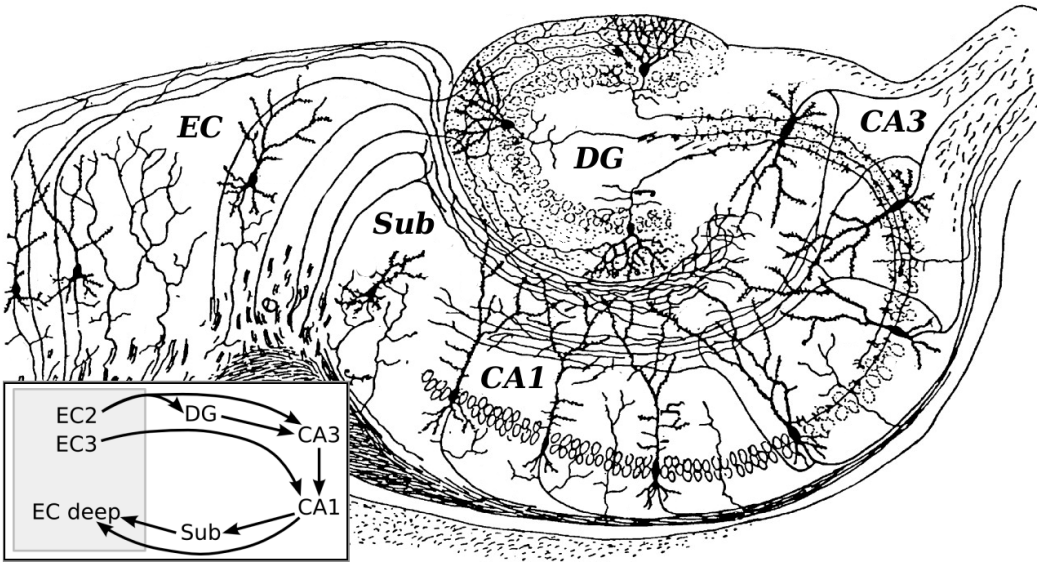

FIGURE 1.1: **Drawing of the neural circuitry of the rodent hippocampus.** Cajal's drawing indicates the regions constituting the hippocampal formation including the dentate gyrus (DG), Cornu Ammonis 3 (CA3), CA1 and Subiculum (Sub). The inset in the lower left depicts the basic connectivity among those regions and the entorhinal cortex (EC). Santiago Ramón y Cajal (1911) Histologie du Système nerveux de l'Homme et des Vertébrés, Paris: A. Maloine. Source: Wikimedia commons

A more detailed view however, reveals a variety of cell types, layers and additional connections, of which I will only mention the ones most relevant to this thesis; the topic is extensively covered in 'The hippocampus book' (Andersen et al., 2006).

The CA areas exhibit prominent cell layers: the deepest layer is the alveus, it contains mostly axons. The next layer is the stratum oriens, which hosts diverse types of interneurons, which will be detailed below. A very densely populated layer is the stratum pyramidale; it contains the cell bodies of the pyramidal neurons, which are the principal cells of the CA areas. The stratum pyramidale is neighboured by the stratum radiatum, and the most superficial layer of the CA fields is the stratum lacunosum–moleculare. In area CA1 the stratum radiatum contains the Schaffer collateral fibers; the CA1 stratum lacunosum–moleculare is the terminal field of the temporoammonic pathway, that arises from the entorhinal cortex and provides direct input from entorhinal cortex, bypassing the dentate gyrus and the CA3 region (Figure 1.1).

The CA1 pyramidal cell layer is continuous with the pyramidal cell layer of the subiculum. In the subiculum however, it is broader and cells are more dispersed than in the CA1 region. Beside the pyramidal cell layer, the subiculum contains a molecular layer and a polymorphic layer. The molecular layer is an extension to the strata lacunosum–moleculare and radiatum of the CA1 region but contains much fewer cell bodys (Ding, 2013).

By means of anterograde tracers it was found that the CA1 region innervates the subiculum in a series of nested loops, i. e. the most distal regions of the CA1 (close to the border to the subiculum) project just over the border and in fact were in some cases also found

to then project back to CA1 in stratum radiatum and statum lacunosum–moleculare. The proximal region of CA1, bordering CA3, targets the distal part of the subiculum while the middle part of CA1 projects to the middle of the subiculum (Amaral et al., 1991; Tamamaki et al., 1987). In addition, the subiculum receives direct excitatory input from the entorhinal cortex layer 3 via the perforant path. These connections are organized in a proximodistal as well as in a septotemporal fashion (Honda et al., 2012).

Area CA1 and the subiculum have both prominent projections to extrahippocampal targets, although they are organized in a different fashion: while in the CA1 region each cell projects to several brain regions outside of the hippocampus, each projection cell in the subiculum has mostly only one target region (Naber and Witter, 1998; Kim and Spruston, 2012). However, most projections from CA1 terminate in the subiculum, therefore the subiculum is the main sub-area from which information is distributed to areas outside of the hippocampus (O'Mara, 2006). The axonal trajectories from the subicular pyramidal cells extend in the deep white matter of the alveus/angular bundle towards the presubiculum or area CA1. The apical dendrites are branching at the top of the cell layer and extend towards the hippocampal fissure (Harris et al., 2001). The target regions of the subiculum are diverse, including cortical and subcortical target areas as indicated in Figure 1.2.

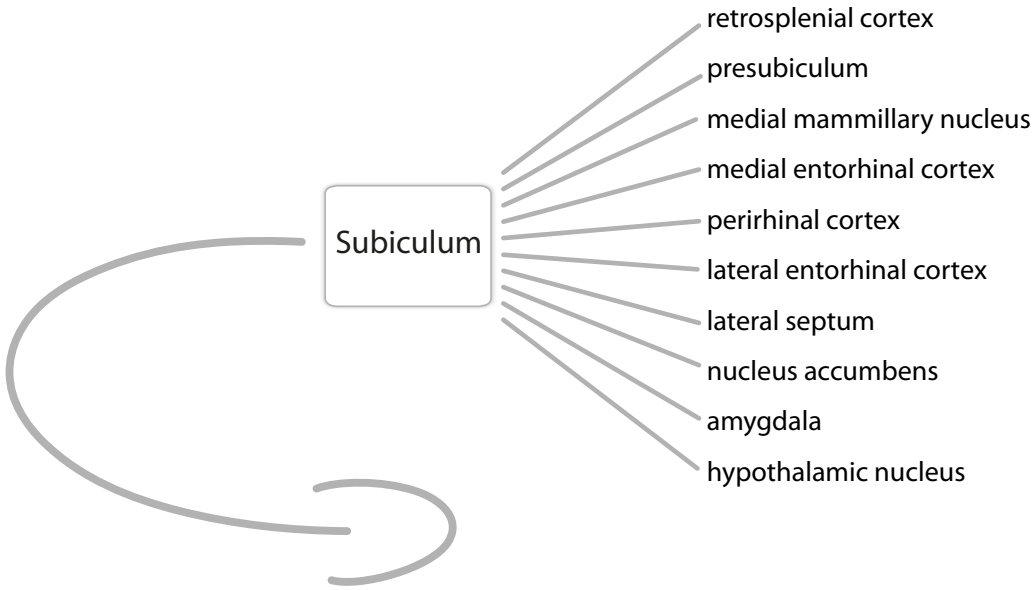

FIGURE 1.2: **The subiculum is one of the main output regions of the hippocampus.** Scheme depicting the hippocampal formation and cortical and subcortical projection areas of the subiculum.

1.2 Neuromodulators

The inputs to the hippocampus from other brain regions also include those from neuromodulatory centers. Neuromodulators are a means to tune and modify hard-wired connections in

a flexible but less specific manner. Numerous neuromodulators have been described, among them acetylcholine, endocannabinoids, norepinephrine, a variety of peptides, dopamine and serotonin. Neuromodulators can have effects on excitatory and inhibitory synaptic transmission, adaptation properties and the membrane potential, and thereby alter processing characteristics. The effects of neuromodulators are generally slower than those of neurotransmitters, they act in a longer lasting and spatially more diffuse manner and are thereby ideally suited to complement the fast action of neurotransmitters. Of note, some of the above mentioned neurochemical substances, including acetylcholine and serotonin can act both in a direct fashion, by binding to and opening an ion channel for example, and indirectly, by triggering an intracellular cascade which in turn might influence neuronal activity. Therefore the modulatory effect of those substances should be classified on the receptor level (Hasselmo, 1995).

Serotonin as a neuromodulator

Serotonin (5-hydroxytrytamin, 5-HT, $C_{10}H_{12}N_2O$) is a monoamine neurochemical that modulates neural activity and a wide range of neuropsychological processes. In animals serotonin is synthesized from the amino acid L-tryptophan by two enzymes, tryptophan hydroylase and aromatic amino acid decarboxylase. The main source of 5-HT in the brain are the neurons of the raphe nuclei (Dahlstroem and Fuxe, 1964). The raphe nuclei are located along the midline of the brainstem around the reticular formation. The neurons from the raphe nuclei send a vast network of projections that terminate in a defined and organized manner in cortical, limbic, midbrain, and hindbrain regions. Nine groups of serotonin-containing cell bodies have been described, B1–B9. The dorsal raphe nucleus consists of B6 and B7. The median raphe nucleus corresponds to B8. The ascending serotonergic projections that innervate the forebrain, including the limbic areas, arise primarily from the dorsal raphe, median raphe and the B9 cell group (Molliver, 1987). Other projections include those to the brainstem and to the spinal cord (Figure 1.3).

The neurons in the dorsal and the median raphe differ in their active and passive electrophysiological properties, such as their responsiveness to 5-HT_{1A} receptor activation (Beck et al., 2004; Kirby et al., 2003). Furthermore, serotonergic axons and terminals exhibit morphological differences: while axons arising from the median raphe are relatively coarse with large varicosities, axons arising from the dorsal raphe nucleus are finer and have smaller varicosities (Mamounas et al., 1991; Kosofsky and Molliver, 1987). The stratum oriens and stratum radiatum of area CA1 are innervated almost exclusively by fine serotonergic axons (Mamounas et al., 1991). Serotonin is released upon action potential generated vesicle release from the axonal terminals.

By the numerous target areas all over the brain the raphe nuclei are well suited to modulate the activity of a wide variety of brain circuits. Serotonin signaling is involved in the

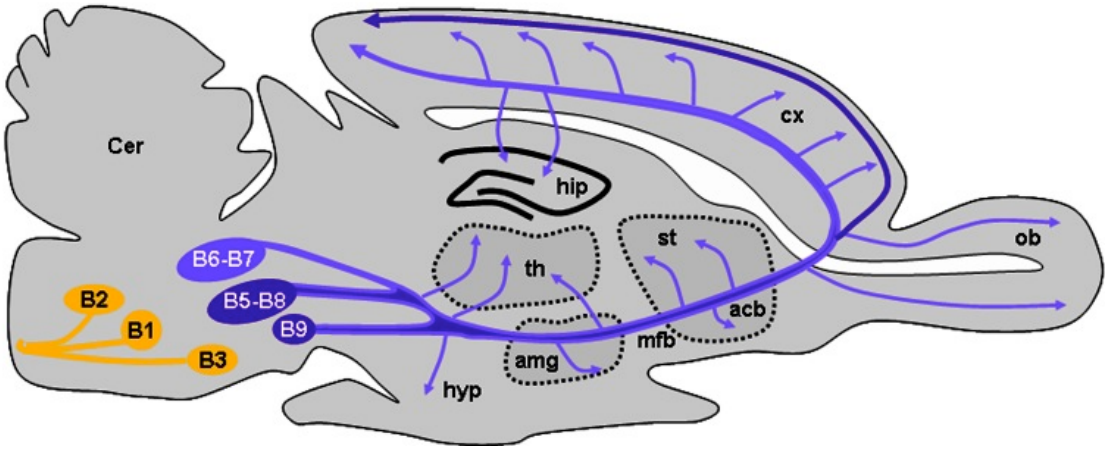

FIGURE 1.3: **The serotonergic neuromodulatory system.** Schematic drawing depicting the location of the serotonergic cell body groups B1–B3 (yellow, posterior groups) and B5–B9 (purple) in a sagittal section of a mouse brain and their major projections. The dorsal raphe nuclei B6 and B7 are depicted in light purple. Arrows indicate regions highly innervated by serotonergic afferents: hypothalamus (hyp), amygdala (amg), thalamus (th), nucleus accumbens (acb), striatum (st), olfactory bulb (ob), cerebral cortex (cx), hippocampus (hip). cer: cerebellum, mfb: medial forebrain bundle. Drawing modified from (Vitalis et al., 2013).

regulations of various cognitive and behavioral functions and dysfunctions, such as sleep, anxiety, pain, mood, learning and their dysfunction in disease syndroms like depression. It acts by binding to the large variety of receptors on the cell's surface of both excitatory and inhibitory gamma-aminobutyric acid (GABA)ergic (inter)neurons. The receptors can be located on the soma, dendrites or presynaptic terminals. Fifteen serotonin receptors have been cloned to date, which are grouped into seven classes based on their signaling mechanism (Kroeze et al., 2002). Except for the 5-HT_3 receptor, a ligand-gated ion channel, all 5-HT receptors are G-protein coupled transmembrane spanning receptors. Upon activation an intracellular second messenger cascade is triggered (Hannon and Hoyer, 2008). Serotonin is cleared by serotonin transporter (SERT) proteins and recycled in a sodium-dependent fashion. This protein is the target of many pharmaceutical drugs commonly used as antidepressant medication. Both immunohistological stainings and electrophysiological experiments have helped to elucidate the numerous cellular effects of serotonin in the hippocampus. For example, it was shown early on that iontophoretically applied serotonin, as well as electrical stimulation of the raphe nuclei inhibit pyramidal cell firing in vivo (Segal, 1975). Aided by an increasing number of receptor subtype specific agonists and antagonists, several cell type and receptor subtype specific actions of serotonin could be identified in the hippocampus. One of the most abundantly expressed 5-HT receptors in the hippocampus is the 5-HT_{1A} receptor. It mediates hyperpolarization of pyramidal cells via G-protein coupled K^+ channels (GIRK channels) (Segal, 1980; Andrade and Nicoll, 1987).

5-HT has also been reported to suppress the induction of long-term potentiation at commissural synapses in stratum radiatum of hippocampal region CA3 (Villani and Johnston, 1993). In contrast, the excitatory input from the entorhinal cortex onto CA1 pyramidal cells via the temperoammonic pathway is selectively potentiated by endogenous serotonin (Cai et al., 2013).

1.3 The role of the hippocampal formation in memory, spatial navigation and disease

Ever since the famous patient H.M. was diagnosed with a severe anterograde amnesia after both his hippocampi had been surgically removed because he suffered from untreatable epilepsy, the hippocampal formation has been implicated in learning and memory (Scoville and Millner, 1957). This case demonstrated that the human hippocampus is necessary for declarative and more specifically, for episodic memory, the ability to remember and describe specific personal experiences (Steinvorth et al., 2005). Furthermore, the hippocampus supports the consolidation of memories for episodic long-term storage (Bayley et al., 2006). However, following surgical removal of the hippocampus perception, cognition, as well as short-term memory remain largely intact. It has been suggested that the hippocampus serves to provide relational organization that encompasses associations between objects and/or events, the spatial-temporal context in which they occurred and the sequential association between events, for review see (Eichenbaum, 2004). In a set of elegant experiments Fortin et al. showed that in rodents the memory for the sequential order of events (in this case the presentation of different odors) is hippocampus-dependent whereas the memory for prior occurrence of events, independent of their order, is not hippocampus-dependent (Fortin et al., 2002).

In rodents one of the most prominent functional features of the hippocampus is its ability to encode a spatial map. In the early 70s, cells with spatially modulated activity were discovered in the hippocampus (O'Keefe and Dostrovsky, 1971). These cells are active whenever the animal is in a certain position in an arena or along a linear track and silent in other locations, therefore these cells have been called 'place cells' (O'Keefe and Nadel, 1978). Place cells have also been found in the dentate gyrus, CA3 (Jung and McNaughton, 1993; Lee and Wilson, 2004) as well as in the subiculum (Sharp and Green, 1994). Further research has revealed other types of spatially modulated cells in the hippocampus and associated regions: grid cells, their activity forms a grid-like map of an environment (Moser et al., 2008), and border-cells. Border cells have been predicted by models of place fields (Hartley et al., 2000) and then have later been found experimentally both in the MEC (Solstad et al., 2008; Savelli et al., 2008) and the subiculum (Lever et al., 2009). These cells are active whenever the animal is in a certain distance to a border or demarcation of

the environment. Other cells with a clearly defined function in spatial navigation include head-direction cells and the recently described speed-cells (Kropff et al., 2015; Sun et al., 2015). In addition, conjunctive cells, that combine properties of two or more types of spatial modulation and/or behavior have been found.

The properties of the place cells in the subiculum differ to some extent from those found in area CA1: their firing fields are larger or display multiple firing peaks, with less sharp edges. Furthermore, it has been suggested that subicular place cells generate the same map after changes in the environment (Sharp and Green, 1994; Sharp, 2006) whereas hippocampal place cells in the CA areas have other or no place fields in different environments, a phenomenon called 'remapping', which has been first described in (Muller and Kubie, 1987).

Generally, compared to neighbouring brain regions, such as area CA1 and the entorhinal cortex, the subiculum has been much less studied and knowledge about the spatial firing properties of subicular pyramidal cells are still limited. Although it is puzzling that one of the major output regions of the hippocampus exhibits a lower degree of spatial selectivity than its input region, these broader place fields might serve the purpose of signaling the approximate position. Given that the firing rate of area CA1 place cells is quite low and the fraction of cells with only one or no field in a given environment is quite high (Thompson and Best, 1989; Karlsson and Frank, 2008; Rich et al., 2014), it might be useful to employ a more coarse representation at the cost of precision.

The formation of a spatial map and the retrieval of it, providing a spatial context for memory, is obviously of great importance for survival, e.g. in order to remember where food is stored, where dangerous predators linger or to be able to find the way home. Furthermore, spatial memory shares features with episodic memory (a term which classically requires self-awareness, which might be questionable in rodents), in which items are recalled in an orderly fashion, similar to the sequential recall of a spatially structured environment as a sequence of place cell activity. It is therefore likely that the structural basis for episodic and spatial memory are alike and quantitatively similar computations are performed (Frank et al., 2006).

Concerning the specific role of the subiculum and the question whether the hippocampal formation functions as one functional unit, it has been shown that damage limited to either the CA regions and the dentate gyrus, or the subiculum alone leads to impairments in learning but combined lesions of all these regions results in more profound deficits (Morris et al., 1990; Jarrard et al., 1986). For non-spatial learning tasks there is conflicting evidence for the necessity of hippocampal regions (Bunsey and Eichenbaum, 1995; Burton et al., 2000). The subiculum and the CA1 region have been suggested to have diverse functional roles in the delayed non-match-to-sample task (DNMS). In this task, rodents, typically rats, are presented a sample and after a certain delay period the animal is requested to choose between the previously presented sample and an alternative. A trial is performed

correctly if the animal chooses the non-familiar sample (non-matched). With synchronous recordings in the subiculum and the CA1 region in rats performing this task, it has been found that during the delay period firing of subicular neurons is increased during the first 15 seconds while hippocampal neurons exhibited a decreased firing rate. This relationship was reversed in later delay phases ($\geq$ 15 seconds): CA1 neurons increased their ensemble firing rate while subicular cells' firing rate decreased, suggesting complementary roles of CA1 and the subiculum during mnemonic tasks (Deadwyler and Hampson, 2004).

The subiculum has been implicated in a number of diseases, such as the in the initiation of epileptic events, e.g. (Cohen et al., 2002), for a review see (Stafstrom, 2005). The ventral subiculum in particular might play a role in drug addiction (Vorel et al., 2001). The subiculum has also been described as one of the regions with the most obvious cytoarchitectural changes observed in schizophrenia, summarized in (Harrison and Eastwood, 2001). Furthermore, in sections from patients who had Alzheimer's disease, a remarkable cell loss in the subiculum as well as in the CA1 region was observed. This cell loss was not present in age-matched controls and also not in the adjacing pre- or para-subiculum of Alzheimer's disease patients. In addition, a large number of neurofibrillary tangles were seen in the subiculum and CA1, not so in presubiculum and CA3. Possibly these alterations might separate the hippocampal output from its targets in the Alzheimer's diseased brain (Hyman et al., 1984; Davies et al., 1988).

1.4 Hippocampal oscillations

In order to achieve functionality the high number of cells in the brain have to be coordinated. Higher brain function does not rely on single cells but is achieved by the concerted action of many neurons and neuron types. This demands for one or several mechanisms that turn subsets of cells on and off in a dynamic fashion to fulfill behavioral and cognitive demands. As the brain is a network of functional units on diverse levels, which are coupled within and among specific anatomical structures, oscillations are a natural way to coordinate the activity of populations of cells (Buzsáki and Draguhn, 2004) .

The hippocampal formation exhibits oscillations at various frequencies that are correlated with behavior. Oscillatory activity can be observed with various methods, both from the outside and the inside of the brain. Electroencephalograms (EEGs) for instance can be measured on the skull surface whereas local field potentials (LFPs) are measured within the brain from a spatially more restricted area. A typical LFP recording picks up the signals from around 250 µm surrounding the electrode (Katzner et al., 2009), depending also on the type of electrode that is used. The LFP can be described as the sum of currents flowing across the membranes of cells in the vicinity of the recording electrode. Furthermore the shape and polarity of the signal depends on the exact positioning of the electrode. It is determined by the organization of the cells within reach of the electrode, i.e. if the cells are

organized in a columnar fashion or more distributed. For example the field signal in the CA1 region is very prominent because of the clear and dense organization of the pyramidal cells in this area, for review see (Buzsáki et al., 2012). When penetrating the brain with a field electrode, the signal changes polarity while crossing the cell body layers and dendritic layers. The polarity is reversed in dendritic layers by 180 ° as compared to the pyramidal cell layers because they act as current sink or source, respectively (Buzsáki, 1986). On the cellular level, oscillations can also be observed as membrane fluctuations that correlate with the extracellular signal (Ylinen et al., 1995b; Kamondi et al., 1998).

The oscillations in the hippocampus can be distinguished by the main frequency they exhibit. One of the most prominent hippocampal oscillations are theta oscillations. Theta oscillations can be observed most prominently during locomotion and during rapid-eye-movement (REM) sleep. The peak frequency ranges between 4–12 Hz, depending on the state of the animals (anesthetized or sleeping versus awake). Furthermore, the frequency of the theta oscillations correlates with the speed of the animal, it shifts to higher frequencies with increasing moving speed (Sławińska and Kasicki, 1998). They can be generated within the CA1 subfield (Goutagny et al., 2009) but usually occur simultaneously in respective hippocampal subregions. They can travel both in the canonic direction, from CA3 to CA1 to the subiculum or in reversed order (Jackson et al., 2014). While theta oscillations have long been believed to be dependent on cholinergic input from the medial septum (Zhang et al., 2010; Vandecasteele et al., 2014), a recent study demonstrates the importance of glutamatergic input from the medial septum in the generation and modulation of theta oscillations (Fuhrmann et al., 2015). Theta oscillations have been hypothesized to play a role in the formation of place fields and phase precession, the ordered advancement of spike timing during traversal of a place field (O'Keefe and Recce, 1993). The phase of spiking thereby encodes the exact position in the place field by employing a temporal code (Jensen and Lisman, 2000). However, the view that theta oscillations are important for spatial navigation has been challenged by findings in bats. These animals have very clear place and grid fields, very good navigational skills and an overall extremely similar structure of the hippocampus as rodents, but do not show any consistent theta oscillations (Yartsev et al., 2011).

Another prominent oscillatory pattern observed in the hippocampus are gamma oscillations; they exhibit frequencies between 30 to 100 Hz. Gamma oscillations often occur concurrently with theta oscillations, both during waking and rapid eye movement (REM) sleep. The faster gamma oscillation can be nested in the slower theta oscillation, which means that the amplitude of the gamma oscillation is modulated by the phase of theta (Bragin et al., 1995; Montgomery et al., 2008). This phase-amplitude cross-frequency coupling has been shown to increase during learning of a conditional discrimination task (Tort et al., 2009). Moreover, the phases of the theta oscillation and the subbands of the gamma oscillation are also coupled (Belluscio et al., 2012). It has been suggested that the two

interacting oscillations serve to represent multiple items, e.g. places, in an orderly fashion. These items are encoded in the cycles of the gamma oscillation which occur at different phases of the theta rhythm; evidence for this hypothesis has been recently discussed by Lisman and Jensen (Lisman and Jensen, 2013). Gamma oscillations can be induced in vitro by activation of metabotropic glutamate receptors (Whittington et al., 1995), muscarinic acetylcholine receptor (Fisahn et al., 1998) or kainate receptors (Fisahn, 2005). During gamma oscillations pyramidal cell spiking leads perisomatic-targeting interneuron firing by a few milliseconds (Bragin1995,Mann2005,Csicsvari2003). The mechanisms involved in the generation of gamma oscillations have been recently reviewed by Buzsaki and Wang (Buzsáki and Wang, 2012).

Sharp wave-ripples, memory consolidation and functional ensembles

The fastest physiological oscillations are ripples, which exhibits frequencies between 120–200 Hz. They are accompanied by an underlying slow component, called sharp wave (Buzsáki, 1986), together they are referred to as sharp wave-ripples (SWRs). SWRs occur during sleep, rest, consummatory behavior and during grooming. Approximately 10% of the whole pyramidal cell population fire one or more action potentials in a given SWR (Ylinen et al., 1995a). In the CA1 region, SWRs can be generated at different positions and travel within area CA1 in both directions, towards subiculum or CA3 and along the dorso-ventral axis (Patel et al., 2013). SWRs occur temporally locked in sub-areas of the hippocampal formation, including area CA3, CA1 and the subiculum. Furthermore, they are locked to up down state transitions in the neocortex (Sirota et al., 2003). The mechanism of SWR generation is still a matter of debate. It has been suggested that fast oscillations are generated in the axonal plexus of excitatory cells that are coupled among each other via gap junctions (Draguhn et al., 1998; Traub and Bibbig, 2000; Bähner et al., 2011). Others have suggested that either interneuron-pyramidal cell interactions are critically involved in the generation of SWRs (English et al., 2014) or that parvalbumin positive interneurons are sufficient for the generation of SWRs (Schlingloff et al., 2014).

SWRs have long been hypothesized to play a role in the consolidation and retrieval of memory (Buzsáki, 1989). In accordance with this notion, sleep has been shown to be beneficial for memory consolidation (Marshall et al., 2006; Wilhelm et al., 2013; Inostroza and Born, 2013), for review see (Diekelmann and Born, 2010). Indeed it has been shown that SWRs play a causal role during spatial memory formation in rodents both during sleep and awake SWRs. In these experiments SWRs were interrupted by electrical stimulation either during sleep phases after learning a spatial task or during the task (Girardeau et al., 2009; Ego-Stengel and Wilson, 2010; Jadhav et al., 2012). Memory consolidation involves transfer to long-term storage areas and long-lasting synaptic changes. These processes are likely enabled by the reactivation of cells that have been active during memory acquisition,

i.e. during exploration (Wilson and McNaughton, 1994). Reactivation occurs preferentially during SWRs, both in awake state as well as during sleep. However it has also been observed during gamma oscillation (Johnson and Redish, 2007). During replay events, a sequence of place cells, that is encountered during exploration is 'replayed', i.e. the place cells coding for the respective place fields are reactivated in the same or reversed order, thereby encoding a specific path.

More general, a pattern of coordinated activity might represent a memory trace, or a memory engram encoding a path or an association. Recently it has been shown that artificially activating an ensemble of dentate gyrus granule cells, that has previously been active during a learning task, in this case fear-conditioning, leads to the appropriate behavioural output, freezing, if the animal is in the context in which the association was learned (Liu et al., 2012). Surprisingly, protein synthesis is not required for context-specific, light induced freezing (Ryan et al., 2015).

How are members of an ensemble of cells, be it cells representing a sequence of visited places or cells that represent an association bound together? On the cellular and molecular level, activity dependent processes might alter the synaptic strength of certain synapses. These processes require the exact timing of pre- and postsynaptic activity, as proposed by Hebb (Hebb, 1949). This type of plasticity has been confirmed at many synapses throughout the brain (Levy and Steward, 1983; Bell et al., 1997; Markram et al., 1997; Bi and Poo, 1998) and has been termed spike-timing dependent plasticity (STDP), for review see (Caporale and Dan, 2008). Ultimately the response to a stimulation of constant strength is enhanced in long-term potentiation (LTP) (Bliss and Lømo, 1973) and decreased in long-term depression (LTD). Ionotropic glutamate receptors, N-methyl-D-aspartate (NMDA) receptors, are necessary for the induction of plasticity as it has been shown that blockade of this receptor type prevents LTP induction (Murphy et al., 1997) and impairs place learning in rats (Morris et al., 1986). Following the induction of LTP, α-amino-3-hydroxy-5-methyl-4-isoxazolepropionic acid (AMPA) receptors are inserted into the postysnaptic membrane whereas following the induction of LTD AMPA receptors are removed from the postsynaptic membrane. In line with this, it has been shown that NMDA receptors in the CA3 region are necessary for pattern completion (Nakazawa et al., 2002). Furthermore, by means of genetically interrupting the Schaffer collateral input from CA3 to CA1 it has been demonstrated that this excitatory input is necessary for system memory consolidation. Interestingly, in these experiments SWRs still occurred in the CA1 region, albeit at a lower frequency. However, the experience-dependent coordinated firing patterns of CA1 neurons were impaired, providing additional evidence that replay of sequences is necessary for memory consolidation (Nakashiba et al., 2009). A causal link between LTP and associative memory, in this study fear conditioning, has recently been made (Nabavi et al., 2014). Whether similar mechanisms are at play for more complex types of memory, such as spatial learning, remains to be established.

1.5 Cell (sub)type diversity in the hippocampal formation

As detailed above, function can be achieved by the coordinated activity of cells. Additionally, cells in the hippocampus and in the brain in general are very diverse and are specialized to fulfill specific functions. Neurons can be classified according to the type of neurotransmitter they release, their morphology, and molecular markers. Very coarsly, neurons can be divided into excitatory and inhibitory neurons. Excitatory principal neurons, such as pyramidal cells and also the granule cells of the dentate gyrus are considered projection neurons, i.e. they target other brain regions. Although generally assumed to be less diverse than interneurons (see paragraph 1.5.2 below), recent evidence, including our study (see paragraph 2.3) points towards intrinsic differences among pyramidal cells. The primary neurotransmitter employed by excitatory neurons is glutamate. Excitatory neurons target both interneurons as well as other excitatory cells. Inputs from a specific area often innervate a certain part of the dendritic tree, e.g. the medial entorhinal cortex input via the temperoammonic pathway targets the apical dendrites of CA1 pyramidal cells.

1.5.1 Pyramidal cells in the subiculum and neighbouring regions

Excitatory cells exhibit a diverse morphology, however I will focus here on the pyramidal cells of the CA region and the subiculum with the name-giving typical triangular cell shape. Pyramidal cells of the CA region and the subiculum exhibit a large apical dendrite and a smaller set of basal dendrites.

In the subiculum two types of pyramidal cells, according to their response to current injections in vitro has been described: bursting and regular firing cells, e.g. (Stewart, 1997). The bursting cells fire two or more closely timed action potentials at the beginning of the step current pulse whereas the action potentials of regular firing cells have a longer interspike interval (Figure 1.4).

FIGURE 1.4: **Burst and regular firing pyramidal cells in the subiculum.** Burst and regular firing cells can be distinguished in vitro by their characteristic firing pattern in response to current pulse injections. Scale bars: 20 mV, 25 ms. Modified from (Wozny et al., 2008b)

.

Besides this difference, subicular pyramidal also exhibit morphological differences: the regular firing cell subtype exhibits longer basal dendrites than the bursting cell subtype, whereas the average total length of tuft dendrites is shorter in regular firing cells than in bursting cells. The input resistance is significantly larger in regular firing cells than in bursting cells, the same holds true for the sag ratio (Graves et al., 2012). In addition the bursting and regular firing type display different pharmacological responsiveness (Graves et al., 2012; Greene and Mason, 1996; Kintscher et al., 2012) and different forms of LTP (Wozny et al., 2008b,a), for review see (Behr et al., 2009). A recent study demonstrated a reversed STDP learning rule at the proximal excitatory synapse of the subiculum (Pandey and Sikdar, 2014). The most obvious differentiating parameter of these cells, however, is their property to elicit action potentials in a characteristic temporal pattern in response to depolarizing step current injections, as described above. The dominating view is that bursting and regular firing cells are not convertible (Stewart, 1997; Graves et al., 2012), but see also (Staff et al., 2000). The mechanism underlying burst firing is voltage independent, and burst firing is primarily driven by non-inactivating, high-voltage activated Ca^{2+} tail currents (Jung et al., 2001).

The proportion of bursting to regular firing cells increases along the proximo-distal axis of the subiculum (proximo-distal with respect to the neighbouring CA1 region). Furthermore the target regions of the subiculum are also arranged in a proximo-distal position dependent manner. As a result, the targets of bursting and regular firing cells are largely different, suggesting parallel streams of information (Kim and Spruston, 2012). Burst firing cells project mostly to the medial entorhinal cortex and presubiculum, which are both brain areas mostly involved in the processing of spatial information. The regular firing type projects mostly to lateral entorhinal cortex as well as nucleus accumbens, brain regions associated with the retrieval of non-spatial memory, such as context and object-related information (Tsao et al., 2013). Despite these differences it remained as yet unknown, if these cells also exhibit functional differences.

Recently, few studies have explored correlations between cellular and functional properties and local connectivity. For example, in the visual cortex pyramidal cells with similar response properties, i.e. cells that share the same tuning curve are preferentially connected among each other (Ko et al., 2011). Moreover, cells exhibiting c-fos expression, an immediate early gene commonly used to indicate previous activation, have been shown to be preferentially connected in primary somatosensory cortex (Yassin et al., 2010). These patterns demonstrate that in many brain regions pyramidal cells are functionally diverse and that these differences are reflected in the network architecture.

In addition to structural differences among pyramidal cells, there are also genetic factors that are likely to contribute to functional cell identity and to the formation of subgroups that are activated together to form functional ensembles. Along these lines Deguchi et al have shown that principal cells in the hippocampal formation, including dentate granule cells and

pyramidal cells of the CA regions 1 and 3 are preferentially connected to each other if they were born on the same day. However electrophysiological evidence and therefore evidence for functional synapses is still missing. Interestingly, cells born around the same time point were not only preferentially connected to each other but also shared the same genetic variants (Deguchi et al., 2011). In another approach, all cells in the CA1 pyramidal layer that were decendents of the same precursor cell were labeled. These sister cells were arranged in clusters and exhibited more synchronous inhibitory inputs than non-sister pyramidal cells, whereas the excitatory input as well as connection probability (both electrical and chemical) were comparably low (Xu et al., 2014).

1.5.2 Inhibitory interneuron diversity in the hippocampus

The 'counterpart' of the above described excitatory pyramidal cells are interneurons. The primary neurotransmitter that is released from interneurons is GABA, which acts mostly inhibitory. The axons of inhibitory interneurons are often extensive and widely distributed, connecting to many postsynaptic partners, including both excitatory and inhibitory neurons. Together with their high firing rate, inhibitory interneurons are expected and have been proven to have a high impact on hippocampal dynamics. The high diversity of inhibitory interneurons in the hippocampus is well accepted. They can be classified according to their preferred target zones on post-synaptic partner neurons, their axonal ramification, their genetic expression profile and their functional specialization (Markram et al., 2004; Klausberger and Somogyi, 2008) (Figure 1.5).

One of the most well studied interneurons of the hippocampus are fast spiking, parvalbumin expressing interneurons (these two populations, fast spiking and parvalbumin immunoreactive cells are not identical, but most fast spiking interneurons are parvalbumin positive). They preferentially innervate the periosomatic region of their target cells, enabling them to tightly control the output of the postsynaptic cell. Their firing rate in vivo is high and they are densely innervating their surrounding pyramidal cells as well as other interneurons. They are involved in many oscillatory patterns of the hippocampus. For instance, parvalbumin positive interneurons control the timing of pyramidal cell firing relative to the theta cycle. Eliminiating parvalbumin positive interneuron firing shifts the phase of the pyramidal cell firing to the trough of theta oscillations (Royer et al., 2012). During SWRs, both fast-spiking interneurons as well as bistratified cells, increase their firing rate (Ylinen et al., 1995a).

Oriens-lacunosum moleculare interneurons

Oriens lacunosum-moleculare (O-LM) interneurons are dendrite–targeting GABAergig interneurons. Their somata have elongated shapes and thick dendrites extending horizontally to both directions, towards CA3 and the subiculum. The axon arborizes extensively in

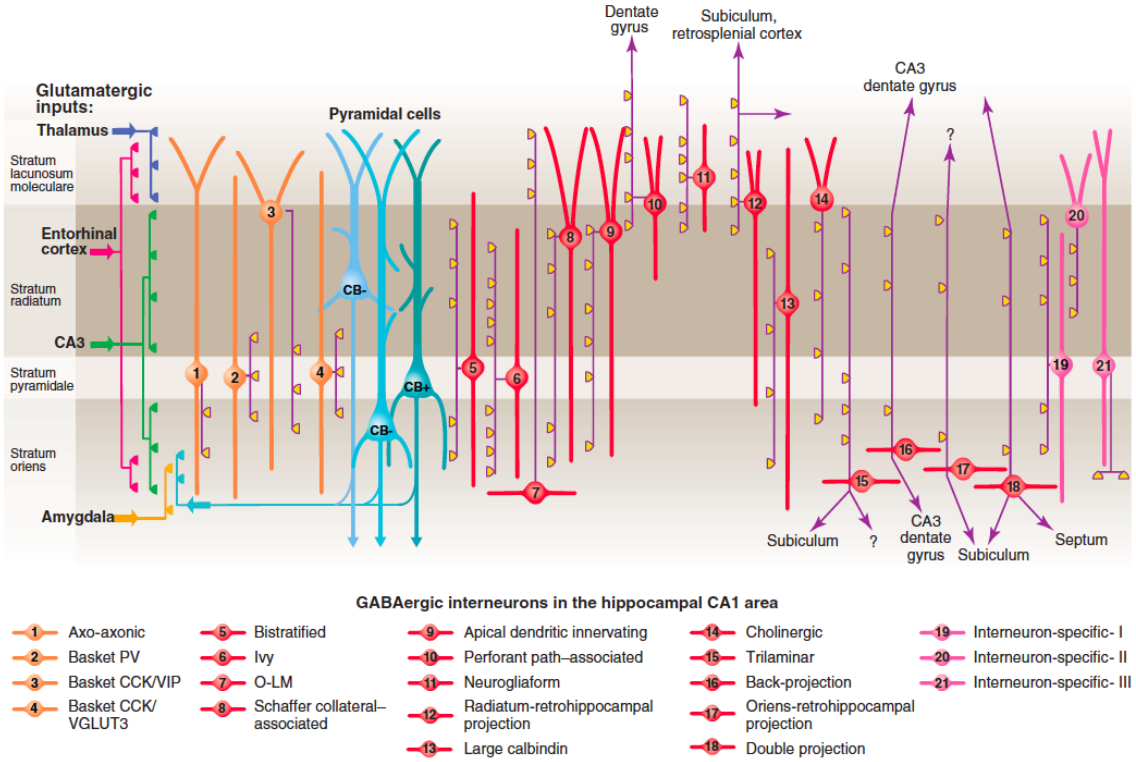

FIGURE 1.5: **Interneuron diversity in the hippocampal region CA1.** The scheme depicts the cellular diversity of the CA1 region. Excitatory input from different sources arrives in the four-layered structure area CA1 (left). Twentyone interneuron types have been described by Klausberger and Somogyi (axons in purple). The O-LM interneuron (7) reaches with its output synapses into stratum lacunosum moleculare, where the input from the entorhinal cortex arrives. Blue: pyramidal cells, they can be distinguished based on the the expression of calbindin (CB). Source: (Klausberger and Somogyi, 2008)

stratum lacunosum-moleculare (Lacaille et al., 1987). They receive both excitatory and inhibitory input with increasing number of synapses towards the distal dendrites as shown by electron microscopy (Martina et al., 2000). They are mostly innervated by local pyramidal cells (Sik et al., 1995; Blasco-Ibáñez and Freund, 1995). O-LM interneurons also receive exciatory, cholinergic input from the medial septum and the diagonal band of Broca and are coupled among each other via gap junctions (Leão et al., 2012). The pyramidal-O-LM synapse is strongly facilitating (Ali and Thomson, 1998), which is in contrast to other glutamatergic synapses, which are mostly depressing (Deuchars and Thomson, 1996; Markram et al., 1997; Feldmeyer et al., 2006). The axon originates mostly from a dendrite, implying a role both in the integration of synaptic input and the axonal output. Indeed, Martina et al. showed that in O-LM interneurons action potentials can be initiated in dendrites; sodium channels allow for fast and active propagation of action potentials along the dendrites (Martina et al., 2000).

O-LM interneurons express metabotropic glutamate receptors mGluR1 (Blasco-Ibáñez and Freund, 1995), their activation leads to strong depolarization and oscillatory responses (McBain et al., 1994). Additionally they express somatostatin (Kosaka et al., 1988; Freund

and Buzsáki, 1996), and recently a more specific marker, *Chrna2*, became available (Leão et al., 2012).

O-LM interneurons do not constitute a homogenous population: recently a subdivision among O-LM interneurons with different developmental origin has been found: one subset of O-LM interneurons is derived from the caudal ganglionic eminence and expresses 5-HT_{3A}receptors and another subset is derived from the medial ganglionic eminence and lacks expression of 5-HT_{3A}receptors (Chittajallu et al., 2013). O-LM interneurons display a hyperpolarization-activated current that has been described to contribute to the excitability of this cell type (Maccaferri and McBain, 1996) as well as to theta–resonance (Griguoli et al., 2010), but see (Kispersky et al., 2012).

O-LM interneurons in area CA1 target the distal apical dendrite of pyramidal cells, where input from entorhinal cortex arrives via the temperoammonic pathway (Maccaferri and McBain, 1995). Indeed, active O-LM interneurons inhibit entorhinal cortex input and can also inhibit LTP of the temperoammonic pathway (Leão et al., 2012). In contrast, intrahippocampal input from CA3 onto CA1 pyramidal cells via the Schaffer collaterals is enabled by active O-LM cells by disinhibition of feedforward inhibition, this way hippocampal output can be controlled (Maccaferri and Dingledine, 2002; Leão et al., 2012).

Interneurons play an important role during oscillatory network activity. They are generally much more densely connected than pyramidal cells and more active and have thereby a strong influence on network activity. O-LM cells can discharge at the trough of theta-oscillations in vivo (Klausberger et al., 2003; Varga et al., 2012; Katona et al., 2014) and in vitro (Gloveli et al., 2005), which has led to the assumption that O-LM cells can act as pacemakers in a theoretical model of hippocampal network oscillations (Tort et al., 2007). However this view has been challenged by an in vitro study employing dynamic clamp experiments, which suggests that O-LM cells can act as amplifiers in the theta range and exhibit locked spiking to theta-modulated input but do not act as resonators (Kispersky et al., 2012). Furthermore it has been described that O-LM cells are enabled to follow theta-modulated input by the activation of kainate receptors (Goldin et al., 2007), which is in line with findings that kainate receptor blockade interferes with theta oscillations in vivo (Huxter et al., 2007).

Beside their role during theta oscillations, O-LM interneurons have also been shown to be occasionally activated during SWRs: in awake head-fixed mice running on a treadmill (Varga et al., 2012) and in vitro (Pangalos et al., 2013). Spike timing was late during SWRs and both during theta and SWRs, O-LM spiking lagged behind the activation of fast spiking inhibitory basket cells (Varga et al., 2012). However, in awake behaving animals firing rates decreased or were unaltered during SWRs as compared to baseline activity both during wakefulness and sleep (Katona et al., 2014). In yet another study using urethane anesthetized mice, O-LM interneuron firing residing in intermediate CA1 has been analyzed with respect to dorsal and intermediate CA1 ripples (Forro et al., 2015). Here, almost all

cells were activated compared to baseline firing rate, both with respect to intermediate as well as dorsal CA1 ripples. These partially conflicting results could be explained by the low number of cells analyzed in some of the studies and also by the existence of two subgroups of O-LM interneurons that might be differently engaged during oscillations (Chittajallu et al., 2013).

Chapter 2

Functional diversity of subicular principal cells during hippocampal ripples

2.1 Motivation and research goals

SWRs play an important role in the consolidation of memory in which specific activity patterns or sequences are reactivated. During this consolidation phase the results of hippocampal processing are believed to be transferred to cortical and subcortical regions for long-term storage and to be integrated into other memory content previously encoded. One of the major output structures of the hippocampus contributing to this distribution is the subiculum. While pyramidal cell activation during SWRs has been extensively studied in the CA1 region, it is unknown how subicular principal cells participate during SWRs[1]. Furthermore the bursting and regular firing pyramidal cell phenotype in the subiculum has been only described in vitro, and it is unclear whether these cell types can be identified in vivo. In addition, the mechanisms underlying pyramidal cell participation in the subiculum and the underlying excitatory and inhibitory currents remain to be determined. I have addressed these questions by combining field potential and patch-clamp recordings in awake mice and in acute brain slices. Furthermore we have investigated the local network topology of the subiculum using multi-patch-clamp recordings in vitro.

2.2 Statement of contribution

I have substantially contributed to the concept and design of this study. The in vivo experiments were established by myself with the help of James Poulet. The data for Figures

[1] In the original article as well as in the discussion in chapter 4, I often refer to 'ripples' instead of SWRs, as the detection of SWRs in vivo was based on the fast component only.

1, 2, 3, 4, 5 (E,F) and 6 were entirely carried out by myself (all in vivo experiments and the majority of the in vitro SWR experiments). I also developed the analysis routines and performed the analysis for all in vivo experiments and some of the in vitro SWR experiments. The data for Figure 5 G - J were carried out by myself and Nikolaus Maier together. For the data displayed in Figure 7 I have prepared for almost all experiments the brain slices and performed the histological analysis by confocal microscopy. The multi-patch clamp recordings (Figure 7) were performed and analyzed by Yangfan Peng and Jochen Winterer. The manuscript was written by myself, all other authors commented on the manuscript.

2.3 Original research article

Claudia Böhm, Yangfan Peng, Nikolaus Maier, Jochen Winterer, James F.A. Poulet, Jörg R.P. Geiger and Dietmar Schmitz. Functional Diversity of Subicular Principal Cells during Hippocampal Ripples. *The Journal of Neuroscience*, 35(40):13608 —13618, Oct 2015

Systems/Circuits

Functional Diversity of Subicular Principal Cells during Hippocampal Ripples

Claudia Böhm,[1] Yangfan Peng,[2] Nikolaus Maier,[1] Jochen Winterer,[1] James F.A. Poulet,[1,3,4] Jörg R.P. Geiger,[2,4] and Dietmar Schmitz[1,3,4,5,6]

[1]Neuroscience Research Center and [2]Institute of Neurophysiology, Charité Universitätsmedizin Berlin, 10117 Berlin, Germany, [3]Max-Delbrück Center for Molecular Medicine, 13092 Berlin, Germany, [4]Cluster of Excellence NeuroCure, 10117 Berlin, Germany, [5]Bernstein Center for Computational Neuroscience, 10115 Berlin, Germany, and [6]Center for Neurodegenerative Diseases Berlin, 10117 Berlin, Germany

Cortical and hippocampal oscillations play a crucial role in the encoding, consolidation, and retrieval of memory. Sharp-wave associated ripples have been shown to be necessary for the consolidation of memory. During consolidation, information is transferred from the hippocampus to the neocortex. One of the structures at the interface between hippocampus and neocortex is the subiculum. It is therefore well suited to mediate the transfer and distribution of information from the hippocampus to other areas. By juxtacellular and whole-cell-recordings in awake mice, we show here that in the subiculum a subset of pyramidal cells is activated, whereas another subset is inhibited during ripples. We demonstrate that these functionally different subgroups are predetermined by their cell subtype. Bursting cells are selectively used to transmit information during ripples, whereas the firing probability in regular firing cells is reduced. With multiple patch-clamp recordings *in vitro*, we show that the cell subtype-specific differences extend into the local network topology. This is reflected in an asymmetric wiring scheme where bursting cells and regular firing cells are recurrently connected among themselves but connections between subtypes exclusively exist from regular to bursting cells. Furthermore, inhibitory connections are more numerous onto regular firing cells than onto bursting cells. We conclude that the network topology contributes to the observed functional diversity of subicular pyramidal cells during sharp-wave associated ripples.

Key words: connectivity; hippocampus; *in vivo*; multiple recordings; oscillation; subiculum

Significance Statement

Memory consolidation is dependent on hippocampal activity patterns, so called hippocampal ripples. During these fast oscillations, memory traces are transferred from the hippocampus to the neocortex via the subiculum. We investigated the role of single cells in the subiculum during ripples and found that, dependent on their subtype, they are preferentially activated or inhibited. In addition, these two subtypes, the bursting and regular firing type, are differentially integrated into the local network: inhibitory cells are more densely connected to regular firing cells, and communication between regular and bursting cells is unidirectional. Together with earlier findings on different preferential target regions of these subtypes, we conclude that memory traces are guided to target regions of the activated cell type.

Introduction

The hippocampal formation exhibits robust networks oscillations, which are correlated to different behavioral states (O'Keefe and Nadel, 1978). Sharp-wave associated ripples (SWRs) are observed during slow-wave sleep, awake immobility, and consummatory behavior (O'Keefe and Nadel, 1978; Buzsáki, 1986). They are related to memory consolidation in rodents and primates (Girardeau et al., 2009; Ego-Stengel and Wilson, 2010; Logothetis

Received Dec. 11, 2014; revised Aug. 20, 2015; accepted Aug. 23, 2015.

Author contributions: C.B., Y.P., J.F.A.P., J.R.P.G., and D.S. designed research; C.B., Y.P., N.M., and J.W. performed research; C.B., Y.P., N.M., and J.W. analyzed data; C.B. and D.S. wrote the paper.

This work was supported by the Deutsche Forschungsgemeinschaft (Cluster of Excellence NeuroCure, SFB 665/958, GRK 1123), the Bernstein Center for Computational Neuroscience, and the Center for Neurodegenerative Diseases, Berlin, Germany. J.F.A.P. was supported by a European Research Council (ERC) starting grant (ERC-2010-StG-260590). We thank Susanne Rieckmann for technical assistance; Jörg Rösner for help with confocal microscopy; Richard Kempter and Christian Wozny for discussion; and Michael Brecht, Richard Kempter, and Anja Gundlfinger for comments on the manuscript.

The authors declare no competing financial interests.

This article is freely available online through the *J Neurosci* Author Open Choice option.

Correspondence should be addressed to either of the following: Dietmar Schmitz, Charitéplatz 1, 10117 Berlin, Germany, E-mail: dietmar.schmitz@charite.de; or Claudia Böhm, Howard Hughes Medical Institute, Janelia Research Campus, Ashburn, VA 20147, E-mail: boehmc@janelia.hhmi.org.

C. Böhm's current address: Howard Hughes Medical Institute, Janelia Research Campus, Ashburn, VA 20147.

DOI:10.1523/JNEUROSCI.5034-14.2015

et al., 2012; Jadhav et al., 2012; Inostroza and Born, 2013) and occur temporally correlated in respective areas of the hippocampal formation, including the subiculum (Chrobak and Buzsáki, 1994). Concomitantly, during SWR, subcortical areas involved in sensory processing are silenced, thereby minimizing interference in hippocampal-neocortical interaction and enabling an efficient information transfer (Logothetis et al., 2012). These findings are in line with the beneficial effect of slow-wave sleep in memory consolidation (Marshall et al., 2006; Inostroza and Born, 2013; Wilhelm et al., 2013). At the cellular level, the consolidation of memory traces during SWR is thought to be based on the reactivation of neuronal ensembles that have been activated during exploration in a temporally compressed fashion (Lee and Wilson, 2002; Davidson et al., 2009; Karlsson and Frank, 2009), thereby stabilizing the synaptic connections between ensemble members (Markram et al., 1997) not only within the hippocampus but also in the cortex (Ji and Wilson, 2007; Mehta, 2007). One of the major output areas of the hippocampus is the subiculum (Witter, 2006). It is densely innervated by the CA1 region of the hippocampus in a series of nested loops (Amaral et al., 1991) and sends projections to various cortical and subcortical structures in a topographic fashion (Witter et al., 1990; Naber et al., 2000; Witter, 2006). In contrast to CA1 pyramidal cells, subicular pyramidal cells exhibit a low degree of axonal collateralization and project mostly to only one target region (Naber and Witter, 1998; Kim and Spruston, 2012). *In vitro*, two types of pyramidal cells have been described in the subiculum: regular firing cells and intrinsically bursting cells (for review, see Behr et al., 2009). These cells have been shown to display different properties with respect to pharmacological responsiveness, dendritic morphology, and projection area (Kim and Spruston, 2012; Graves et al., 2012). However, it remains unclear whether these subtypes are also functionally diverse and whether this diversity is reflected in the local network topology. To address these questions, we combined single-cell *in vivo* electrophysiology during a defined behavioral state with multiple simultaneous patch-clamp recordings *in vitro*. This allowed us to reveal a pyramidal cell subtype-specific activation during SWR and a local synaptic circuitry that exhibits unidirectional connectivity from regular to bursting cells as well as an inhibitory circuitry that favors inhibition onto regular firing cells.

Materials and Methods

Ethics statement

Animal maintenance and experiments were in accordance with the respective guidelines of local authorities (Berlin state government, T0100/03 and G0151/12) and followed the German animal welfare act and the European Council Directive 2010/63/EU on protection of animals used for experimental and other scientific purposes.

Animal surgery and electrophysiology in vivo

All *in vivo* experimental procedures followed previously described methods (Crochet and Petersen, 2006; Maier et al., 2011). Male p24 to p33 C57BL/6J mice were anesthetized and implanted with a lightweight metal head holder and a plastic recording chamber centered over the CA1-subicular region. After surgery, animals were allowed to recover for at least 1 d before habituation to head restraint started. Habituation was repeated for several days until the animal sat calmly for a period of at least 1 h. On the day of the experiment, two small craniotomies for local field potential (LFP) and single-cell recordings were made under isoflurane anesthesia (1.5%). Animals were then allowed to recover for at least 2 h before recordings started. Coordinates for craniotomies were determined stereotactically on the left hemisphere: for LFP recordings in distal CA1, the glass pipette was inserted at 2.5 mm posterior of bregma and 2.5 mm medial from the midline at an angle of ~30 degree tilted from the vertical. The patch electrode was inserted vertically 3 mm posterior of bregma and 1.8–2 mm lateral of the midline. For LFP recordings, we used glass pipettes (5–7 MΩ) filled with Ringer's solution containing the following (in mM): 135 NaCl, 5 KCl, 5 HEPES, 1.8 $CaCl_2$, and 1 $MgCl_2$. To determine the recording depth of the area of interest (i.e., CA1 stratum pyramidale), the LFP electrode was lowered until clear ripple activity was observed, usually at 1100–1300 μm. Then the second electrode was inserted through the more posterior craniotomy, aimed to target the subiculum. It was advanced until signal polarity of both electrodes was equal and ripple activity could also be seen on the subiculum electrode (at ~1500 μm). Searching for cells began ~50 μm above the so-determined depth with a new pipette. For whole-cell and juxtacellular recordings, 5–7 MΩ glass electrodes filled with intracellular solution containing the following (in mM): 135 K-gluconate, 4 KCl, 4 MgATP, 10 Na_2-phosphocreatine, 0.3 Na_3GTP, and 10 HEPES (pH adjusted to 7.3 with KOH; 2 mg/ml biocytin).

No constant current injections were used. Membrane potentials are not corrected for liquid junction potential. On average, the initial membrane potential was −59.8 ± 0.7 mV (mean ± SEM, $n = 46$ cells), and the average spike height was 70.3 ± 2.2 mV (mean ± SEM, $n = 46$ cells) as calculated at rheobase from baseline voltage before current injection to spike peak. Cells with an initial membrane potential positive to −50 mV were excluded. Recording positions in the subiculum were verified by biocytin staining of the recorded cell, an electrode track, or traces of ejected biocytin. All *in vivo* signals were amplified with a Multiclamp 700B (Molecular Devices), filtered at 10 kHz, and digitized at 20 kHz (ITC-18; HEKA Elektronik). The reconstruction of the pyramidal cell shown in Figure 3*A* was performed on a DAB staining of the biocytin-filled neuron using the Neurolucida software (MicroBrightField).

Electrophysiology in vitro*: slice preparation*

Male C57BL/6N mice of age 3–6 weeks were decapitated following isoflurane anesthesia. Brains were transferred to ice-cold ACSF slicing solution containing (in mM) the following: 87 NaCl, 2.5 KCl, 3 $MgCl_2$, 0.5 $CaCl_2$, 25 glucose, 50 sucrose, 1.25 NaH_2PO_4, and 26 $NaHCO_3$, pH 7.4. Horizontal slices (400 μm thick) of ventral to mid-hippocampus were cut on a slicer (VT1200S; Leica) and stored in an interface chamber (32°C–34°C) and perfused with standard ACSF containing (in mM) the following: 119 NaCl, 2.5 KCl, 1.3 $MgCl_2$, 2.5 $CaCl_2$, 10 glucose, 1.0 NaH_2PO_4, and 26 $NaHCO_3$. The perfusion rate was ~1 ml/min. All ACSF was equilibrated with carbogen (95% O_2, 5% CO_2). Slices were allowed to recover for at least 1 h after preparation. Minislices of the subiculum were prepared from full slices and cut shortly after preparation on an agar block in oxygenized ACSF. A scalpel was used to separate both: connections between CA1 and the subiculum, and between the subiculum and the entorhinal cortex. After cutting, the slices were retransferred to the interface chamber and allowed to recover for at least 1 h. In some experiments, subiculum minislices were cut immediately before the experiments. Data obtained from either approach were pooled.

Recordings of ripple-associated currents in vitro

As described previously (Maier et al., 2009), recordings were performed in standard ACSF at 31°C–32°C in a submerged-type recording chamber perfused at high rate (5–6 ml/min). For LFP recordings, glass microelectrodes (tip diameter 5–10 μm; resistance 0.2–0.3 MΩ) were filled with ACSF before use. Whole-cell recordings of subicular principal neurons and interneurons were performed with glass electrodes (2–5 MΩ) filled with 120 mM K-gluconate, 10 mM HEPES, 3 mM Mg-ATP, 10 mM KCl, 5 mM EGTA, 2 mM $MgSO_4$, 0.3 mM Na_2-GTP, and 14 mM phosphocreatine. The pH was adjusted to 7.4 with KOH. Voltage-clamp recordings at the reversal potential of excitation and inhibition were performed using intracellular solution containing 120 mM gluconic acid, 10 mM HEPES, 5 mM EGTA, 10 mM KCl, 2 mM $MgSO_4$, 1 mM Na_2-GTP, and 3 MgATP. The pH was adjusted to 7.4 with CsOH. Using the Multiclamp 700A amplifier (Molecular Devices), extracellular LFP signals were amplified 1000-fold, and whole-cell data were amplified 5- and 25-fold for voltage-clamp and current-clamp recordings. Signals were filtered (1–8 kHz) and digitized at 10 or 20 kHz with 16-bit resolution (6036 E card; National Instruments);

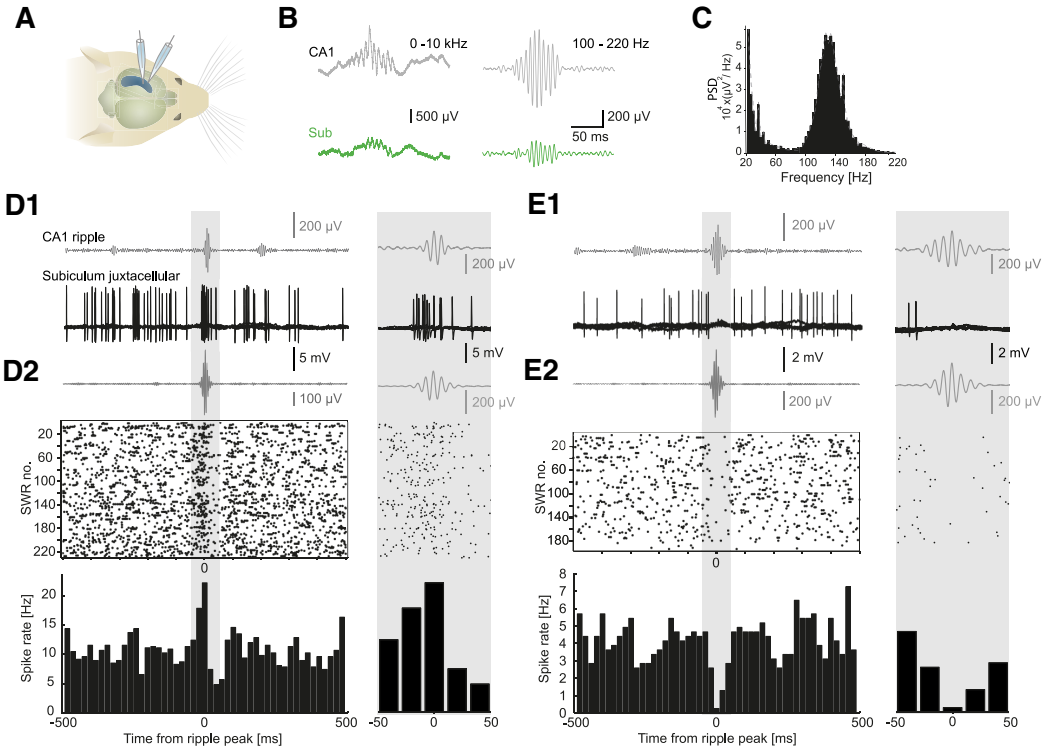

Figure 1. Subicular neurons are differentially modulated during ripples in awake mice. ***A***, Recording configuration. ***B***, Example ripple in simultaneous LFP recordings in area CA1 (gray) and the subiculum (green) during quiet wakefulness. Left, 0–10 kHz. Right, Same as left but bandpass filtered between 100 and 220 Hz. ***C***, Power spectral density of the ripple peak-aligned averages from 35 LFP recordings. Gray lines indicate ± SEM. ***D***, ***E***, Juxtacellular recordings in the subiculum with opposing spike modulation during CA1 ripples (***D*** and ***E*** represent one cell each). Zooms of the shaded areas are shown to the right. ***D1***, ***E1***, Top, Average of 5 ripples (LFP) aligned to the peak of the oscillation. Bottom, Overlay of corresponding juxtacellular recording. ***D2***, ***E2***, Top, Mean ripple LFP aligned to the peak of the oscillation. Middle, Raster plot of corresponding spikes. Each dot represents a spike. Each row represents all spikes that occur within 1 s (100 ms in zoom) around a ripple with its peak aligned to time point 0. Bottom, Histograms of the above raster plot; time bins, 20 ms.

data were stored using Igor Pro (Wavemetrics). The parvalbumin-positive interneuron shown in Figure 6*B* was reconstructed using the "Simple Neurite Tracer" (Longair et al., 2011).

Connectivity

The slices were prepared as described above. To ensure comparable slice condition and quality, we tested in each slice whether SWRs were generated and used only those slices in which this was the case. The temperature in the recording chamber was adjusted to 34°C. Cells in the subiculum were identified using infrared differential contrast microscopy (BX51WI, Olympus) and selected within a distance of 50–100 μm from each other. In a subset of experiments, GAD67-GFP-expressing mice were used to aid the identification of interneurons. We performed somatic whole-cell patch-clamp recordings (pipette resistance 2.5–5 MΩ) of up to eight cells simultaneously. Each of the simultaneously recorded cells was consecutively stimulated with a train of 4 action potentials at 50 Hz, elicited by 0.5- to 2-ms-long current injections of 2–3.5 nA. For the characterization, increasing steps of current were injected (500 ms, increment: 40–50 pA). The resting membrane potential of pyramidal cells was −62.7 ± 0.25 mV, that of fast-spiking interneurons −64.4 ± 1.3 mV, and that of non–fast-spiking interneurons −62.5 ± 0.9 mV on average. In a few experiments, hyperpolarizing holding current was applied to keep the membrane potential at −60 mV. The intracellular solution contained 135 mM potassium gluconate, 6 mM KCl, 2 mM $MgCl_2$, 0.2 mM EGTA, 5 mM Na_2-phosphocreatine, 2 mM Na_2-ATP, 0.5 mM Na_2-GTP, 10 mM HEPES buffer, and 0.2% biocytin. The pH was adjusted to 7.20 with KOH. Recordings were performed using Multiclamp 700B amplifiers (Molecular Devices). Signals were filtered at 6 kHz, sampled at 20 kHz, and digitized using the Digidata 1440 and pClamp 10 (Molecular Devices).

Data analysis

Analysis of in vivo *data*. To detect ripples, the LFP signal was filtered with a Butterworth bandpass filter at 100–220 Hz in forward and reverse direction to prevent phase distortion. Any offset was corrected for by subtracting the mean. The absolute (i.e., rectified) value of the signal was smoothed using a Savitzky–Golay filter with a spanning window of 300 data points. A first threshold for the length of candidate events was set to 2 SDs of the smoothed and rectified signal. Positive detected events had to be above this threshold for a duration of at least 21 ms. In these periods, maxima were detected that had to pass the criterion of 4.5 SDs of the filtered but not smoothed signal (detection is more adequate in the unflattened signal). In addition, a criterion for the minimum distance between the peaks of two events was used (40 ms). In case of failure of this criterion, the ripple with the smaller peak was discarded. The so-determined peaks of the ripples were used for alignment both of the LFP signal and the simultaneous single-cell recordings.

Spikes in whole-cell current-clamp recordings were detected with a thresholding algorithm on the ascending flank at −20 mV, and the maximum in the following 2.5 ms was considered the peak. The signal had to fall below the threshold again, before a new spike was considered, which was relevant for spike detection in bursts. For spike detection in juxtacellular recordings, a similar algorithm was used where the threshold was set individually in each recording according to spike height. Cells with a peak to through width shorter than 0.4 ms were excluded as presumptive interneurons.

To generate the surrogate data for each cell, the number of ripples n observed in the data was determined. Then, n random time points were generated in ripple-free periods, and time windows of the same length as used to determine the spike count during ripples (40 ms) were used to

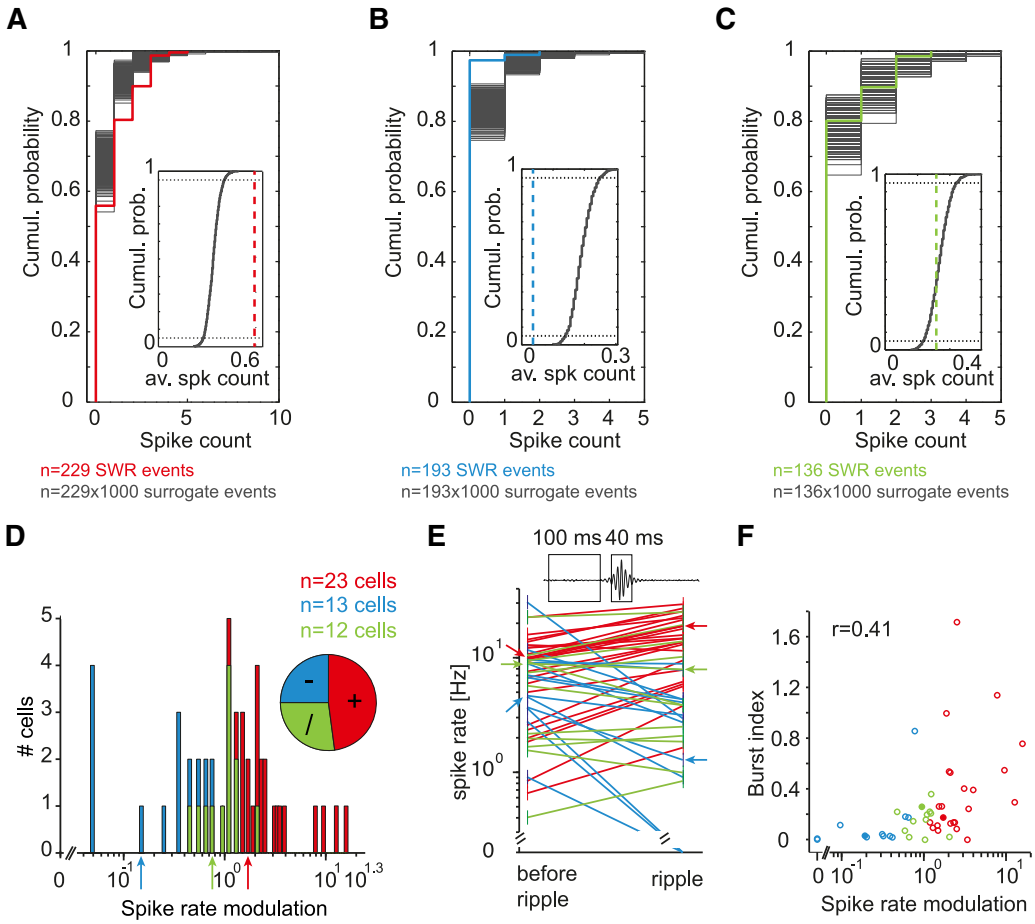

Figure 2. Analysis of juxtacellular recordings. ***A–C***, One cell each. ***A*** shows the analysis for the cell in Figure 1*D* and ***B*** for the cell in Figure 1*E*. Red/blue/green lines indicate cumulative distribution of spike counts observed during ripple events (40 ms around the ripple peak). Gray represents the same number and length of time windows were randomly chosen in ripple-free periods and the cumulative distribution of the spike count was plotted. This procedure was repeated 1000 times. Insets in gray, Distribution of the mean firing rate of each set of surrogate "ripples." Dashed colored lines indicate the mean spike count during ripples. The shift of the red line to the right in the cell in ***A*** indicates a higher spike count than expected from choosing random time windows of the same size. The shift to the left (blue) in the cell displayed in ***B*** indicates a decrease in firing rate during ripples. ***C***, The green line is within the expected range from the randomly generated dataset; this cell's discharge rate is not modulated by ripples. Insets, Gray dotted lines indicate that the corresponding spike count on the *x*-axis occurs in ≤5% of the cases when choosing random time windows. ***D***, Distribution of spike rate modulation. The spike rate modulation was assessed as the ratio of the firing rate during ripples and the overall firing rate (average over the whole duration of the recording). The bins from 0 to 1 (decrease in spike rate) have 0.1 width (i.e., the first bin contain cells with modulation between 0 and 0.1), whereas the bins for increased spike rate (spike rate modulation >1) have 0.2 width (i.e., the first bin contains cells with modulation between 1 and 1.2). For better visualization on log scale, the bar width does not represent bin width; bars are centered on the corresponding bin. Colored arrows indicate the bins containing the example cells (***A–C***). Inset, Fraction of cells that display different types of modulation during ripples. ***E***, Comparison of spike rates before ripples and during ripples. Inset, Time windows used for analysis with respect to LFP. Colored arrows indicate the example cells (***A–C***). ***F***, The burst index (number of spikes in bursts/number of remaining spikes, both calculated from the whole recording duration) is correlated with the spike rate modulation (spike rate during ripples/overall spike rate). Filled circles represent the bins containing the example cells (***A–C***). *r*, correlation coefficient. ***D–F***, Blue represents cells with a significant decrease in spiking. Red represents cells with a significant increase in spiking. Green represents cells without significant modulation. $p > 0.05$ (as determined by comparison with the surrogate datasets).

calculate the spike count in ripple-free periods. This procedure was repeated 1000 times. For each set of surrogate "ripples," the mean count was calculated and the distribution thereof was compared with the mean of the real observed count during ripples. If the probability to observe this real count in the surrogate data was <5%, we considered the cell to be modulated by ripple activity. A similar method was used previously to estimate the modulation of interneuron spiking during ripples (Katona et al., 2014).

To determine whether a cell was depolarized or hyperpolarized during ripples, spikes were cut, and the averaged membrane potential before and after the ripple (−80 ms to −40 and 40 to 80 ms) was used as a baseline, and the deviation of the average membrane potential during the peak of the ripple (−20 to 20 ms) was used to measure the modulation. When spikes were cut out in whole-cell current-clamp recordings, all data points between 3 ms before the peak and 5 ms after the peak were deleted and replaced by linear interpolation. For cell classification in whole-cell current-clamp recordings, we considered only the spike pattern at rheobase in response to depolarizing pulses in the beginning of the recording, when the network was still mostly silenced. Cells where this was not unambiguously possible, due to high spontaneous network activity (presumably because the time to seal and open the cell were in these cases long enough for the network to recover), are not included in any analysis that requires this classification (see Fig. 4*C*,*D*). In total, we recorded 46 cells in whole-cell current-clamp mode: 10 cells could be classified as regular firing cells, 25 as bursting cells, and 11 could not be identified unambiguously.

The "ongoing network activity" (see Fig. 4*B*) refers to periods later on during the recordings, when the network expresses stable activity levels, including periods with and without ripples. A burst was defined as at least 3 spikes with an interspike interval of <8 ms, a spike was considered

a member of a burst if a preceding or following spike was within 8 ms, meaning that also the last and first spike of a burst were considered members of the burst. The burst index was defined as the number of spikes in bursts divided by the number of remaining spikes (single spikes and doublets). For statistical comparison, the Mann–Whitney or the Wilcoxon signed-rank test was used. To test for normal distribution, the Lilliefors test was used.

Analysis of in vitro *data.* LFP SWRs recorded in area CA1 or in minislices of the subiculum were detected using a threshold-based algorithm. From simultaneously sampled voltage-clamp data, 200 ms stretches of signal of SWR-associated postsynaptic currents were cut after alignment to the peak of the averaged postsynaptic currents of the respective recording; the postsynaptic current stretches were baseline-corrected by subtracting the mean of the first 75 ms in each window. For estimation of synaptic input during SWRs the total charge transfer was calculated by trapezoidal integration over the windows of data (trapz function in MATLAB, The MathWorks). The mean charge transfer values were calculated for each cell for comparison of synaptic input in regular and burst firing neurons. For statistical comparison of charge transfer and the ratio of excitatory and inhibitory charge transfer, the Mann–Whitney test or Student's *t* test was used, as indicated.

Analysis of connectivity data. Cell subtypes were differentiated by monitoring the firing pattern at rheobase. Synaptic connections were identified when there was a postsynaptic potential corresponding to the presynaptic stimulation in the averaged trace from 40 to 50 sweeps. The 150 ms baseline just before the stimulation and the postsynaptic peak during the first action potential were used for the analysis of the EPSP/IPSP amplitudes with pClamp 10 (Molecular Devices). Only those pairs in which the first postsynaptic peak was clearly discernible were used for analysis of the amplitude. Postsynaptic potentials were clearly discernible from electrical crosstalk between electrodes by their relative timing, kinetics, and amplitudes. We used the Fisher's exact test for statistical comparison of the connection probabilities. The statistical significance of postsynaptic amplitudes was calculated using the Mann–Whitney test.

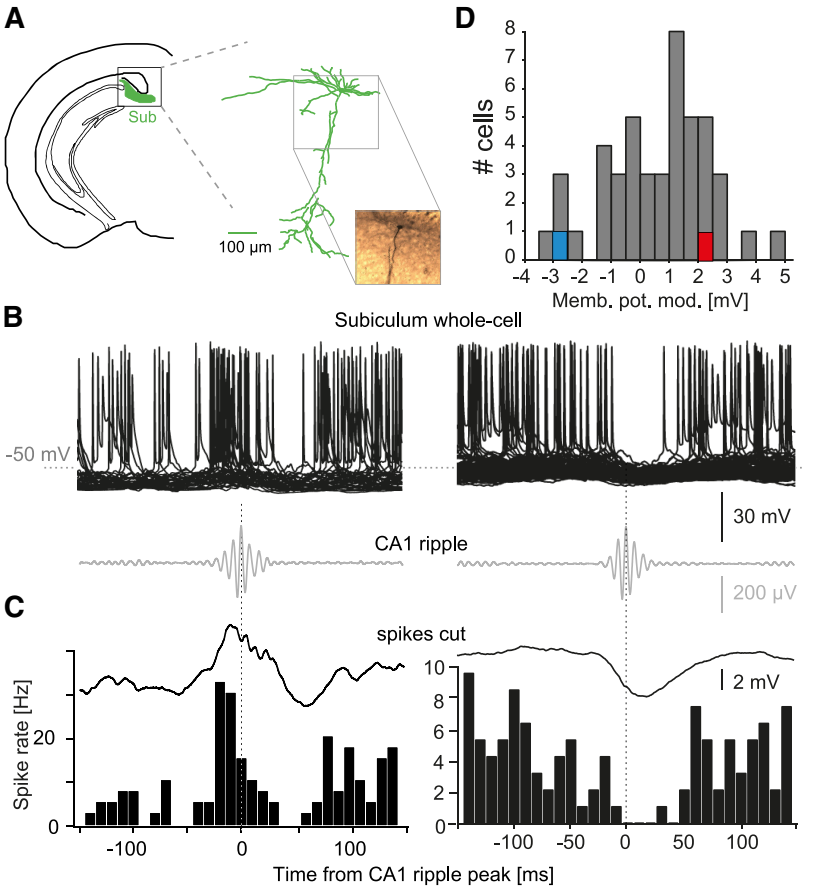

Figure 3. Pyramidal cells in the subiculum display depolarization or hyperpolarization during ripples. ***A***, Left, Coronal slice. Green represents the subiculum (adapted from Paxinos and Franklin, 2012). Right, Morphological reconstruction of a pyramidal cell in the subiculum recorded *in vivo*. Right, Bottom, Micrograph of the indicated area shows the stained cell in tissue. ***B***, Examples of whole-cell current-clamp recordings. Left and right columns represent one cell each. Top, Overlay of membrane potential traces aligned to the corresponding ripple peak of the LFP (left, 40 traces; right, 92 traces). Bottom, Mean ripple LFP. ***C***, Top, Averages of the membrane potential with spikes cut. Bottom, Mean histogram of spike rate of the traces in ***B***; time bins, 10 ms. ***D***, Distribution of average membrane potential modulation of all cells recorded. The example cells shown in ***B*** and ***C*** are indicated by colored boxes.

Results

Pyramidal cells in the subiculum are functionally diverse *in vivo*

LFP and simultaneous single-cell recordings were performed in awake head-fixed mice. The animals were habituated to the head fixation for a few days until they sat calmly for at least 1 h. During the recordings, the animals were alert, they whisked, their eyes were always open, and they were mostly still during the recording (Crochet and Petersen, 2006). Ripples were recorded in the CA1 region of the hippocampus; they appeared as short (50–100 ms) aperiodic, recurrent events, and displayed a frequency peak at 120–150 Hz (Chrobak and Buzsáki, 1996) (Fig. 1*A–C*). With an additional electrode placed in the subiculum, we confirmed that ripples in CA1 and the subiculum occurred temporally coupled in our recording conditions (Chrobak and Buzsáki, 1994) (Fig. 1*B*). In the juxtacellular recording configuration, we then recorded from putative pyramidal cells (for details, see Materials and Methods) in the subiculum and correlated their activity with ripples in area CA1: we aligned the juxtacellular recording to the peak of the corresponding ripple oscillation to visualize any changes in discharge rate (Fig. 1 *D*, *E*). We found cells in which the discharge rate increased during ripples, cells in which the discharge rate decreased, and cells in which it seemed unchanged. To quantify these opposing types of spike rate modulation, we generated for each cell a surrogate dataset, consisting of the spike counts in random time windows in ripple-free periods, and compared those with the spike count observed during ripples (for details, see Materials and Methods). A right shift in the observed cumulative distribution of the spike count (Fig. 2*A*, red line, corresponds to the cell shown in Fig. 1*D*) compared with the surrogate data (gray line(s)) indicates an increase in spike count and a left shift indicates a decrease (Fig. 2*B*, blue line, corresponds to the cell shown in Fig. 1*E*). Our analysis revealed indeed two subsets of cells that were opposingly modulated: some cells elicited more spikes and some cells elicited less spikes than expected from the surrogate dataset ($n = 23$, $n = 13$, respectively). Twelve cells

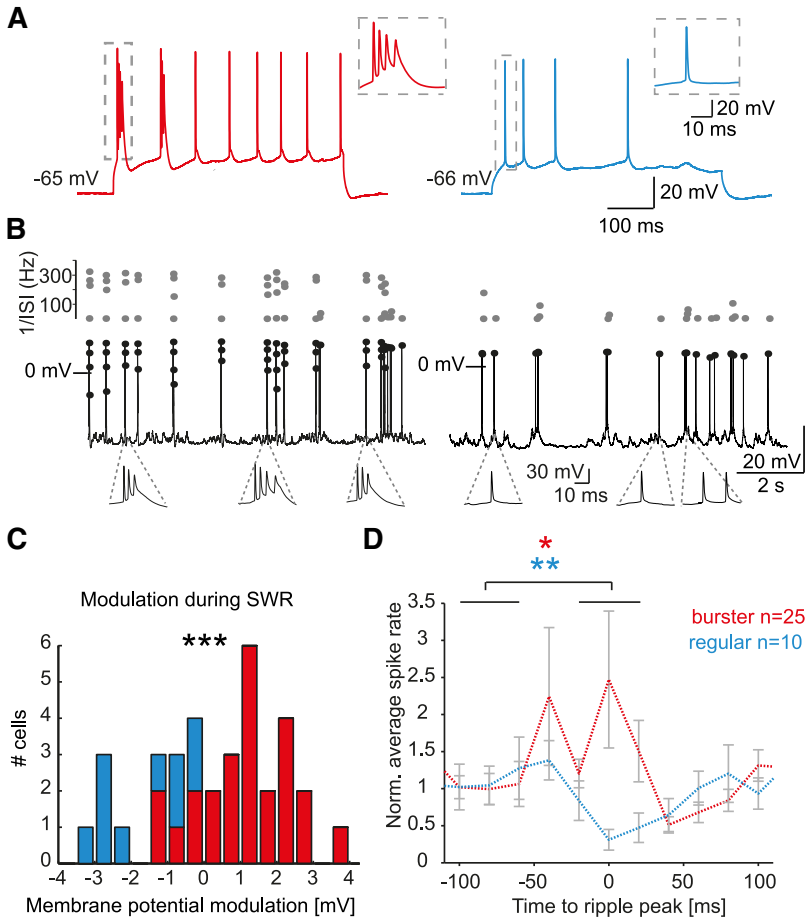

Figure 4. Subicular cell subtype predicts modulation during ripples *in vivo*. ***A***, Firing pattern in response to 500 ms step current pulse in a burst (red) and a regular firing cell (blue). ***B***, Ongoing network activity of the cells displayed in ***A***. Black dots indicate peaks of spikes. Top, 1/interspike interval (gray dots). ***C***, Distribution of membrane potential modulation in bursting (red) and regular (blue) firing cells. Cell subtype classification is solely based on the firing pattern at rheobase in response to step current pulses (for details, see Materials and Methods). The mean membrane potential modulation is significantly different from that of regular firing cells. ***$p < 0.001$ (Mann–Whitney test). ***D***, Time course of spike rate around the ripple peak. The average spike rate for each cell was normalized to its overall firing rate and the result averaged across all cells of bursting (red) or regular (blue) firing type, respectively. Time bins, 20 ms. Error bars indicate SEM across cells. Significance was assessed as paired comparison of the average (not normalized) spike rate in the indicated bins before and during the ripple for all bursting cells (red asterisk) and all regular firing cells (blue asterisks). *$p < 0.05$ (Wilcoxon signed-rank test). **$p < 0.01$ (Wilcoxon signed-rank test).

were not significantly modulated during ripples. In these cells, the spike rate observed was within the distribution of the randomly generated datasets (an example is shown in Fig. 2*C*). A summary of the spike rate modulation of all cells recorded is shown in Figure 2*D*, and a comparison of the spike rates before and during the ripple is shown in Figure 2*E*. The mean overall firing rate across all cells was 7.9 ± 0.9 Hz and was similar in cells that were activated and cells that were silenced or not modulated during ripples (7.1 ± 1.1 Hz, activated, $n = 23$; 9.8 ± 2.1 Hz, silenced, $n = 13$; 7.4 ± 0.6 Hz, not modulated, $n = 12$; mean ± SEM). The overall firing rate found here is in line with previous studies (Kim et al., 2012; Jackson et al., 2014) and is substantially higher than in other hippocampal or parahippocampal regions, such as the dentate gyrus, CA3, CA1, and entorhinal cortex (Mizuseki and Buzsáki, 2013). Furthermore, we analyzed the temporal structure of spiking as the ratio of number of spikes in bursts divided by the number of remaining spikes (burst index). The burst index, also in periods without ripples, was correlated with the spike rate modulation observed during ripples, pointing toward intrinsic differences in these cells (Fig. 2*F*; correlation coefficient $r = 0.41$, $p = 0.004$).

To further investigate the ripple-associated modulation of discharge in subicular pyramidal cells, we performed whole-cell current-clamp recordings. These recordings were done under the same conditions as the juxtacellular recordings (i.e., in awake head-fixed mice). Similar to the procedure for the juxtacellular recordings, we aligned the membrane potential to the peak of the ripple oscillation. We found a subset of cells that displayed on average a depolarization during ripples, often followed by a hyperpolarization (Fig. 3*B*,*C*, left column). In a second subset of cells, we observed a hyperpolarization during the peak of the ripple oscillation (Fig. 3*B*,*C*, right column). To assess the membrane potential modulation during ripples, we subtracted the average of the membrane potential before and after the ripple peak (−80 to −40 ms and 40 to 80 ms) for each cell from the average membrane potential during the ripple (−20 to 20 ms). The membrane potential modulation ranged from a clear depolarization to a clear hyperpolarization, whereas some cells were not clearly modulated (i.e., a membrane potential modulation close to zero, $n = 46$ cells in total; Fig. 3*D*). Those depolarizations or hyperpolarizations were accompanied by an increase or decrease of spiking, respectively (Fig. 3*C*). The membrane potential modulation did not correlate with the initial membrane potential (i.e., the membrane potential registered at opening of the cell) ($r = 0.08$, data not shown).

In addition to the possibility to monitor changes in membrane potential, whole-cell current-clamp recordings also allow for characterizing the firing pattern in response to step current pulses as routinely done in recordings *in vitro*. Subicular pyramidal cells *in vitro* exhibit either intrinsic bursting or regular spiking upon moderate depolarization (Taube, 1993). Therefore, we asked whether a similar distinction was present *in vivo*, and, if it was present, whether these distinct cell subtypes were consistent with the differential membrane potential modulation during ripples. To this end, we investigated the firing pattern in response to step current injections. Indeed, we observed differences in the responses of neurons due to 500 ms step current injections: at rheobase, we observed either one or several bursts of action potentials at the beginning of the step current pulse or we observed a more regular firing pattern consisting of single action potentials (Fig. 4*A*; in the following called bursting and regular firing cells, for details, see Materials and Methods). In line with their intrinsic discharge pattern, these cells also exhibited different firing patterns during ongoing spontaneous network activity, including

periods outside of ripples: bursting cells fired often several closely timed action potentials and only few single spikes (Fig. 4*B*); hence, the burst index was higher in bursting and lower in regular firing cells (0.98 ± 0.34, bursting cells, $n = 25$; 0.15 ± 0.04, regular firing cells, $n = 9$; one cell was excluded from this analysis as it was entirely silent, during ongoing network activity, mean ± SEM, Mann–Whitney test, $p = 0.003$). Next, we asked whether the intrinsic discharge properties in response to step current pulses correlate with the differential modulation of the membrane potential and the differential discharge modulation during ripples. Indeed, the membrane potential modulation was negative for all regular firing cells ($n = 10$) and positive for most (20 of 25) bursting cells (Fig. 4*C*; i.e., all cells displaying a depolarization were burst firing cells, membrane potential modulation in bursting vs regular firing cells: $p < 0.001$, Mann–Whitney test). The maximum depolarization of bursting cells was on average 6 ± 4 ms before the ripple peak, and the minimum membrane potential in regular firing cells was on average 10.7 ± 4.0 ms after the ripple peak. Furthermore, the average spike rate decreased around the peak of the ripple for regular firing cells and increased for burst firing cells (Fig. 4*D*). These data confirm and extend our results from the juxtacellular recordings: juxtacellularly recorded cells with a decrease in spike rate during ripples likely correspond with regular firing cells and cells with an increase in spike rate correspond with the bursting phenotype of cells. This correspondence is also in line with a positive correlation of burst index and spike rate modulation in the juxtacellular recordings (Fig. 2*F*). Additionally, using a network-independent parameter for classification by depolarizing step current injections, we found in whole-cell recordings a higher burst index for bursting cells than for regular firing cells. Together, these experiments show that the burst firing subtype correlates with increased activity, whereas the regular firing subtype with decreased activity during ripples. Hence, we conclude that bursting and regular firing cells can act as functional distinct entities during ripples.

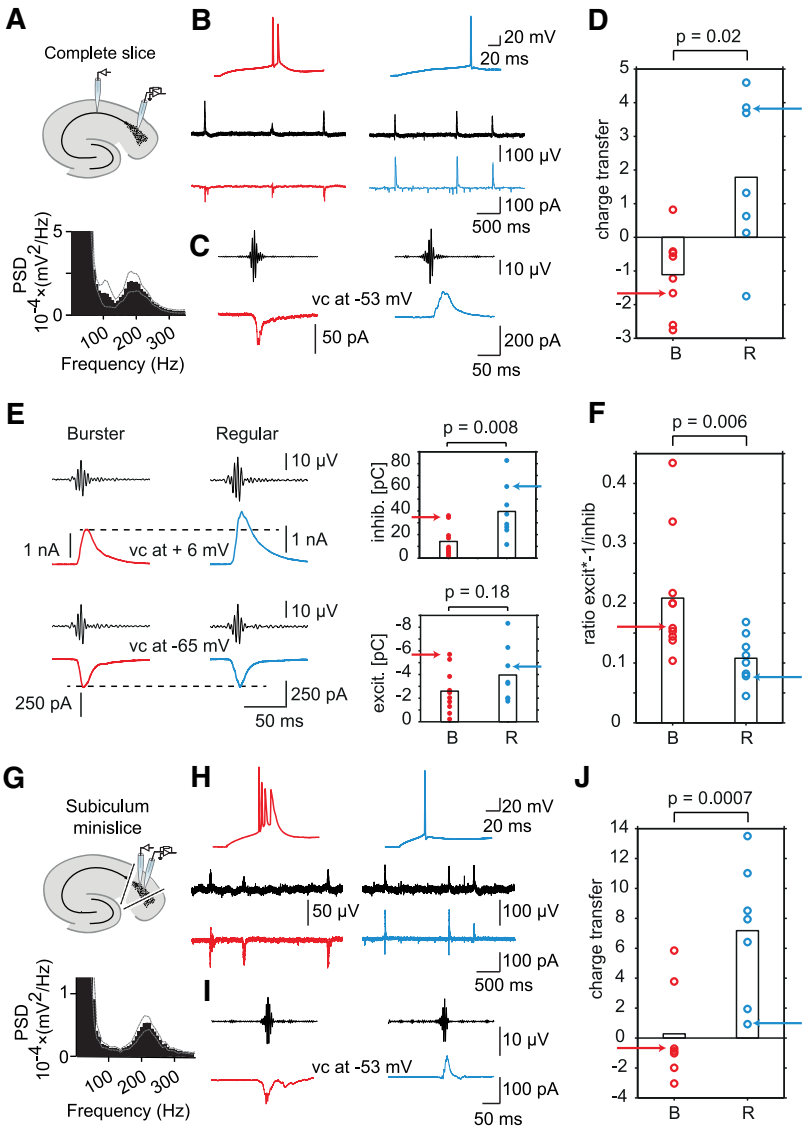

Figure 5. Bursting and regular firing cells are differentially engaged in SWRs *in vitro*. ***A***, Top, Recording configuration: LFP in CA1 and simultaneous voltage-clamp recording in subicular cells. Bottom, Average power spectral density (PSD) of the data displayed in ***B*** (left, middle). ***B***, Top, Discharge patterns of a bursting (red) and a regular spiking cell (blue). Middle, Field potential SWR recorded in CA1 with associated synaptic currents (bottom). ***C***, Averages (aligned to the ripple peak) of 20 CA1 ripples (filtered, 120–300 Hz) and their postsynaptic currents (cells as in ***B***). ***D***, Left, Mean charge transfer values for regular and bursting neurons ($n = 7$ and $n = 8$; $p = 0.02$). ***E***, Field potential SWR recorded in CA1 with associated synaptic currents recorded at 6 mV and −65 mV using cesium-based intracellular solution in a bursting (red) and a regular firing cell (blue). Right, Summary of inhibitory and excitatory charge transfer in regular and bursting cells ($n = 10$ and $n = 8$). ***F***, Ratios of averaged excitatory/inhibitory charge transfer for bursting and regular firing cells ($n = 10$ and $n = 8$; $p = 0.006$). ***G***, Recording configuration and PSD. ***H***, ***I***, Same as in ***B***, ***C***, but for subiculum minislice recordings. ***J***, Mean charge transfer values for regular and bursting neurons ($n = 7$ each; $p = 0.0007$). Arrows indicate example traces.

Mechanisms of functional diversity assessed *in vitro*

To disentangle whether the origin of this differential activation is intrinsic to the subiculum or governed by extrinsic (hippocampal or cortical) sources, we made use of an *in vitro* model of SWR in acute hippocampal slices (Hájos et al., 2009; Maier et al., 2009). We recorded the LFP SWR in area CA1 and postsynaptic currents in bursting and regular firing neurons in the subiculum (Fig. 5*A*). Regular firing cells received primarily outward currents, whereas bursting cells received net inward currents during SWR (charge transfer in regular firing cells: 1.8 ± 0.9 pC, $n = 7$, bursting cells: −1.1 ± 0.4 pC, $n = 8$, $p = 0.02$, Mann–Whitney test; Fig. 5*B–D*). To determine whether this difference in net currents arises from systematic differences of excitatory or inhibitory synaptic inputs or both, we performed voltage-clamp recordings at the reversal potentials of excitation and inhibition (−65 mV and 6 mV, for AMPA receptor- and GABAA receptor-mediated currents, re-

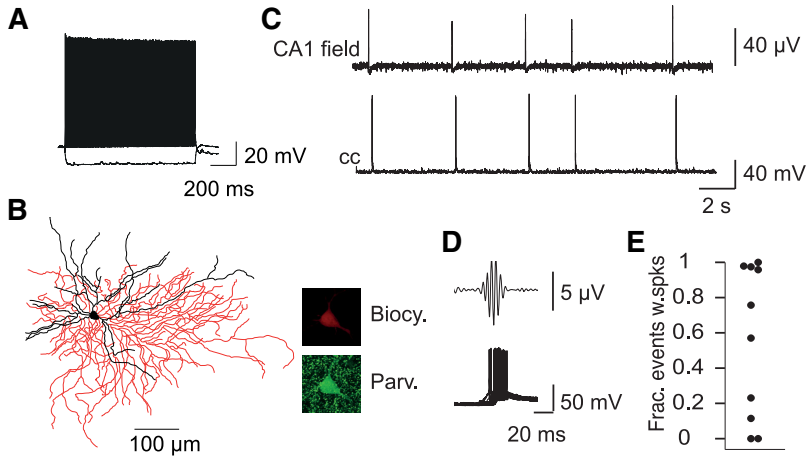

Figure 6. Fast-spiking interneurons are activated during SWR *in vitro*. ***A***, Firing pattern of a fast-spiking interneuron. ***B***, Left, Reconstruction of this cell. Black: dendrite; red: axon. Right, The cell was stained with biocytin and expressed parvalbumin. ***C***, Top, LFP recorded in CA1. Bottom, Simultaneous current-clamp recording of the cell shown in ***A*** and ***B***. ***D***, Left, Top, Averaged and aligned ripple oscillation. Bottom, Overlay of SWR-aligned current-clamp recording of this cell. ***E***, Fraction of SWR events in which spikes were emitted for all fast-spiking interneurons ($n = 10$); overlapping data points are horizontally shifted for better visualization.

spectively; Fig. 5*E*). Cells were briefly characterized by step current injection using potassium gluconate intracellular solution; hereafter, the patch pipette was gently withdrawn, and the same cell was repatched with cesium based intracellular solution to allow for improved voltage clamp and for clamping cells at positive potentials, which is a requirement to record at the reversal potential of AMPA receptors. Excitatory currents during SWR were comparable in regular (-4.0 ± 0.8 pC, $n = 8$) and burst firing cells (-2.6 ± 0.6 pC, $p = 0.18$, $n = 10$, unpaired Student's *t* test). In contrast, we found that inhibitory currents associated with SWR were significantly larger in regular compared with burst firing cells (charge transfer: 39.6 ± 8.1 pC in regular firing cells vs 14.2 ± 3.9 pC in burst firing cells, $p = 0.008$, unpaired Student's *t* test; Fig. 5*E*, right). Accordingly, the ratio between the absolute value of excitation and inhibition was also significantly different in both subgroups of cells (Fig. 5*F*; 0.11 ± 0.01 in regular firing cells vs 0.21 ± 0.03 in bursting cells, $p = 0.006$, Mann–Whitney test). Based on these findings, we conclude that the differential recruitment of bursting and regular firing cells during SWR arises mainly from a difference in the strength of synaptic inhibition onto those two subtypes. These data confirm and complement our *in vivo* results and demonstrate that, in the absence of cortical inputs, hippocampal signaling onto the subiculum is sufficient to differentially recruit subicular principal neurons. To probe whether this differential activation is inherited from the hippocampus or can be internally generated within the subiculum, we prepared minislices that only contained the subicular area (see Materials and Methods). Subicular minislice LFP recordings revealed spontaneous network oscillations in the ripple frequency range (Fig. 5*G*). Although the incidence was decreased in minislices compared with complete slices (0.43 ± 0.1 event/s in complete slices vs 0.15 ± 0.0 events/s in minislices), the oscillation frequency was largely similar (205 ± 6 Hz in complete slices vs 220 ± 7 Hz in minislices). In voltage-clamp recordings, we found that regular firing cells primarily received net inhibitory currents during SWR, whereas in bursting cells net inputs were less positive or even negative, similar to recordings in whole slice conditions (charge transfer in regular firing cells: 7.2 ± 1.7 pC, $n = 7$, bursting cells: 0.2 ± 1.2 pC, $n = 7$, $p = 0.0007$, Mann–Whitney test; Fig. 5*H–J*). Hence, the differential recruitment of subicular principal cells appears to arise from within the subicular network and is likely to be mediated by a differential SWR-associated inhibitory signaling onto burst versus regular firing cells.

Therefore, we next investigated in complete slices the recruitment of one major class of inhibitory interneurons, the parvalbumin-expressing fast-spiking interneurons, during SWR (Fig. 6*A*,*B*). Voltage-clamp recordings revealed strong excitatory input during SWR onto these cells, charge transfer: -11.03 ± 3.9 pC on average ($n = 9$). In line with this, most cells elicited spontaneous spikes during SWR (8 of 10 cells; Fig. 6*C*,*D*,*E*). The fraction of events per cell in which spikes were evoked was on average 0.56 ± 0.14 ($n = 10$). We conclude that fast-spiking interneurons are a likely source of the inhibitory currents observed in pyramidal cells during SWR and might contribute to the differential modulation of bursting and regular firing cells during SWR.

To test whether the functional differences we found during SWR *in vivo* and *in vitro* are reflected in the local network topology, we established multiple simultaneous recordings of pyramidal cells and interneurons (Fig. 7*A*). We performed up to eight parallel recordings of subicular pyramidal neurons and interneurons and tested their synaptic connection probability as well as their transmission properties. In total, we recorded 245 regular spiking pyramidal cells, 200 bursting cells, and 149 interneurons, of which 85 were fast-spiking interneurons. We elicited four action potentials at 50 Hz in the presynaptic cell, which led to EPSPs or IPSPs in the postsynaptic cell if they were connected (Fig. 7*B*,*C*). Among bursting neurons, we found a connection probability of 3.7% (15 of 408), similar to that among regular firing cells: 4.7% (28 of 592), whereas the projections from regular onto bursting cells were more numerous, 7.3% (13 of 179). In stark contrast, we found no connection in the opposite direction (0 of 181; Fig. 7*E*, left). In addition, we analyzed the amplitudes of the EPSP evoked from the first action potential in connected pairs. In some connected pairs, a clear EPSP was only discernible after more than one action potential and is therefore not included in the analysis. The amplitudes of EPSPs from the first action potential were larger in regular to burst firing cell connections (0.5 ± 0.2 mV, $n = 10$) compared with connections among burst firing cells (0.1 ± 0.0 mV, $n = 14$, $p < 0.05$, Mann–Whitney test). The amplitude among regular firing cells was 0.3 ± 0.1 mV ($n = 23$; Fig. 7*F*, left). Together, these data show that the local excitatory wiring of the subiculum is not random but is ruled by subtype-specific connection probabilities.

As a pyramidal cell subtype-specific inhibitory wiring scheme might contribute to the different modulation of burst and regular firing cells during SWR, we next investigated connection probabilities among interneurons and pyramidal cells. Indeed, we found that the inhibitory connections onto regular firing cells were more numerous than onto bursting cells (35%, 81 of 229 interneuron to bursting cells vs 46%, 95 of 208 interneuron to regular firing cells, $p = 0.03$, Fisher's exact test; Fig. 7*E*). The

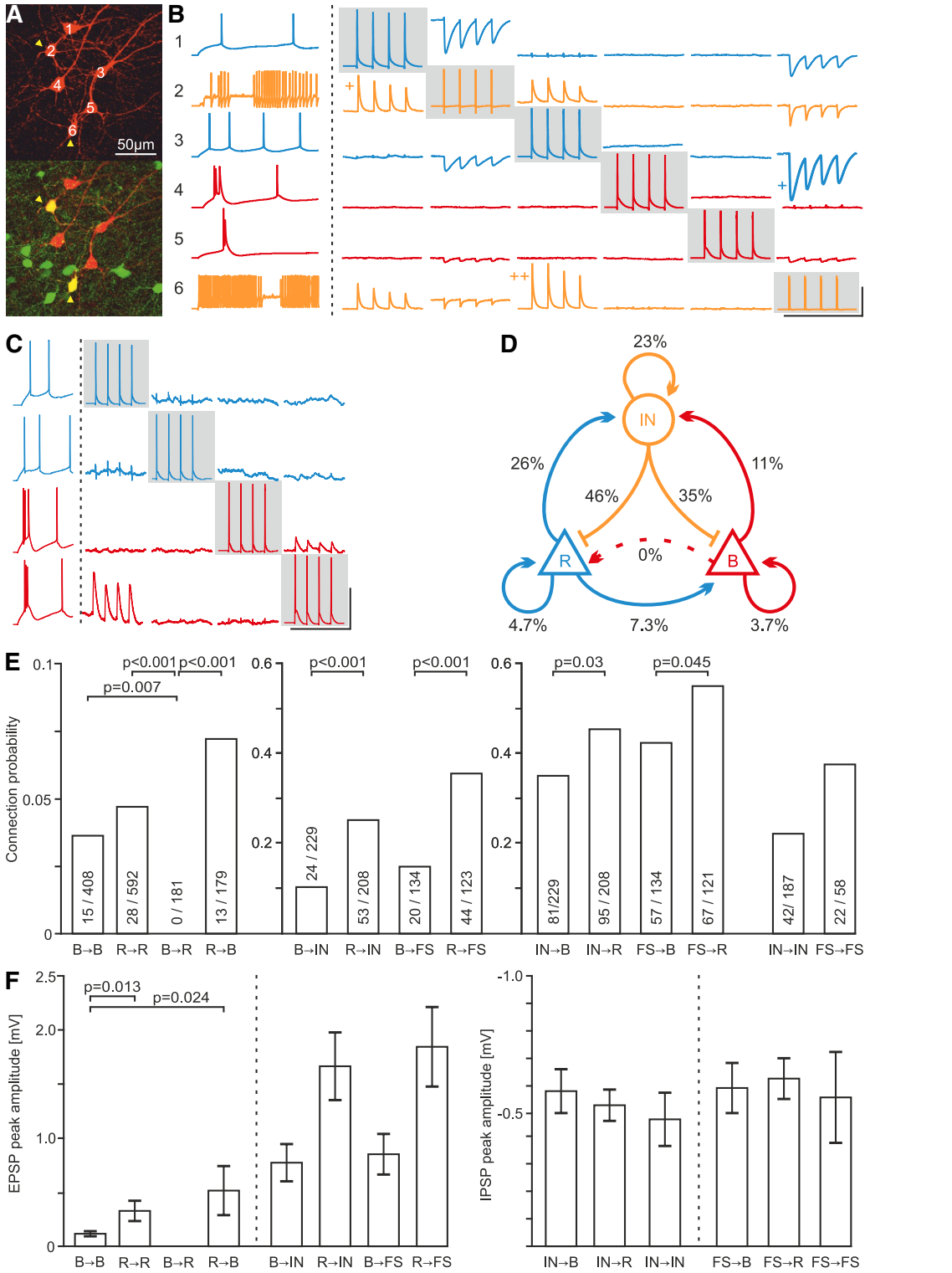

Figure 7. Subtype-specific connection probability and synaptic strength. ***A***, Biocytin staining of six cells recorded simultaneously (top). Using GAD67-eGFP transgenic mice (bottom, interneurons in green), two interneurons (bottom, orange arrowheads) and four pyramidal cells were identified. ***B***, Recorded traces in current-clamp mode. The firing pattern at rheobase is used for cell (sub)type classification (left). Blue represents regular firing pyramidal cells. Yellow represents interneurons. Red represents bursting pyramidal cells. Each neuron is consecutively stimulated with 4 action potentials (gray boxes). The postsynaptic responses are shown in the same column. Calibration: horizontal, 250 ms; vertical: 2 mV; +, 4 mV; ++, 8 mV, 50 mV for action potentials. ***C***, Example traces of excitatory connections between pyramidal cells. Left, Firing patterns. Calibration: horizontal, 250 ms, 200 ms for firing pattern; vertical, 0.5 mV, 50 mV for action potentials. Because of close positioning of the patch pipettes, stimulation artifacts are sometimes registered on other channels. ***D***, Scheme of the subtype-specific connection (*Figure legend continues.*)

amplitude of interneuron to regular firing pyramidal cell connections was −0.5 ± 0.1 mV ($n = 79$), and the amplitude of interneuron to bursting pyramidal cells was −0.6 ± 0.1 mV ($n = 77$) (Figure 7*F*, right). Furthermore, inhibitory interneurons received more connections from regular firing cells (26%, 53 of 208) than from burst firing cells (11%, 24 of 229, $p < 0.001$, Fisher's exact test; Fig. 7*E*). The postsynaptic amplitudes from regular firing and burst firing cells onto interneurons were similar (1.7 ± 0.3 mV, $n = 53$, vs 0.8 ± 0.2 mV, $n = 23$, respectively, $p = 0.081$, Mann–Whitney test; Figure 7*F*). As the inhibitory input during SWR is likely to stem from fast-spiking interneurons, we analyzed the connection probability of subicular pyramidal cells and fast-spiking interneurons separately. Indeed, we found that fast-spiking interneurons project more often onto regular firing cells (55%, 67 of 121) than onto bursting cells (43%, 57 of 134, $p = 0.045$, Fisher's exact test; Fig. 7*E*). The postsynaptic amplitudes from fast-spiking interneurons to regular firing cells was −0.6 ± 0.1 mV ($n = 55$) and to burst firing cells −0.6 ± 0.1 mV ($n = 53$) ($p = 0.117$, Mann–Whitney test; Figure 7*F*). A summary of the connection probabilities is shown in Figure 7*D*. These data suggest that the functional diversity of burst and regular firing pyramidal cells might be enabled by the subtype-specific local network topology.

Discussion

Using whole-cell patch-clamp recordings, we have shown here that bursting and regular firing cells in the subiculum are discernible *in vivo*. Further, we show that these two pyramidal cell subpopulations exhibit a functional difference: burst firing cells are activated, whereas the firing probability of regular firing cells is reduced during ripples. In line with this, we found that, in SWR-associated synaptic inputs, the ratio of excitation to inhibition is larger for bursting than for regular firing cells. Whereas it has been shown that the strength of pyramidal cell activation in CA1 can vary depending on their anatomical position within the pyramidal cell layer (Mizuseki et al., 2011), we show here that in the subiculum only a subset of cells, the bursting cells, are activated while another subset is inhibited (Eller et al., 2015). Because SWRs have been shown to be important for learning of spatial memory tasks, and only the burst firing cells are activated during SWR, it is likely that this population of cells transmits mostly spatial information, whereas regular firing cells might contribute to the transmission of nonspatial contents. Moreover, considering the different preferential extrahippocampal target areas of burst and regular firing cells (Kim and Spruston, 2012), we assume that mainly target regions of the burst firing cells receive excitatory input from the subiculum during SWR. Indeed, neuronal activity that is temporally locked to hippocampal sharp waves could be shown in both the medial entorhinal cortex (Chrobak and Buzsáki, 1994; Wu et al., 2006) and the presubiculum (Chrobak and Buzsáki, 1994), which are target areas of burst firing cells (Kim and Spruston, 2012). It is tempting to speculate that there is no or less SWR-associated input to the lateral entorhinal cortex, a target area mostly innervated by regular firing cells. This would imply a pivotal role of the subiculum in separating information streams and distributing this information to cortical targets. Furthermore, recent studies demonstrated that the canonical flow of information from CA3 via CA1 to the subiculum can be reversed during theta oscillations in intact hippocampal preparations as well as *in vivo* (Jackson et al., 2014) and that the subiculum might receive input from entorhinal cortex during SWR (Norimoto et al., 2013). Together with anatomical data, the influence of the subiculum on "upstream" target regions is likely to be stronger than previously anticipated (Sun et al., 2014).

Our analysis of the neuronal network topology revealed that the subtype-specific functional differences observed during SWR are also reflected in the local network wiring: the subiculum exhibits an excitatory network with unidirectional connectivity between regular and bursting cells. A local network topology that is determined by long-range projection targets has been described recently in the cortex. Principal cells that either project to the same target region or to different target regions can be preferentially connected (Morishima and Kawaguchi, 2006; Brown and Hestrin, 2009; Morishima et al., 2011). Here, we find that principal cells that project to the same target regions are connected among themselves; in addition, there is exclusive unidirectional connectivity from one group of principal cells, regular firing cells, to the other, burst firing cells, but not vice versa. This shows that functional specialization and long-range targets are closely linked to local network topology.

Our findings from the minislice experiments suggest that the local network of the subiculum is able to generate the subtype-specific modulation by itself. Furthermore, we show here that burst firing cells are preferentially activated and that there is a high connection probability between regular and bursting cells. However, it seems unlikely that the strong unidirectional regular to burst firing connection can explain the preferential activation during ripples because we do not have evidence for activation of regular firing cells during ripples. Nevertheless, we cannot exclude the possibility that a fraction of regular firing cells is activated and might aid the initiation of ripple events. Our data suggest that regular firing cells receive stronger inhibitory inputs during SWR than burst firing pyramidal cells. By multiple patch-clamp recordings, we could further show that the local subicular network favors inhibition onto regular firing cells. These findings are in contrast to the previously described homogeneous inhibitory innervation found in neocortex (Packer and Yuste, 2011) but in line with the subtype-specific innervation described for entorhinal cortex (Varga et al., 2010), CA1 (Lee et al., 2014), and the striatum (Gittis et al., 2010). For the subiculum, this subtype specificity of inhibitory connections is likely to endow functional preference of burst and regular firing cells during ripples.

←

(*Figure legend continued.*) probabilities in the subiculum. ***E***, Connection probability between the different subtypes determined as the number of connected pairs divided by the number of tested connections. No connections were found projecting from bursting to regular firing pyramidal cells. B, Burst firing cell; R, regular firing cell; IN, interneurons; FS, fast-spiking interneurons. Statistical test: Fisher's exact test. ***F***, Mean of postsynaptic potential amplitudes. Error bars indicate SEM. Statistical test: Mann–Whitney test.

References

Amaral DG, Dolorfo C, Alvarez-Royo P (1991) Organization of CA1 projections to the subiculum: a PHA-L analysis in the rat. Hippocampus 1:415–435. CrossRef Medline

Behr J, Wozny C, Fidzinski P, Schmitz D (2009) Synaptic plasticity in the subiculum. Prog Neurobiol 89:334–342. CrossRef Medline

Brown SP, Hestrin S (2009) Intracortical circuits of pyramidal neurons reflect their long-range axonal targets. Nature 457:1133–1136. CrossRef Medline

Buzsáki G (1986) Hippocampal sharp waves: their origin and significance. Brain Res 398:242–252. CrossRef Medline

Chrobak JJ, Buzsáki G (1994) Selective activation of deep layer (v-vi) retrohippocampal cortical neurons during hippocampal sharp waves in the behaving rat. J Neurosci 14:6160–6170. Medline

Chrobak JJ, Buzsáki G (1996) High-frequency oscillations in the output net-

works of the hippocampal-entorhinal axis of the freely behaving rat. J Neurosci 16:3056–3066. Medline

Crochet S, Petersen CC (2006) Correlating whisker behavior with membrane potential in barrel cortex of awake mice. Nat Neurosci 9:608–610. CrossRef Medline

Davidson TJ, Kloosterman F, Wilson MA (2009) Hippocampal replay of extended experience. Neuron 63:497–507. CrossRef Medline

Ego-Stengel V, Wilson MA (2010) Disruption of ripple-associated hippocampal activity during rest impairs spatial learning in the rat. Hippocampus 20:1–10. CrossRef Medline

Eller J, Zarnadze S, Bäuerle P, Dugladze T, Gloveli T (2015) Cell type-specific separation of subicular principal neurons during network activities. PLoS One 10:e0123636. CrossRef Medline

Girardeau G, Benchenane K, Wiener SI, Buzsáki G, Zugaro MB (2009) Selective suppression of hippocampal ripples impairs spatial memory. Nat Neurosci 12:1222–1223. CrossRef Medline

Gittis AH, Nelson AB, Thwin MT, Palop JJ, Kreitzer AC (2010) Distinct roles of GABAergic interneurons in the regulation of striatal output pathways. J Neurosci 30:2223–2234. CrossRef Medline

Graves AR, Moore SJ, Bloss EB, Mensh BD, Kath WL, Spruston N (2012) Hippocampal pyramidal neurons comprise two distinct cell types that are countermodulated by metabotropic receptors. Neuron 76:776–789. CrossRef Medline

Hájos N, Ellender TJ, Zemankovics R, Mann EO, Exley R, Cragg SJ, Freund TF, Paulsen O (2009) Maintaining network activity in submerged hippocampal slices: importance of oxygen supply. Eur J Neurosci 29:319–327. CrossRef Medline

Inostroza M, Born J (2013) Sleep for preserving and transforming episodic memory. Annu Rev Neurosci 36:79–102. CrossRef Medline

Jackson J, Amilhon B, Goutagny R, Bott JB, Manseau F, Kortleven C, Bressler SL, Williams S (2014) Reversal of theta rhythm flow through intact hippocampal circuits. Nat Neurosci 17:1362–1370. CrossRef Medline

Jadhav SP, Kemere C, German PW, Frank LM (2012) Awake hippocampal sharp-wave ripples support spatial memory. Science 336:1454–1458. CrossRef Medline

Ji D, Wilson MA (2007) Coordinated memory replay in the visual cortex and hippocampus during sleep. Nat Neurosci 10:100–107. CrossRef Medline

Karlsson MP, Frank LM (2009) Awake replay of remote experiences in the hippocampus. Nat Neurosci 12:913–918. CrossRef Medline

Katona L, Lapray D, Viney TJ, Oulhaj A, Borhegyi Z, Micklem BR, Klausberger T, Somogyi P (2014) Sleep and movement differentiates actions of two types of somatostatin-expressing gabaergic interneuron in rat hippocampus. Neuron 82:872–886. CrossRef Medline

Kim SM, Ganguli S, Frank LM (2012) Spatial information outflow from the hippocampal circuit: distributed spatial coding and phase precession in the subiculum. J Neurosci 32:11539–11558. CrossRef Medline

Kim Y, Spruston N (2012) Target-specific output patterns are predicted by the distribution of regular-spiking and bursting pyramidal neurons in the subiculum. Hippocampus 22:693–706. CrossRef Medline

Lee AK, Wilson MA (2002) Memory of sequential experience in the hippocampus during slow wave sleep. Neuron 36:1183–1194. CrossRef Medline

Lee SH, Marchionni I, Bezaire M, Varga C, Danielson N, Lovett-Barron M, Losonczy A, Soltesz I (2014) Parvalbumin-positive basket cells differentiate among hippocampal pyramidal cells. Neuron 82:1129–1144. CrossRef Medline

Logothetis NK, Eschenko O, Murayama Y, Augath M, Steudel T, Evrard HC, Besserve M, Oeltermann A (2012) Hippocampal-cortical interaction during periods of subcortical silence. Nature 491:547–553. CrossRef Medline

Longair MH, Baker DA, Armstrong JD (2011) Simple neurite tracer: open source software for reconstruction, visualization and analysis of neuronal processes. Bioinformatics 27:2453–2454. CrossRef Medline

Maier N, Morris G, Johenning FW, Schmitz D (2009) An approach for reliably investigating hippocampal sharp wave-ripples in vitro. PLoS One 4:e6925. CrossRef Medline

Maier N, Tejero-Cantero A, Dorrn AL, Winterer J, Beed PS, Morris G, Kempter R, Poulet JF, Leibold C, Schmitz D (2011) Coherent phasic excitation during hippocampal ripples. Neuron 72:137–152. CrossRef Medline

Markram H, Lübke J, Frotscher M, Sakmann B (1997) Regulation of synaptic efficacy by coincidence of postsynaptic APs and EPSPs. Science 275:213–215. CrossRef Medline

Marshall L, Helgadóttir H, Mölle M, Born J (2006) Boosting slow oscillations during sleep potentiates memory. Nature 444:610–613. CrossRef Medline

Mehta MR (2007) Cortico-hippocampal interaction during up-down states and memory consolidation. Nat Neurosci 10:13–15. CrossRef Medline

Mizuseki K, Buzsáki G (2013) Preconfigured, skewed distribution of firing rates in the hippocampus and entorhinal cortex. Cell Rep 4:1010–1021. CrossRef Medline

Mizuseki K, Diba K, Pastalkova E, Buzsáki G (2011) Hippocampal ca1 pyramidal cells form functionally distinct sublayers. Nat Neurosci 14:1174–1181. CrossRef Medline

Morishima M, Kawaguchi Y (2006) Recurrent connection patterns of corticostriatal pyramidal cells in frontal cortex. J Neurosci 26:4394–4405. CrossRef Medline

Morishima M, Morita K, Kubota Y, Kawaguchi Y (2011) Highly differentiated projection-specific cortical subnetworks. J Neurosci 31:10380–10391. CrossRef Medline

Naber PA, Witter MP (1998) Subicular efferents are organized mostly as parallel projections: a double-labeling, retrograde-tracing study in the rat. J Comp Neurol 393:284–297. CrossRef Medline

Naber PA, Witter MP, Silva FHL (2000) Networks of the hippocampal memory system of the rat: the pivotal role of the subiculum. Ann N Y Acad Sci 911:392–403. CrossRef Medline

Norimoto H, Matsumoto N, Miyawaki T, Matsuki N, Ikegaya Y (2013) Subicular activation preceding hippocampal ripples in vitro. Sci Rep 3:2696. CrossRef Medline

O'Keefe J, Nadel L (1978) The hippocampus as a cognitive map. Oxford: Oxford UP.

Packer AM, Yuste R (2011) Dense, unspecific connectivity of neocortical parvalbumin-positive interneurons: a canonical microcircuit for inhibition? J Neurosci 31:13260–13271. CrossRef Medline

Paxinos G, Franklin K (2012) The mouse brain in stereotactic coordinates, Ed 4. San Diego: Academic.

Sun Y, Nguyen AQ, Nguyen JP, Le L, Saur D, Choi J, Callaway EM, Xu X (2014) Cell-type-specific circuit connectivity of hippocampal CA1 revealed through Cre-dependent rabies tracing. Cell Rep 7:269–280. CrossRef Medline

Taube JS (1993) Electrophysiological properties of neurons in the rat subiculum in vitro. Exp Brain Res 96:304–318. Medline

Varga C, Lee SY, Soltesz I (2010) Target-selective gabaergic control of entorhinal cortex output. Nat Neurosci 13:822–824. CrossRef Medline

Wilhelm I, Rose M, Imhof KI, Rasch B, Büchel C, Born J (2013) The sleeping child outplays the adult's capacity to convert implicit into explicit knowledge. Nat Neurosci 16:391–393. CrossRef Medline

Witter MP (2006) Connections of the subiculum of the rat: topography in relation to columnar and laminar organization. Behav Brain Res 174:251–264. CrossRef Medline

Witter MP, Ostendorf RH, Groenewegen HJ (1990) Heterogeneity in the dorsal subiculum of the rat: distinct neuronal zones project to different cortical and subcortical targets. Eur J Neurosci 2:718–725. CrossRef Medline

Wu CP, Huang HL, Asl MN, He JW, Gillis J, Skinner FK, Zhang L (2006) Spontaneous rhythmic field potentials of isolated mouse hippocampal-subicular-entorhinal cortices in vitro. J Physiol 576:457–476. CrossRef Medline

Chapter 3

Serotonin attenuates feedback excitation onto O-LM interneurons

3.1 Motivation and research goals

The raphe nuclei send serotonergic projections to numerous target regions, and serotonin is thereby capable of influencing synaptic transmission all over the brain. The hippocampus is implicated in many important brain functions such as memory formation and consolidation. Hippocampal function is dependent both on internal processing and on interaction with cortical structures providing input to the hippocampus, such as the entorhinal cortex. O-LM interneurons of the CA1 region are involved in controlling intrahippocampal input onto CA1 pyramidal cells as well as external input from the entorhinal cortex. To gain insights into the rules governing internal and external input onto CA1 pyramidal cells it is therefore important to investigate what sources modulate O-LM interneuron activity. Serotonin has been shown to modulate pyramidal cells and other types of interneurons, but as yet it was unknown if and how serotonin influences O-LM interneuron activity. The goal of this study was therefore to illuminate the role of serotonin in the modulation of glutamatergic transmission onto this cell type. I used patch-clamp recordings in acute hippocampal slices as well as calcium imaging to investigate these questions.

3.2 Statement of contribution

I have contributed in part to the design and concept of this study. The data for Figure 1, 2 (A,B), 4 (A,B), 6 and 7 were fully acquired and analyzed by myself. The data for Figure 5 and 2C were acquired by Maria Pangalos, Jochen Winterer and myself and analyzed by myself. Maria Pangalos and myself acquired the data for Figure 2D together and I have analyzed them. Jochen Winterer performed the paired recordings displayed in Figure 3

and Figure 4C. The manuscript was written by Jochen Winterer and myself and all other authors commented on the manuscript.

3.3 Original research article

Claudia Böhm, Maria Pangalos, Jochen Winterer and Dietmar Schmitz. Serotonin Attenuates Feedback Excitation onto O-LM Interneurons. *Cerebral Cortex*, 25(11):4572–4583, Nov 2015

Cerebral Cortex, November 2015;25: 4572–4583

doi: 10.1093/cercor/bhv098
Advance Access Publication Date: 28 May 2015
Original Article

ORIGINAL ARTICLE

Serotonin Attenuates Feedback Excitation onto O-LM Interneurons

Claudia Böhm[1], Maria Pangalos[1], Dietmar Schmitz[1,2,3,4,5,†], and Jochen Winterer[1,†]

[1]Neuroscience Research Center, Charité – Universitätsmedizin Berlin, 10117 Berlin, Germany, [2]Bernstein Center for Computational Neuroscience Berlin, Humboldt-Universität zu Berlin, 10115 Berlin, Germany, [3]Cluster of Excellence "NeuroCure", Charité – Universitätsmedizin Berlin, 10117 Berlin, Germany, [4]Einstein Foundation Berlin, 10117 Berlin, Germany, and [5]Deutsches Zentrum für Neurodegenerative Erkrankungen (DZNE), c/o Charité – Universitätsmedizin Berlin, Neuroscience Research Center, 10117 Berlin, Germany

Address correspondence to Dietmar Schmitz, Neuroscience Research Center, CharitéCrossOver, Charité – Universitätsmedizin Berlin, Charitéplatz 1, 10117 Berlin, Germany. Email: dietmar.schmitz@charite.de; Jochen Winterer, Neuroscience Research Center, CharitéCrossOver, Charité – Universitätsmedizin Berlin, Charitéplatz 1, 10117 Berlin, Germany. Email: jochen.winterer@charite.de

[†]These authors contributed equally to this work.

Abstract

The serotonergic system is a subcortical neuromodulatory center that controls cortical information processing in a state-dependent manner. In the hippocampus, serotonin (5-HT) is released by ascending serotonergic fibers from the midbrain raphe nuclei, thereby mediating numerous modulatory functions on various neuronal subtypes. Here, we focus on the neuromodulatory effects of 5-HT on GABAergic inhibitory oriens lacunosum-moleculare (O-LM) cells in the hippocampal area CA1 of the rat. These interneurons are thought to receive primarily local excitatory input and are, via their axonal projections to stratum lacunosum-moleculare, ideally suited to control entorhinal cortex input. We show that 5-HT reduces excitatory glutamatergic transmission onto O-LM interneurons. By means of paired recordings from synaptically connected CA1 pyramidal cells and O-LM interneurons we reveal that this synapse is modulated by 5-HT. Furthermore, we demonstrate that the reduction of glutamatergic transmission by serotonin is likely to be mediated via a decrease of calcium influx into presynaptic terminals of CA1 pyramidal cells. This modulation of excitatory synaptic transmission onto O-LM interneurons by 5-HT might be a mechanism to vary the activation of O-LM interneurons during ongoing network activity and serve as a brain state-dependent switch gating the efficiency of entorhinal cortex input to CA1 pyramidal neurons.

Key words: 5-HT, CA1, paired recordings, presynaptic neuromodulation

Introduction

The hippocampus receives a dense serotonergic innervation originating from the midbrain raphe nuclei, both from the Median raphe nucleus and to a lesser extend from the Dorsal raphe nucleus (Freund et al. 1990; Vertes 1991, 1999). Earlier studies on the cellular neurophysiology of serotonergic signaling predominantly focused on the neuromodulation of intrinsic cellular properties and the neuromodulation of synaptic transmission on hippocampal pyramidal neurons. In these studies, multiple

important effects of 5-HT have been identified, mediated by a number of distinct pre- and/or postsynaptic receptors (Segal 1980; Andrade and Nicoll 1987; Barnes and Sharp 1999). In contrast, relatively few studies investigated the neuromodulatory effects of 5-HT on GABAergic inhibitory interneurons in the hippocampus (Varga et al. 2009; Winterer et al. 2011; Chittajallu et al. 2013). Complicated by the high diversity of interneurons it has not yet been possible to establish a clear picture of how serotonin acts on these neuronal subtypes (Parra et al. 1998).

GABAergic interneurons are recognized as key players in the synchronization of neuronal activity on various timescales and in the generation of oscillatory patterns in the brain. These different types of interneurons exhibit morphological, immunohistochemical, and electrophysiological characteristics and are differentially involved in oscillations at different frequencies (Maccaferri and Lacaille 2003; Maccaferri 2005; Somogyi and Klausberger 2005). One of the major classes of GABAergic interneurons in the stratum oriens of the CA1 subfield of the hippocampus are oriens lacunosum-moleculare (O-LM) interneurons. These interneurons fire correlated with hippocampal rhythms (Klausberger et al. 2003; Goldin et al. 2007; Varga et al. 2012; Pangalos et al. 2013; Katona et al. 2014) and have been hypothesized to coordinate cell assemblies (Tort et al. 2007). O-LM cells can be considered as classical feedback inhibitory neurons due to their predominantly local excitatory input from CA1 pyramidal cells. Their axonal projections impinge on distal apical dendrites of CA1 pyramidal cells as well as on local inhibitory interneurons targeting the proximal portions of CA1 pyramidal dendrites. In this respect O-LM interneurons are ideally suited to gate the activity in area CA1, where they are able to facilitate the input from the Schaffer collaterals via an indirect disinhibition of the proximal dendritic compartments while reducing the input of the temporoammonic (TA) pathway by inhibiting the distal apical dendrites of CA1 pyramidal neurons (Leão et al. 2012).

Here, we show that 5-HT reduces excitatory glutamatergic inputs onto O-LM interneurons and lowers their spike probability in area CA1 of the hippocampus. We identify one source of excitatory input that is modulated by 5-HT by paired recordings of synaptically connected CA1 pyramidal neurons and O-LM interneurons. Furthermore, our results indicate that this modulation is mediated by a decrease of calcium influx into presynaptic terminals of CA1 pyramidal cells.

Material and Methods

Ethics Statement

Animal husbandry and experimental intervention was performed according to the European Council Directive 2010/63/EU regarding the protection of animals used for experimental and other scientific purposes. All animal maintenance and experiments were performed in accordance with the guidelines of local authorities, Berlin (T0100/03).

Preparation

Hippocampal slices were prepared from Wistar rats (P16-24, both sexes) as previously described (Schmitz et al. 2003). In brief, the animals were anesthetized with isoflurane, decapitated and the brains were removed. Tissue blocks containing the subicular area and hippocampus were mounted on a Vibratome (Leica VT1200 S) in a chamber filled with ice-cold artificial cerebrospinal fluid, ACSF, containing (in mM): NaCl, 87; sucrose, 75; $NaHCO_3$, 26; KCl, 2.5; NaH_2PO4, 1.25; $CaCl_2$, 0.5; $MgCl_2$, 7; glucose, 25, saturated with 95% O_2, 5% CO_2, pH 7.4. Transverse slices were cut at 300 μm thickness. The slices were taken from ventral to medial hippocampus. They were kept at 35°C for 30 min and then stored in a submerged chamber, where they were kept for 1–4 h before being transferred to the recording chamber. Another subset of slices was transferred directly after cutting to an interface chamber where they were stored at ~32°C before being transferred to the recording chamber. The effect of serotonin was robust in both storage conditions.

In the recording chamber, slices were perfused with ACSF containing (in mM): NaCl, 119; $NaHCO_3$, 26; glucose, 10; KCl 2.5, $CaCl_2$, 2.5; $MgCl_2$ 1.3; NaH_2PO_4, 1 at a rate of 4–5 mL/min at 31–34°C. All ACSF was equilibrated with 95% O_2 and 5% CO_2.

Electrophysiology

Whole-cell recording electrodes were filled with (in mM): K-gluconate 120–135, HEPES 10, Mg-ATP 2, KCl 20, EGTA 0.5, Phosphocreatine 5 adjusted to 7.3 with KOH. For paired recordings, the electrode for the presynaptic CA1 pyramidal neuron was filled with (in mM): K-gluconate 105, HEPES 10, Na_2-ATP 2, Na_2-GTP 0.3, Mg-ATP 2, KCl 40, $MgCl_2$ 2, EGTA 0.1, Na_2-phosphocreatine 1, L-glutamate 0.1, adjusted to 7.3 with KOH. For staining and reconstruction of the recorded neurons, ~0.25% biocytin was added to the intracellular solution. Depolarizing current steps of 1 s duration were applied to characterize the cells' discharge behavior.

Excitatory postsynaptic responses were evoked by electrical stimulation (100 μs at intervals of 50 ms) in *stratum oriens* of area CA1 via a broken patch-pipette (~8 μm) filled with ACSF. Experiments were done in the presence of the GABA-A receptor antagonist gabazine (1 μM) and NBQX (100 nM) to prevent epileptiform activity and to minimize polysynaptic activity except where pairs or extracellular evoked spikes (Fig. 2*D*) were recorded. mEPSCs were recorded in the presence of tetrodotoxin (TTX) (1 μM) and gabazine (1 μM).

Peaks of extracellularly evoked spikes exhibited a delay of ~4–8 ms to the stimulus. The interstimulus interval was set to 125 ms. In this set of experiments, the membrane potential of O-LM interneurons was kept constant at −60 mV.

Access resistances ranged between 9 and 31 MΩ (on average 14.2 ± 0.8 MΩ) for O-LM interneurons. They were continuously monitored during the recording and were not allowed to vary >30% during the course of the experiment. In current-clamp configuration, bridge balance compensation was used. In some experiments in voltage-clamp configuration slight changes in series resistance were compensated. Electrode resistances ranged from 3 to 5 MΩ.

Morphology of O-LM Interneurons and CA1 Pyramidal Neurons

After recording, slices were transferred into a fixative solution containing 4% paraformaldehyde and 0.2% saturated picric acid in 0.1 M phosphate buffer. To reveal the presynaptic axonal arborization and dendritic arbors in detail, the biocytin-filled cells were subsequently visualized with 3,3′-diaminobenzidine tetrahydrochloride (0.015%) using standard ABC kit (Vector) and reconstructed with the Neurolucida 3D reconstruction system (MicroBrightField, Inc., Williston, VT, USA).

Glutamate Uncaging

20 mL of 50 or 200 μM (MNI)-caged-L-glutamate (Tocris, Bristol, UK) were reperfused at 2.5–3.0 mL/min. For uncaging, we used a UV pulsed laser (Rapp Optoelektronik, Wedel, Germany) attached

with a 200 μm optical fiber coupled into the epifluorescence port of the microscope with an OSI-BX adapter (Rapp Optoelektronik, Wedel, Germany) and focused on the specimen by the objective lens. This yielded an illuminated circle of 20–50 μm. The duration of the laser flash was 2 ms. The laser power under the objective corresponding to the stimulus intensity level used was monitored using a photo diode array-based photodetector (PDA-K-60, Rapp Optoelectronics, Wedel, Germany) and did not change over time.

Glutamate was uncaged over the cell soma in the presence of the GABA-A receptor antagonist gabazine (1 μM) and NBQX (100 nM, to prevent epileptiform activity).

Fluorescence Measurements

The axonal fibers in CA1 *stratum oriens* were locally labeled with a pressure stream of the low-affinity calcium indicator magnesium green AM (Invitrogen, Molecular Probes) dissolved in 5% Pluronic for photodiode measurements (Breustedt et al. 2003). The indicator was injected into area CA1 stratum oriens, the filling pipette pointing toward the alveus (Fig. 6A). Recordings were started 40–90 min after slices were labeled. Axons were stimulated extracellularly (Fig. 6A) and epifluorescence was measured with a single photodiode from a spot a few hundred micrometers away from the loading site. The signals from the photodiode were digitized by data acquisition hardware (PCI-6036E National Instruments, Austin, TX) at 5 kHz. The fluorescence intensity was measured alternating every 30 s with and without stimulus and the change in fluorescence intensity (ΔF) relative to the initial baseline of fluorescence (F) was calculated. To exclude any postsynaptic contribution to the signal all recordings were performed in NBQX (20 μM) and D-AP5 (50 μM).

Data Analysis

Data were acquired and analyzed with Igor Pro software (WaveMetrics, Lake Oswego, OR), NeuroMatic and custom written MATLAB scripts (The MathWorks, Natick, MA).

Values in the text and the figures are expressed as mean ± standard error of the mean (SEM) unless indicated otherwise (as median and interquartile range, IQR). The nonparametric Wilcoxon rank test was used for statistical comparisons in sets of experimental data where normality could not be assumed. To compare the numbers of successfully evoked spikes in control versus fenfluramine, McNemar's test was used (Fig. 2D). For normal distributed sets of data a paired or unpaired Student's T-test was used. Differences were considered statistically significant if $P < 0.05$. All traces are averages of 5–10 sweeps unless otherwise stated. For display purposes some traces were low-pass filtered (<2 kHz) and a 50 Hz notch filter to remove line hum was applied if necessary. In paired recordings (Fig. 4C) successful synaptic transmission was counted as such if the postsynaptic amplitude was larger than 1.5 standard deviations of the baseline (in the absence of spontaneous events).

Drugs

5-Hydroxytryptamine creatine sulfate complex (5-HT), (RS)-N-ethyl-1-[3-(trifluormethyl)phenyl]propan-2-amin(fenfluramine) (both from Sigma), 2,3-dihydroxy-6-nitro-7-sulfamoyl-benzo[*f*] quinoxaline-2,3-dione (NBQX), 4-[6-imino-3-(4-methoxyphenyl) pyridazin-1-yl] butanoic acid hydrobromide (SR95531, gabazine), D-(–)-2-amino-5-phosphonopentanoic acid (D-AP5), 4-Methoxy-7-nitroindolinyl-caged-L-glutamate (MNI-caged-L-glutamate), (4*R*,4a*R*,5*R*,6*S*,7*S*,8*S*,8a*R*,10*S*,12*S*)-2-azaniumylidene-4,6,8,12-tetrahydroxy-6-(hydroxymethyl)-2,3,4,4a,5,6,7,8-octahydro-1*H*-8a,10-methano-5,7-(epoxymethanooxy) quinazolin-10-olate (TTX), 5-propoxy-3-(1,2,3,6-tetrahydro-4-pyridinyl)-1H-pyrrolo[3,2-b] pyridine hydrochloride (CP 94253 hydrochloride), (±)-8-hydroxy-2-dipropylaminotetralin hydrobromide (8-OH-DPAT hydrobromide), (5′α,10α)-9,10-dihydro-12′-hydroxy-2′-(1-methylethyl)-5′-(phenylmethyl)-ergotaman-3′,6′,18-trione mesylate (dihydroergocristine mesylate), (*R*)-(+)-7-chloro-8-hydroxy-3-methyl-1-phenyl-2,3,4,5-tetrahydro-1*H*-3-benzazepine hydrochloride (SCH23390 hydrochloride) (all from Tocris), Magnesium green AM (Invitrogen, Molecular Probes).

Results

O-LM interneurons were identified by their location in *stratum oriens*, the characteristic elongated shape of their somata and the horizontally oriented dendrites as well as their electrophysiological properties: the typical firing pattern in response to depolarizing current pulses and the prominent sag potential in response to hyperpolarizing current pulses (Fig. 1A, right, top). O-LM interneurons displayed a strong facilitation in response to consecutive synaptic stimuli (Fig. 1A, right bottom), as described previously (Ali and Thomson 1998; Losonczy et al. 2002; Biró et al. 2005). A subset of the recorded cells, identified by the above described criteria, were further validated by biocytin stainings in which we could identify the vertically projecting axons with an extensive arborization in stratum lacunosum-moleculare (Fig. 1A, left).

5-HT Reduces Glutamatergic Transmission on O-LM Interneurons

To study the excitatory synaptic transmission onto O-LM interneurons, cells were held in voltage-clamp mode at −60 mV. First, we examined the effect of 5-HT on the frequency of spontaneous excitatory postsynaptic currents (sEPSCs). The frequency decreased from 4.1 ± 0.6 Hz to 2.3 ± 0.3 Hz during application of 5-HT. This effect was fully reversible during washout: 5.8 ± 0.6 Hz ($n = 8$; control vs. 5-HT: $P = 0.0032$; 5-HT vs. wash: $P = 0.0003$, Student's T-test; Fig. 1B,C, left). The amplitude of sEPSCs did not change significantly (baseline: 21.4 ± 3.1 pA vs. 19.2 ± 1.6 pA during application of 5-HT, $P = 0.39$, paired Student's T-test, $n = 8$; recovery: 23.7 ± 3.0 pA, Fig. 1B,C, right).

Next, we examined the effect of 5-HT on stimulus-induced glutamatergic transmission in O-LM interneurons which was evoked by a stimulating electrode positioned at the border of the *alveus* and *stratum oriens* (Fig. 2A). 5-HT profoundly and reversibly reduced the amplitude of evoked excitatory postsynaptic currents (eEPSCs) by 50.86% (median, IQR: 28.16%, $n = 12$; Fig. 2B1,B2; baseline amplitude is significantly different from amplitude during application of 5-HT, $P = 0.0005$, paired sample Wilcoxon rank test). Upon application of 5-HT, we further observed a change in the holding current of the recorded cells: O-LM interneurons displayed a mean inward current of −61.6 ± 13.0 pA ($n = 13$; data not shown) indicative of a postsynaptic expression of 5-HT receptors in O-LM interneurons (Lee et al. 1999; Chittajallu et al. 2013).

Fenfluramine Mimics the Effect of 5-HT on Glutamatergic Transmission

To address the question whether physiological release of 5-HT from serotonergic fibers in the hippocampus induces similar effects, we used the compound fenfluramine, which is thought to provoke the release of serotonin: fenfluramine disrupts the

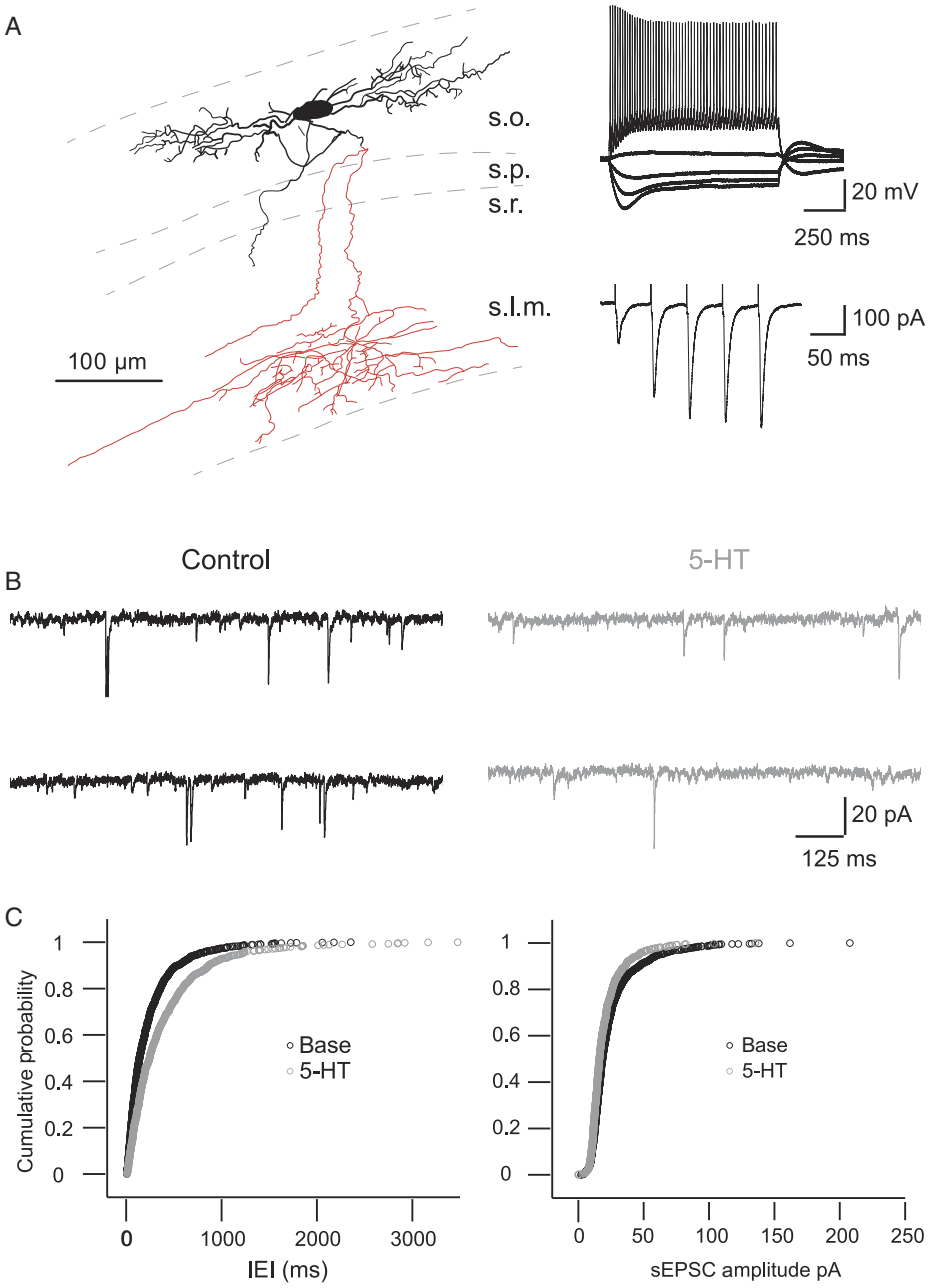

Figure 1. 5-HT inhibits spontaneous EPSCs in O-LM interneurons. (*A*) Left, reconstruction of an O-LM interneuron (dashed: outline of cell layers, black: cell body and dendrites, red: axon). Right top, typical voltage responses of an O-LM cell to de- and hyperpolarizing current pulses. Right bottom, strongly facilitating excitatory postsynaptic current amplitudes to consecutive extrasynaptic stimuli. (*B*) Example traces of spontaneous EPSCs under control conditions and in 10 µM 5-HT. (*C*) Cumulative probability of interevent intervals (IEI, left) and amplitude of spontaneous EPSCs (right) under control conditions, in 10 µM 5-HT and after wash ($n = 8$). s.l.m., *stratum lacunosom-moleculare*; s.o., *stratum oriens*, s.p., *stratum pyramidale*; s.r., *stratum radiatum*.

vesicular storage of 5-HT and consecutively reverses the serotonin transporter. As a result, the extracellular concentration of 5-HT is increased. In the following sets of experiments, we tested whether the inhibitory effect of serotonin on EPSCs could be mimicked by fenfluramine induced release of endogenous 5-HT from hippocampal serotonergic fibers. We observed a clear and reversible reduction of the EPSC amplitude by application of fenfluramine by 26.15%, median, IQR: 8.95% (amplitude before and during fenfluramine application is significantly different, paired sample Wilcoxon rank test $P = 0.0156$, Fig. 2C1,C2, $n = 7$). Furthermore, we investigated the effect of fenfluramine on the spiking probability of O-LM interneurons. Spikes could be readily evoked by a theta stimulation protocol in which 5 brief current pulses with an interstimulus interval of 125 ms were delivered. The number of spikes elicited was either strongly reduced or all spikes were abolished under fenfluramine (number of successfully evoked spikes in control vs. fenfluramine: $P < 0.000001$, McNemar's test, Fig. 2D).

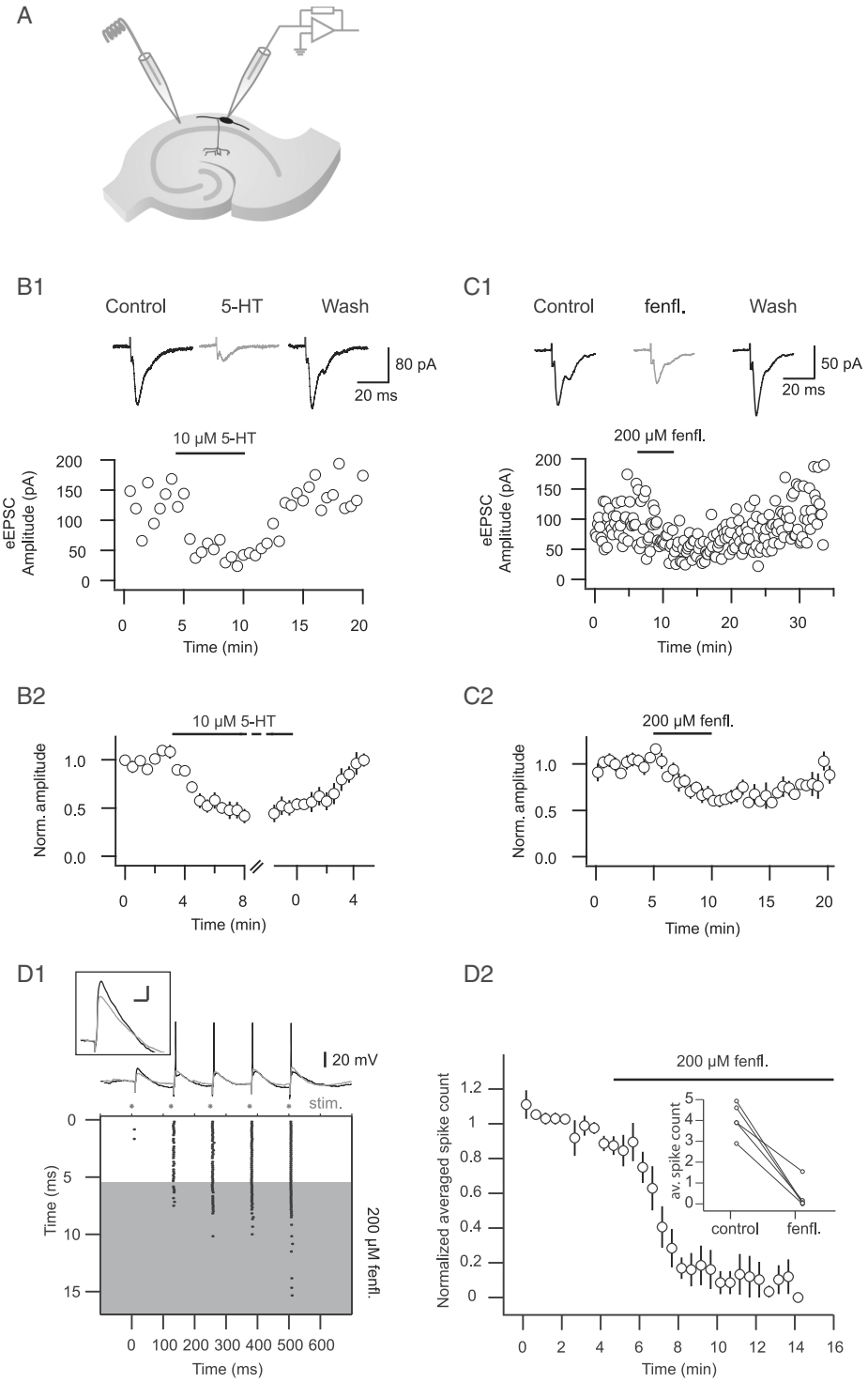

Figure 2. Bath-applied as well as endogenously released 5-HT decreases stimulus-evoked EPSCs. (*A*) Recording configuration with an extracellular stimulating electrode positioned at the border of the *alveus* and *stratum oriens*. (*B1*) Top, example traces of stimulus-evoked EPSCs. Bottom, time course of the EPSC amplitude before, during and after washout of 10 µM 5-HT. (*B2*) Summary of the time course of the normalized and binned EPSC amplitudes ($n = 12$). (*C1*) Top, example traces of stimulus-evoked EPSCs. Bottom, time course of the EPSC amplitude before, during and after washout of 200 µM fenfluramine. (*C2*) Summary of time course of the normalized and binned EPSC amplitudes ($n = 7$). (*D*) Endogenously released 5-HT reduces spiking probability. (*D1*) Example experiment where spikes were evoked in an O-LM interneuron by extracellular stimulation. Five pulses at theta frequency (interstimulus interval: 125 ms) were delivered. * Indicate stimulus time points. Top, example traces in control conditions (black) and in fenfluramine (200 µM, gray). (Inset) EPSP evoked by the first stimulus in control condition (black) and in fenfluramine (gray), average of 4 traces each, scale bar, *x*: 20 ms, *y*: 5 mV. Bottom, time course of experiment displayed as raster plot of spikes evoked in response to stimulation. Spikes were abolished shortly after washing in fenfluramine (gray area). (*D2*) Summary, spike count normalized to the summed and averaged spike counts of trials under control conditions. Inset, averaged spike counts under control conditions and in fenfluramine ($n = 5$).

5-HT Reduces Excitatory Synaptic Transmission at the CA1 Pyramidal Cell–O-LM Interneuron Synapse

O-LM interneurons are considered as classical feedback inhibitory interneurons as they receive excitatory input predominantly from recurrent CA1 pyramidal cell axons (Blasco-Ibáñez and Freund 1995). To test the assumption that 5-HT acts at the CA1 pyramidal–O-LM interneuron synapse, we performed paired recordings from synaptically connected CA1 pyramidal cells and O-LM interneurons. In this set of experiments, we tested 18 simultaneously recorded CA1 pyramidal cell–O-LM interneuron pairs, 5 of which were synaptically connected. Post hoc neuroanatomical analysis confirmed the cellular identities of O-LM and pyramidal neurons in all 5 synaptically connected paired recordings (Fig. 3A). O-LM interneurons displayed a strong facilitation of the postsynaptic amplitude in response to consecutive action potentials (APs) elicited in the presynaptic pyramidal cell (Fig. 3B1). The mean baseline amplitude of the first unitary EPSC (uEPSC) was 7.2 ± 0.4 pA ($n = 4$; one of the O-LM interneurons displayed a reliably detectable postsynaptic current only after the fourth presynaptic AP and was therefore not considered for analysis). After application of 5-HT, we observed a profound and fully reversible reduction in the amplitudes of all uEPSCs (Fig. 3B1,B2). 5-HT reduced the amplitude of the first uEPSC to 30.7 ± 6% ($n = 4$; Fig. 3C and D). Taken together, these results confirm the assumption that 5-HT reduces the excitatory drive from local CA1 collaterals onto O-LM interneurons.

Presynaptic Modulation of Glutamatergic Transmission onto O-LM Interneurons

We sought to further characterize the mechanism underlying the observed modulation of glutamatergic inputs onto O-LM interneurons in area CA1. We considered 3 possible scenarios to explain our findings: 1) The observed reduction in amplitude of EPSCs could be due to a modulation on the presynaptic site of excitatory terminals; 2) it could be mediated by modifications at the postsynaptic site, or 3) a combination of both scenarios could account for the effect of 5-HT. To study the location of 5-HT action, we first investigated the effect of 5-HT on miniature EPSCs (mEPSCs), recorded in the presence of the sodium channel blocker TTX. Under these conditions, neurotransmitter release upon spontaneous vesicle fusion can be tested independent of AP-mediated Ca^{2+} influx. There was no significant difference in the incidence or amplitude of mEPSCs after bath application of 5-HT (Fig. 4A, $n = 10$, frequency: control 2.4 ± 0.3 Hz vs. 1.9 ± 0.3 Hz in 5-HT ($P = 0.15$), amplitude: control: 24.3 ± 2.2 pA vs. 22.6 ± 2.1 pA in 5-HT, $P = 0.191$, paired Student's T-test).

To gain further insights into the site of serotonergic action, we performed single-photon laser stimulation of MNI-caged-L-glutamate. In this set of experiments, a constant amount of caged glutamate is uncaged by laser stimulation and therefore the presynaptic site is not involved. However, a decrease in the glutamate evoked EPSC amplitude by the application of 5-HT was not observed (Fig. 4B, $n = 4$). Furthermore, we analyzed the incidence of synaptic failures of the first and second EPSC in the synaptically connected paired recordings. We observed that the failure rate increased upon application of 5-HT ($n = 4$; failure rate of the first EPSC under control condition: 64.1 ± 5% vs. failure rate in 5-HT: 81.6 ± 3%, Fig. 4C. Failure rate of the second EPSC under control condition: 39.2 ± 3% vs. failure rate in 5-HT: 72.7 ± 7%). Summarizing these findings supports the conclusion that a postsynaptic mechanism is unlikely to be responsible for the reduced excitatory glutamatergic transmission onto O-LM

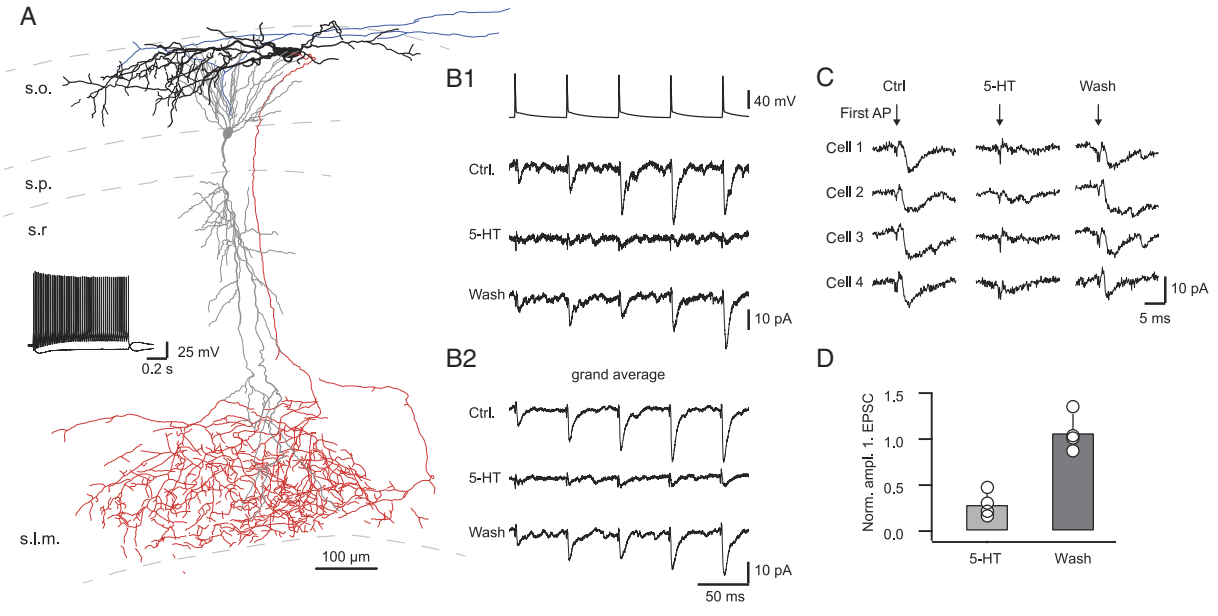

Figure 3. Serotonin reduces glutamatergic excitatory synaptic transmission at the CA1 pyramidal cell–O-LM interneuron synapse. (*A*) Reconstruction of a synaptically connected pyramidal cell–O-LM interneuron pair (dashed: outline of cell layers, black: cell body and dendrites of O-LM interneuron, red: axon of O-LM interneuron; gray: cell body and dendrites of pyramidal cell, blue: axon of pyramidal cell). Middle, left, voltage responses of the shown O-LM cell to de- and hyperpolarizing current pulses. (*B1*) Strongly facilitating unitary excitatory postsynaptic currents to consecutive APs, elicited in the presynaptic pyramidal cell. Below the postsynaptic response to consecutive APs after 5-HT application and after washout of 5-HT are shown. (*B2*) Grand average of the postsynaptic responses of 4 connected pairs in the indicated conditions. (*C*) Traces of uEPSCs evoked by the first presynaptic AP (time point indicated by arrow) in 4 cells under control conditions, after application of 10 µM 5-HT and after washout of 5-HT. (*D*) Summary of the reduction of the normalized first uEPSC amplitude by application of 5-HT and after washout of 5-HT ($n = 4$). s.l.m., *stratum lacunosom-moleculare*; s.o., *stratum oriens*, s.p., *stratum pyramidale*; s.r., *stratum radiatum*.

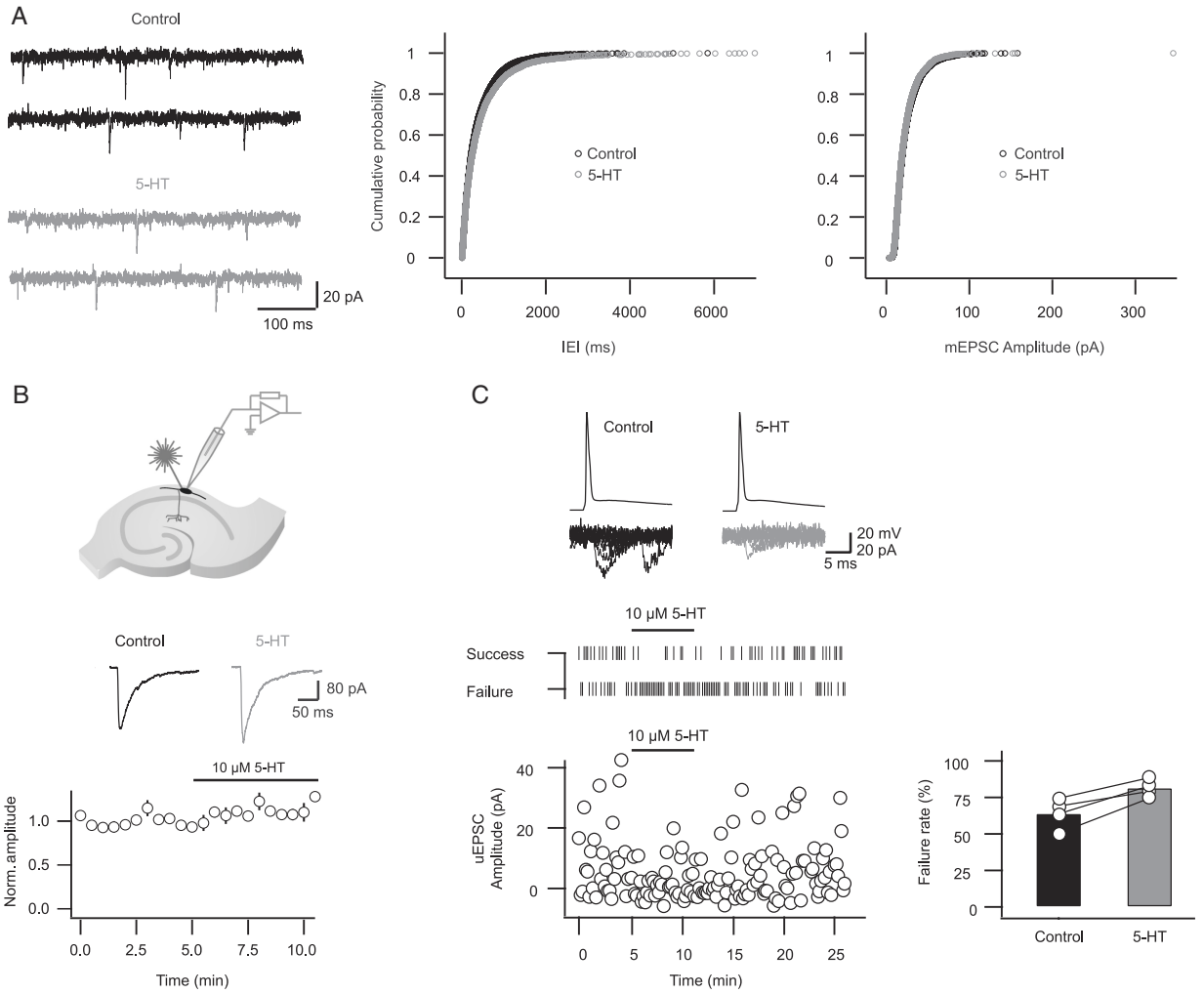

Figure 4. 5-HT acts most likely presynaptically. (*A*) Left, example traces of miniature EPSCs in control conditions (black) and in 10 μM 5-HT (gray). Right, cumulative probability of interevent intervals and amplitude of miniature EPSCs in control conditions and in 10 μM 5-HT ($n = 10$). (*B*) Top, recording configuration for glutamate uncaging. With a laser flash glutamate is uncaged in the immediate vicinity of the soma of an O-LM interneuron. Middle, example traces of the glutamate evoked current before (black) and after the application of 10 μM 5-HT (gray). Bottom, summary of the time course of the glutamate evoked current. Depicted is the normalized and binned peak amplitude. Note that the amplitude is not decreased after application of 5-HT ($n = 4$). (*C*) Left, example of connected pyramidal–O-LM pair, top, overlay of uEPSCs in control conditions and in 5-HT, middle, time course of successful synaptic transmission and failures. Bottom, time course of the uEPSC amplitude (as shown in top row) before, during and after washout of 10 μM 5-HT. Note that the failure rate increases during application of 5-HT. Right, summary of failure rate in synaptically connected paired recordings under control conditions and in 10 μM 5-HT ($n = 4$).

interneurons by serotonin application. Thus, we conclude that the mechanism is most likely presynaptic.

Mechanism of Action

After having localized the site of action, we aimed to identify the 5-HT receptor subtype mediating inhibition of glutamatergic transmission. At first, we confirmed with the unspecific 5-HT antagonist dihydroergocristine mesylate that the reduction in EPSC amplitude can indeed be blocked by antagonizing 5-HT receptors ($n = 7$, median of normalized amplitude in dihydroergocristine mesylate 0.84, IQR: 0.26, EPSC amplitude in dihydroergocristine mesylate vs. EPSC amplitude in dihydroergocristine mesylate and 5-HT: $P = 0.3$, paired Wilcoxon rank test, Fig. 5A). One candidate presynaptic receptor is the 5-HT_{1B} receptor that has been shown to modulate glutamatergic transmission of CA1 pyramidal cells (Winterer et al. 2011). However, application of the 5-HT_{1B} receptor agonist CP 94523 did not mimic the effect of 5-HT on evoked EPSCs (median of normalized amplitude in CP 94523 is 0.834, IQR: 0.28, EPSC amplitude in control vs. EPSC amplitude in CP 94523: $P = 0.15$, paired Wilcoxon rank test, Fig. 5B). Next, we investigated the possibility that presynaptic 5-HT_{1A} receptors might be responsible for mediating the reduction of glutamate release (Schmitz et al. 1995, 1999; Fink and Göthert 2007). Indeed, application of the 5-HT_{1A} agonist 8-OH-DPAT could, in part, mimic the effect of 5-HT on evoked EPSCs (median of normalized amplitude in 8-OH-DPAT: 0.76, IQR: 0.21, EPSC amplitude in control vs. EPSC amplitude in 8-OH-DPAT: $P = 0.016$, paired Wilcoxon rank test, Fig. 5C1). Furthermore, the 5-HT_{1A} receptor antagonist Way100635 reduced the action of 5-HT, when compared with control conditions (median of normalized amplitude: 0.78, IQR: 0.3, EPSC amplitude in Way100635 vs. EPSC amplitude in Way100635 and 5-HT: $P = 0.01$, paired Wilcoxon rank test, Fig. 5C2). We conclude that the presynaptic activation of 5-HT_{1A}

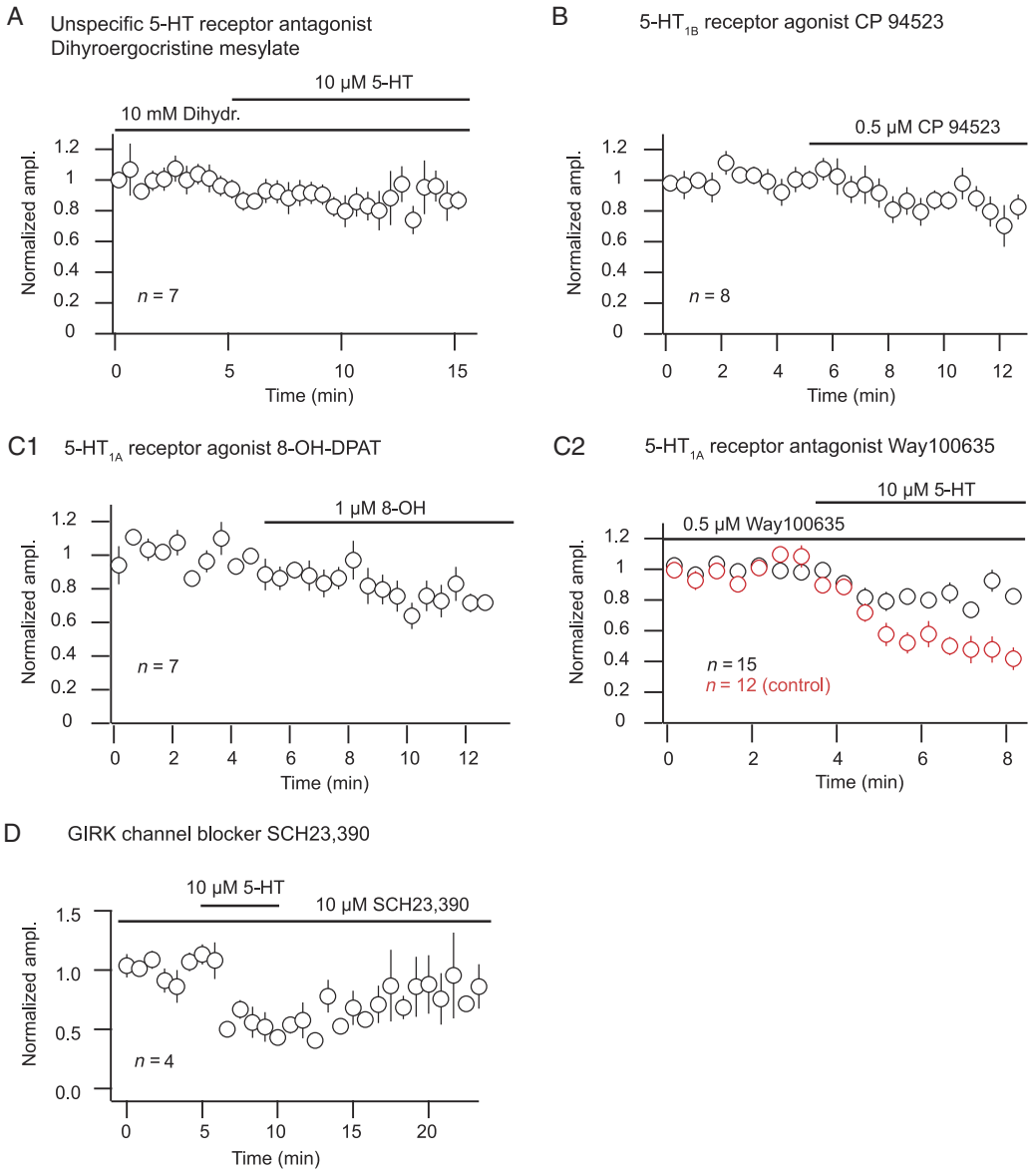

Figure 5. Effect of 5-HT receptor subtype (un)specific compounds on eEPSC amplitude. (*A–D*) Time course of averaged, normalized, and binned amplitude. The paired Wilcoxon sign rank test was used to compare amplitudes in the indicated conditions (tested on raw, not normalized amplitudes). (*A*) In the presence of the unspecific 5-HT receptor antagonist dihydroergocristine mesylate the effect of 5-HT on the EPSC amplitude is abolished. ($n = 7$, $P = 0.30$). (*B*) The 5-HT_{1B} receptor agonist CP 94523 does not mimic the 5-HT effect. ($n = 8$, $P = 0.15$). (*C1*) The 5-HT_{1A} receptor agonist 8-OH-DPAT reduces eEPSC amplitudes ($n = 7$, $P = 0.02$). (*C2*) The 5-HT_{1A} receptor antagonist WAY100635 partially blocks the 5-HT effect on eEPSC amplitude ($n = 15$, $P = 0.01$). For comparison the eEPSC amplitude in control conditions, that is, in the absence of the antagonist is shown ($n = 12$) (red, compare Fig. 2*B*, unpaired Wilcoxon test, $P = 0.0002$). (*D*) In the presence of the GIRK-channel blocker SCH23390 5-HT still reduces the amplitude of eEPSCs ($n = 4$). Also compare Figure 2*B2*.

receptors is partially responsible for the inhibition of glutamatergic transmission onto O-LM interneurons.

5-HT_{1A} receptors might mediate the observed effect of 5-HT on glutamatergic transmission by hyperpolarizing the presynaptic pyramidal cell. This hyperpolarization is mediated by the opening of G-protein-gated inwardly rectifying K^+ channels (GIRK) (Andrade and Nicoll 1987; Segal et al. 1989; Schmitz et al. 1995). However, application of the GIRK-channel blocker SCH23390 did not prevent the reduction of excitatory synaptic transmission onto O-LM interneurons by 5-HT (mean inhibition of amplitude: 42.73% ± 9.7, $n = 4$, Fig. 5*D*).

5-HT receptor activation could target calcium channels via G-proteins (Mizutani et al. 2006) resulting in a reduced Ca^{2+} influx and thereby decreasing Ca^{2+}-dependent vesicle release. To test this hypothesis, we evaluated if 5-HT reduces Ca^{2+} influx into the presynaptic terminals of CA1 pyramidal cell axons that are predominantly contributing to the glutamatergic synaptic transmission onto O-LM interneurons. We adapted an optical recording method described previously (Regehr and Tank 1991; Breustedt et al. 2003), in which the presynaptic fibers in *stratum oriens* are labeled with the low-affinity fluorescent Ca^{2+} indicator dye magnesium green AM. These recordings were done in the

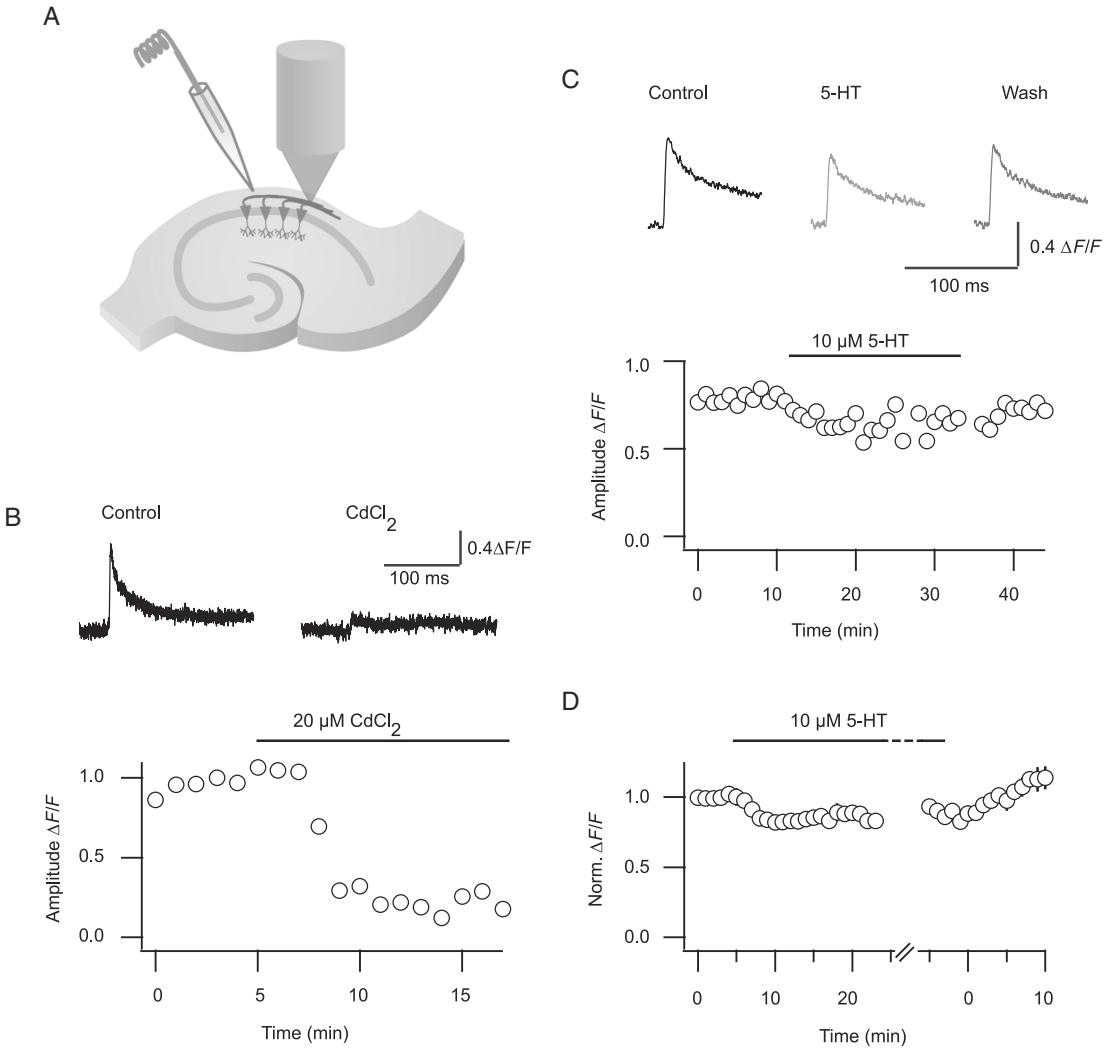

Figure 6. Decreased presynaptic calcium influx can account for the reduction of glutamatergic transmission by 5-HT. (*A*) Ca^{2+}-imaging recording configuration. Axonal fibers were filled with the Ca^{2+}-sensitive dye magnesium green AM (green) by bulk loading and stimulated with an extracellular electrode positioned at the border of the *alveus* and *stratum oriens*. The resulting Ca^{2+} transients were measured with a photodiode. (*B*) Top, example traces of the Ca^{2+} transients in control and in 20 μM $CdCl_2$. Bottom, time course of ΔF/F amplitude of the Ca^{2+} transients shown above. Note that the transient is abolished in the presence of the calcium channel blocker CdCl2. (*C*) Top, example traces of the calcium transient in control, in 10 μM 5-HT and after wash. Bottom, time course of ΔF/F amplitude of the above transients. (*D*) Summary of time course of ΔF/F amplitude ($n = 11$).

presence of NBQX and D-AP5 to exclude a postsynaptic contribution to the signal. AP driven Ca^{2+} influx into the presynaptic terminal was elicited by a single extracellular stimulation electrode positioned at the border of *stratum oriens* and *alveus*. The rise in presynaptic Ca^{2+} was quantified using the transient increase of the fluorescence signal (see Materials and Methods; Fig. 6A). To ensure that the detected signal was actually due to Ca^{2+} influx, we applied the unspecific Ca^{2+} channel blocker $CdCl_2$ which abolished the Ca^{2+} transient (Fig. 6B). We then tested the effect of 5-HT on the presynaptic Ca^{2+} transient and found that indeed 5-HT reversibly decreased the Ca^{2+} transient amplitude by 13.9 ± 3.2% on average ($n = 11$, amplitude in 5-HT is significantly different from control: $P = 0.006$, paired Student's *T*-test, Fig. 6C,D).

To further corroborate this finding, we tested whether a reduction in Ca^{2+} influx can account for the inhibition in glutamatergic transmission induced by serotonin. We therefore reduced the extracellular Ca^{2+} concentration from 2.5 to 2.0 mM ($n = 5$, amplitude in 2.5 mM Ca^{2+} is significantly different from the amplitude in 2 mM Ca^{2+}: $P = 0.0022$, paired Student's *T*-test, Fig. 7A,C) and compared the reduction in amplitude of the calcium transient to the reduction observed under 5-HT: 5-HT application as well as lowering the extracellular Ca^{2+} concentration displayed a comparable amount of reduction of the Ca^{2+} transient (13.9 ± 3.2% in 5-HT vs. 16.0 ± 1.7% in 2 mM Ca^{2+}, the reduction in amplitude observed in 5-HT and lowered Ca^{2+} concentration are not different: $P = 0.6731$, unpaired Student's *T*-test, Fig. 7A,C, left).

We hypothesized that if the reduced calcium influx into the presynaptic terminal is responsible for the inhibition of glutamatergic transmission, a reduction of the extracellular calcium concentration should also be able to mimic the 5-HT effect on EPSCs evoked by electrical stimulation. Indeed, reducing the available calcium by the same amount as in the imaging experiments (0.5 mM), resulted in a reduction of the amplitude of the eEPSCs

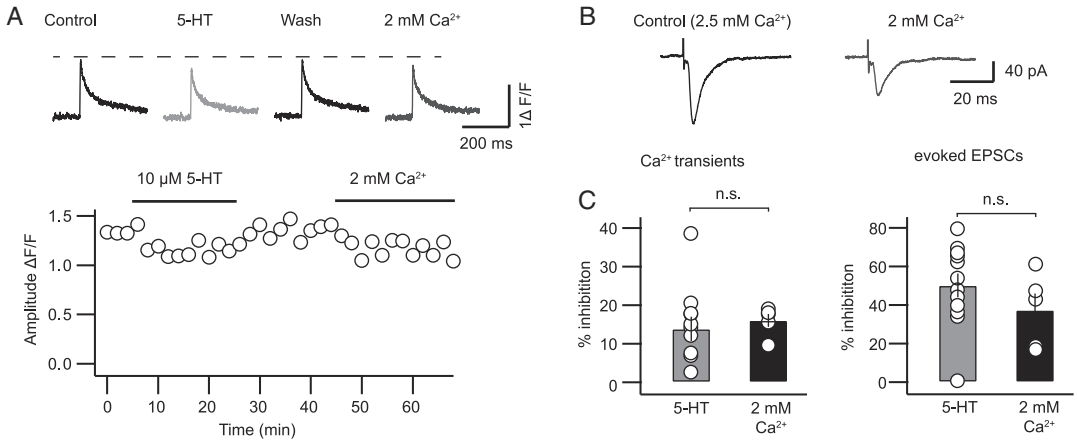

Figure 7. The 5-HT induced reduction of the presynaptic Ca^{2+} transient as well as the reduction of the glutamatergic synaptic transmission can be mimicked by a reduction of the extracellular Ca^{2+} concentration. (A) Top, example traces of Ca^{2+} signals in control conditions, after application of 10 µM 5-HT, after washout of 5-HT and after reduction of the extracellular Ca^{2+} concentration from 2.5 to 2 mM. Bottom, time course of the binned amplitude of the Ca^{2+} transient in control conditions, after application of 10 µM 5-HT, after washout and in 2 mM Ca^{2+}. (B) Example traces of stimulus-evoked EPSCs in control conditions and after reduction of the extracellular Ca^{2+} concentration from 2.5 to 2 mM. (C) Summaries of the effect of 5-HT and the reduced extracellular Ca^{2+} concentration on the amplitude of the Ca^{2+} transients and on the amplitude of stimulus-evoked EPSCs.

by 37.4 ± 8.6% ($n = 5$, Fig. 7B,C right), similar to the reduction we observed with 5-HT ($n = 12$; 50.1 ± 6.1%, Fig. 7C, right, $P = 0.2676$, unpaired Student's *T*-test).

In summary, we could show that 5-HT inhibits excitatory synaptic transmission at the pyramidal cell–O-LM interneuron synapse in CA1. This effect most likely involves a decrease of calcium influx into the presynaptic terminal and is mediated by presynaptic 5-HT receptors.

Discussion

Here we show by means of electrophysiological recordings and Ca^{2+} measurements that 5-HT reversibly reduces excitatory glutamatergic synaptic transmission onto O-LM interneurons, which leads to a decrease in spiking probability of O-LM interneurons in area CA1 of the hippocampus. Our findings indicate that 5-HT decreases the Ca^{2+} influx into the presynaptic terminal of CA1 pyramidal cells and that this modulation is most likely responsible for the reduction in glutamatergic synaptic transmission at the pyramidal cell–O-LM interneuron synapse.

At first, we observed a reduction of the frequency of spontaneous EPSCs in O-LM interneurons by the application of 5-HT. Spontaneous EPSCs are generated either by Ca^{2+}-independent spontaneous fusion of vesicles with the presynaptic plasma membrane (mEPSCs) or by Ca^{2+}-dependent vesicular release in response to spontaneous APs. We found that the observed neuromodulation by 5-HT critically depends on presynaptic APs, as the decrease in the frequency of sEPSCs was lost after application of TTX. The finding that mEPSCs are not affected, neither in frequency nor in amplitude, could be in line with the following scenario: 5-HT could induce a hyperpolarization of the presynaptic pyramidal cell, mediated by the opening of GIRK channels by 5-HT_{1A} receptor activation (Andrade and Nicoll 1987; Segal et al. 1989; Schmitz et al. 1995). This would diminish the frequency of sEPSCs because of a decrease in the number of spontaneous spikes as has been shown in vivo (Richter-Levin and Segal 1992). This possibility seems to be unlikely because application of a GIRK-channel blocker could not prevent the reduction of excitatory synaptic transmission onto O-LM interneurons by 5-HT.

Another potential target of 5-HT might be astrocytes, which have been shown to react on 5-HT (Schipke et al. 2011), and in turn are able to modulate neurotransmission (Araque et al. 1999). However, the time course of reaction to 5-HT in astrocytes (Schipke et al. 2011) differs largely from the type of modulation described here.

The more likely site of action is an activation of 5-HT receptors at the axon terminals of the presynaptic cell, which leads to a decrease in Ca^{2+} influx; this mechanism would not affect the probability of spontaneous vesicle fusion, and is in line with our finding that 5-HT does not affect mEPSCs.

We next investigated the effects of 5-HT on EPSCs evoked by extracellular stimulation in *stratum oriens/alveus* where activation of axonal fibers from CA1 pyramidal cells is most likely. As excitatory connections on O-LM cells originate predominately from local CA1 collaterals (Blasco-Ibáñez and Freund 1995), the 5-HT-mediated decrease in amplitude of stimulus-evoked currents is most likely the result of a depression of glutamatergic transmission from local CA1 pyramidal cells. We confirmed this assumption with paired recordings from synaptically connected CA1 pyramidal neurons and O-LM interneurons. In this set of experiments 5-HT mediated a robust increase of synaptic failures, that is, presynaptic AP initiation without successful synaptic transmission. The very low initial release probability at this synapse and its further reduction due to 5-HT prevented the analysis of changes in short-term facilitation upon 5-HT application. In a further set of experiments, we circumvented a possible serotonergic modulation of the presynaptic site by means of photolytically activating glutamate. In doing so, the amount of glutamate that activates postsynaptic glutamate receptors is kept constant. Under these experimental conditions, we found that 5-HT had no effect on the glutamate evoked response. Together, these observations are suggestive for a presynaptic mechanism mediating the decrease in glutamatergic transmission.

Presynaptic modulation of transmitter release can be mediated via a G-protein-mediated block of Ca^{2+} channels (Thomson 2000; Mizutani et al. 2006; but see Gerachshenko et al. 2009). As a consequence the Ca^{2+} influx into the presynaptic terminal is reduced. We were able to show that indeed application

of 5-HT leads to a decrease in presynaptic Ca^{2+} levels. Although our method does not allow specific loading of axon terminals on O-LM cells, they are likely to constitute a considerable fraction of the loaded fibers; hence, they contribute substantially to the measured Ca^{2+} transient. Since these recordings were performed under blockade of N-methyl-D-aspartate- and alpha-amino-3-hydroxy-5-methyl-4-isoxazole-propionate-receptors, a postsynaptic contribution to the measured Ca^{2+} signal can be excluded. The observed inhibition of Ca^{2+} influx upon 5-HT application was within the expected range since the relationship between Ca^{2+} influx and transmitter release is nonlinear (Mintz et al. 1995; Gundlfinger et al. 2007). Furthermore, we could show that a decrease in extracellular Ca^{2+} concentration is able to mimic the effects of 5-HT. This applies for the experiments where we probed the presynaptic Ca^{2+} influx into the presynaptic terminals by means of fluorescence measurements as well as in the experiments where we tested the stimulus-induced EPSCs in O-LM interneurons.

Under physiological conditions, 5-HT is released in the hippocampus by axons originating from serotonergic neurons in the midbrain raphe nuclei. With the aim of avoiding the exogenous application of serotonin by bath, we made use of fenfluramine to mimic physiological release of serotonin in the hippocampus. Indeed, we observed that also endogenously released serotonin is able to reduce the excitatory synaptic transmission onto O-LM interneurons. O-LM interneurons have been shown to be active during hippocampal theta oscillations (Klausberger et al. 2003; Katona et al. 2014). We aimed to mimic theta-timed input onto O-LM-interneurons by extracellular stimulation and could readily evoke spikes, suggesting that the low release probability can be overcome by an appropriate stimulus. Furthermore, the serotonergic modulation of glutamatergic transmission described here significantly reduces the spiking probability and therefore has an impact on the output of O-LM interneurons

Serotonergic neuromodulation of O-LM interneurons could have an important influence on the dynamics of hippocampal-entorhinal cortex interaction. Active O-LM cells are presumed to inhibit input from the entorhinal cortex via postsynaptic $GABA_A$ receptor activation in *stratum moleculare* and might in addition mediate a reduction of glutamate and GABA release by presynaptic $GABA_B$ receptors (Chalifoux and Carter 2011; Urban-Ciecko et al. 2015). Deactivation of O-LM cells is likely to strengthen entorhinal cortex input to CA1 via the TA pathway (Maccaferri and McBain 1995). Moreover, it has been shown recently that serotonin is able to induce a potentiation of the TA pathway–CA1 synapses (Cai et al. 2013). In this respect, serotonin is acting synergistically to increase the input via the TA pathway: 5-HT reduces the excitatory drive onto O-LM interneurons and consequently releases the target region of the entorhinal projections from inhibition. The finding that O-LM interneurons differentially modulate the input from CA3 and the entorhinal cortex onto hippocampal CA1 neurons (Leão et al. 2012) puts serotonergic neuromodulation of O-LM interneurons at center stage for switching the information flow from direct TA pathway inputs with sensory information to inputs with internal representations stored in CA3.

Funding

This work was supported by the Deutsche Forschungsgesellschaft (DFG) grants SFB 665 and 958, Cluster of Excellence 257, NeuroCure, the Bernstein Center for Computational Neuroscience Berlin, the Bernstein Focus Berlin (BMBF), Deutsches Zentrum für Neurodegenerative Erkrankungen (DZNE), and the Einstein Foundation. Funding to pay the Open Access publication charges for this article was provided by Charité.

Notes

We thank Susanne Rieckmann, Anke Schönherr, Karin Bloch, and Lisa Züchner for excellent technical assistance. We thank the members of the Schmitz laboratory for support and helpful comments. *Conflict of Interest*: None declared.

References

Ali AB, Thomson AM. 1998. Facilitating pyramid to horizontal oriens-alveus interneurone inputs: dual intracellular recordings in slices of rat hippocampus. J Physiol (Lond). 507(Pt 1): 185–199.

Andrade R, Nicoll RA. 1987. Pharmacologically distinct actions of serotonin on single pyramidal neurones of the rat hippocampus recorded in vitro. J Physiol (Lond). 394:99–124.

Araque A, Parpura V, Sanzgiri RP, Haydon PG. 1999. Tripartite synapses: glia, the unacknowledged partner. Trends Neurosci. 22:208–215.

Barnes NM, Sharp T. 1999. A review of central 5-HT receptors and their function. Neuropharmacology. 38:1083–1152.

Biró AA, Holderith NB, Nusser Z. 2005. Quantal size is independent of the release probability at hippocampal excitatory synapses. J Neurosci. 25:223–232.

Blasco-Ibáñez JM, Freund TF. 1995. Synaptic input of horizontal interneurons in stratum oriens of the hippocampal CA1 subfield: structural basis of feed-back activation. Eur J Neurosci. 7:2170–2180.

Breustedt J, Vogt KE, Miller RJ, Nicoll RA, Schmitz D. 2003. Alpha1E-containing Ca2+ channels are involved in synaptic plasticity. Proc Natl Acad Sci USA. 100:12450–12455.

Cai X, Kallarackal AJ, Kvarta MD, Goluskin S, Gaylor K, Bailey AM, Lee H-K, Huganir RL, Thompson SM. 2013. Local potentiation of excitatory synapses by serotonin and its alteration in rodent models of depression. Nat Neurosci. 16:464–472.

Chalifoux JR, Carter AG. 2011. $GABA_B$ receptor modulation of synaptic function. Curr Opin Neurobiol. 21:339–344.

Chittajallu R, Craig MT, McFarland A, Yuan X, Gerfen S, Tricoire L, Erkkila B, Barron SC, Lopez CM, Liang BJ, et al. 2013. Dual origins of functionally distinct O-LM interneurons revealed by differential 5-HT3AR expression. Nat Neurosci. 16:1598–1607.

Fink KB, Göthert M. 2007. 5-HT receptor regulation of neurotransmitter release. Pharmacol Rev. 59:360–417.

Freund TF, Gulyás AI, Acsády L, Görcs T, Tóth K. 1990. Serotonergic control of the hippocampus via local inhibitory interneurons. Proc Natl Acad Sci USA. 87:8501–8505.

Gerachshenko T, Schwartz E, Bleckert A, Photowala H, Seymour A, Alford S. 2009. Presynaptic G-protein-coupled receptors dynamically modify vesicle fusion, synaptic cleft glutamate concentrations, and motor behavior. J Neurosci. 29:10221–10233.

Goldin M, Epsztein J, Jorquera I, Represa A, Ben-Ari Y, Crépel V, Cossart R. 2007. Synaptic kainate receptors tune oriens-lacunosum moleculare interneurons to operate at theta frequency. J Neurosci. 27:9560–9572.

Gundlfinger A, Bischofberger J, Johenning FW, Torvinen M, Schmitz D, Breustedt J. 2007. Adenosine modulates transmission at the hippocampal mossy fibre synapse via direct inhibition of presynaptic calcium channels. J Physiol (Lond). 582:263–277.

Katona L, Lapray D, Viney TJ, Oulhaj A, Borhegyi Z, Micklem BR, Klausberger T, Somogy P. 2014. Sleep and movement differentiates actions of two types of somatostatin-expressing GABAergic interneurons in rat hippocampus. Neuron. 82:827–886.

Klausberger T, Magill PJ, Márton LF, Roberts JDB, Cobden PM, Buzsáki G, Somogyi P. 2003. Brain-state- and cell-type-specific firing of hippocampal interneurons in vivo. Nature. 421:844–848.

Leão RN, Mikulovic S, Leão KE, Munguba H, Gezelius H, Enjin A, Patra K, Eriksson A, Loew LM, Tort ABL, et al. 2012. OLM interneurons differentially modulate CA3 and entorhinal inputs to hippocampal CA1 neurons. Nat Neurosci. 15:1524–1530.

Lee K, Dixon AK, Pinnock RD. 1999. Serotonin depolarizes hippocampal interneurones in the rat stratum oriens by interaction with 5HT2 receptors. Neurosci Lett. 270:56–58.

Losonczy A, Zhang L, Shigemoto R, Somogyi P, Nusser Z. 2002. Cell type dependence and variability in the short-term plasticity of EPSCs in identified mouse hippocampal interneurones. J Physiol (Lond). 542:193–210.

Maccaferri G. 2005. Stratum oriens horizontal interneurone diversity and hippocampal network dynamics. J Physiol (Lond). 562:73–80.

Maccaferri G, Lacaille J-C. 2003. Interneuron diversity series: hippocampal interneuron classifications—making things as simple as possible, not simpler. Trends Neurosci. 26:564–571.

Maccaferri G, McBain CJ. 1995. Passive propagation of LTD to stratum oriens-alveus inhibitory neurons modulates the temporoammonic input to the hippocampal CA1 region. Neuron. 15:137–145.

Mintz IM, Sabatini BL, Regehr WG. 1995. Calcium control of transmitter release at a cerebellar synapse. Neuron. 15:675–688.

Mizutani H, Hori T, Takahashi T. 2006. 5-HT1B receptor-mediated presynaptic inhibition at the calyx of Held of immature rats. Eur J Neurosci. 24:1946–1954.

Pangalos M, Donoso JR, Winterer J, Zivkovic AR, Kempter R, Maier N, Schmitz D. 2013. Recruitment of oriens-lacunosum-moleculare interneurons during hippocampal ripples. Proc Natl Acad Sci USA. 110:4398–4403.

Parra P, Gulyás AI, Miles R. 1998. How many subtypes of inhibitory cells in the hippocampus? Neuron. 20:983–993.

Regehr WG, Tank DW. 1991. Selective fura-2 loading of presynaptic terminals and nerve cell processes by local perfusion in mammalian brain slice. J Neurosci Methods. 37:111–119.

Richter-Levin G, Segal M. 1992. Raphe grafts in the hippocampus, but not in the entorhinal cortex, reverse hippocampal hyperexcitability of serotonin-depleted rats and restore their responsiveness to fenfluramine. Dev Neurosci. 14:166–172.

Schipke CG, Heuser I, Peters O. 2011. Antidepressants act on glial cells: SSRIs and serotonin elicit astrocyte calcium signaling in the mouse prefrontal cortex. J Psychiatr Res. 45:242–248.

Schmitz D, Empson RM, Heinemann U. 1995. Serotonin reduces inhibition via 5-HT1A receptors in area CA1 of rat hippocampal slices in vitro. J Neurosci. 15:7217–7225.

Schmitz D, Gloveli T, Empson RM, Heinemann U. 1999. Potent depression of stimulus evoked field potential responses in the medial entorhinal cortex by serotonin. Br J Pharmacol. 128:248–254.

Schmitz D, Mellor J, Breustedt J, Nicoll RA. 2003. Presynaptic kainate receptors impart an associative property to hippocampal mossy fiber long-term potentiation. Nat Neurosci. 6:1058–1063.

Segal M. 1980. The action of serotonin in the rat hippocampal slice preparation. J Physiol (Lond). 303:423–439.

Segal M, Azmitia EC, Whitaker-Azmitia PM. 1989. Physiological effects of selective 5-HT1a and 5-HT1b ligands in rat hippocampus: comparison to 5-HT. Brain Res. 502:67–74.

Somogyi P, Klausberger T. 2005. Defined types of cortical interneurone structure space and spike timing in the hippocampus. J Physiol (Lond). 562:9–26.

Thomson AM. 2000. Facilitation, augmentation and potentiation at central synapses. Trends Neurosci. 23:305–312.

Tort ABL, Rotstein HG, Dugladze T, Gloveli T, Kopell NJ. 2007. On the formation of gamma-coherent cell assemblies by oriens lacunosum-moleculare interneurons in the hippocampus. Proc Natl Acad Sci USA. 104:13490–13495.

Urban-Ciecko J, Fanselow EE, Barth AL. 2015. Neocortical somatostatin neurons reversibly silence excitatory transmission via $GABA_B$ receptors. Curr Biol 25(6):722–731.

Varga C, Golshani P, Soltesz I. 2012. Frequency-invariant temporal ordering of interneuronal discharges during hippocampal oscillations in awake mice. Proc Natl Acad Sci USA. 109: E2726–E2734.

Varga V, Losonczy A, Zemelman BV, Borhegyi Z, Nyiri G, Domonkos A, Hangya B, Holderith N, Magee JC, Freund TF. 2009. Fast Synaptic Subcortical Control of Hippocampal Circuits. Science. 326:449–453.

Vertes RP. 1991. A PHA-L analysis of ascending projections of the dorsal raphe nucleus in the rat. J Comp Neurol. 313:643–668.

Vertes RP, Fortin WJ, Crane AM. 1999. Projections of the median raphe nucleus in the rat. J Comp Neurol. 407:555–582.

Winterer J, Stempel AV, Dugladze T, Földy C, Maziashvili N, Zivkovic AR, Priller J, Soltesz I, Gloveli T, Schmitz D. 2011. Cell-type-specific modulation of feedback inhibition by serotonin in the hippocampus. J Neurosci. 31:8464–8475.

Chapter 4

Discussion

In the following I will provide a more expansive discussion of issues that are not contained or only touched on in the original research article's discussion. The first part focuses on the study concerning pyramidal cell modulation in the subiculum (Böhm et al., 2015b) and the second part on the O-LM-interneuron study (Böhm et al., 2015a). The last section gives a broader overview on both projects.

4.1 Extended discussion on 'Functional diversity of subicular principal cells during hippocampal ripples'

There are three major findings in this study: first, I have shown that in vivo the pyramidal cell population in the subiculum comprises two major subtypes, i. e. burst and regular firing cells. Second, the biophysical distinction between the two cell types is functionally relevant, as shown by their different modulation during SWRs both in vivo and in vitro. In vitro repatch experiments revealed that increased inhibition is responsible for the different membrane potential modulation. Third, we have investigated the microcircuit of the subiculum on a cellular level using a multiple-electrode patch-clamp approach. Unidirectional connections between bursting and regular firing cells hint at an irreversible identity of these subtypes. Furthermore, the intrinsic network topology provides a possible mechanism for the opposing membrane potential modulation of regular and burst firing cells observed here.

In the following sections I will discuss these findings with respect to pyramidal cell diversity, possible mechanisms, depict functional consequences and illustrate some limitations of our approach and will conclude with an outlook of possible future experiments.

4.1.1 Pyramidal cell diversity

So far, distinctions between subicular burst and regular firing cells in response to current injections have only been described in vitro. A characterization in vivo might have been

precluded by the extracellular recording methods used, because spike sorting algorithms and widely used manual spike sorting rely on wave form and action potential amplitude. These characteristics change within a burst, therefore it might be difficult to assign a burst firing cell to one unit using spike sorting. However, a previous report 'tentatively identified' subicular cell subtypes based on interspike interval and autocorrelation, but the authors note that intracellular recordings would be required to definitely determine their identity (Sharp and Green, 1994). The subtypes identified based on spike train patterns did not show any significant difference in strength of spatial signal (Sharp and Green, 1994).

Using the whole-cell patch clamp technique I have shown that regular and bursting cells are discernible in vivo under physiological conditions and that the output mode, bursting versus regular firing, is also reflected in the ongoing network activity in awake, still mice. This demonstrates that despite the manifold neuromodulators present in an intact awake brain, naturally occurring inputs evoke bursts primarily in burst firing cells.

Interestingly, it has been found in CA1 pyramidal cells that cells with a high burst propensity prior to exploration of a new environment are more likely to become the place cells of that environment than their less bursty peers (Epsztein et al., 2011). Furthermore, In the entorhinal cortex the propensity to fire action potentials in doublets correlates with the type of spatial modulation observed: cells firing predominantly in doublets tended to exhibit grid cell periodicity while those firing less doublets were more often border cells and head-direction cells (Latuske et al., 2015). These studies suggest that the temporal output pattern is functionally relevant in many brain regions.

The delayed non-match-to-sample task is dependent on an intact subiculum at short delays, and subicular principal cells are active during different phases of the task: either their firing rate increases during the presentation of the sample and/or the early delay phase or it is restricted to the delay phase. It would be interesting to see if these functionally distinct cells correlate with the bursting and regular firing cell types, too (Hampson and Deadwyler, 2003).

Recently a study combining sharp microelectrode and extracellular recordings as well as histological analysis revealed differences in modulation during SWRs of CA1 pyramidal cells depending on cell depth. Superficial, preferentially calbindin immunopositive cells tended to depolarize during ripples while deep, calbindin immunonegative pyramidal cells had a predominantly inhibitory drive in urethane anesthetized rats (Valero et al., 2015). Immunohistochemistry revealed a gradient of parvalbumin/gephyrin puncta density from superficial to deep. The authors propose that this bias in perisomatic inhibition, see also (Lee et al., 2014), together with a decreased excitation of deep CA1 pyramidal cells by CA2 pyramidal cells might be responsible for the different modulation (Valero et al., 2015). Together with our data this suggests that pyramidal cell diversity in the hippocampus is a general principle and, further, that cells participating in SWRs are, at least in part preselected by their immunohistochemical identity and their biophysical properties.

In the subiculum, the cell subtype correlates both with long-range projection targets (Kim and Frank, 2009) and local connectivity motifs. This principle has also been found in other regions of the brain: for example in the somatosensory cortex area S1, where cells with similar functional properties project to the same long-range target region (Chen et al., 2013). Similarly, in the visual cortex area V1, response selectivity coincides with connection patterns across layers (Vélez-Fort et al., 2014) and locally (Ko et al., 2011). These data suggest that functional specialization is accompanied or even determined by structural features.

4.1.2 The mechanism(s) underlying the opposing membrane potential modulation during ripples

Employing a model of SWRs in vitro I could show that the difference in membrane potential modulation is largely due to increased inhibitory input onto regular firing cells during SWRs and, further, that parvalbumin positive interneurons receive excitatory input during SWRs and emit action potentials. In a reduced slice preparation, in which both the connections from MEC and the connections from area CA1 were interrupted, SWRs could still be observed and also the differential modulation during SWRs was still present. This suggests that the differential inputs arise from within the local network and cell-type specific input from area CA1 is not needed to generate the cell subtype specific modulation. We therefore investigated the local network topology and found that indeed the inhibitory connection probability onto regular firing cells was higher than onto bursting cells. This analysis included different types of interneurons, but restricting the analysis to fast spiking interneurons also revealed a small but significant difference in the connection probability. We conclude that differential inhibition contributes to the membrane potential differences during ripples. However, additional mechanism might be at work in a more intact preparation. GABAergic neurons are believed to act mostly local, yet, long-range-projecting interneurons have been described in other areas (Melzer et al., 2012), therefore it might well be the case that GABAergic connections from area CA1 or the contralateral hemisphere impinging onto regular firing cells also contribute to the different membrane potential modulation during ripples.

Considering the earlier timing of the membrane depolarization in bursting cells compared to the membrane hyperpolarization of the regular firing cells with respect to the ripple peak in area CA1 (on average, the maximum hyperpolarization in the regular firing cells was 17 ms later than the maximum depolarization in bursting cells, although the variability was quite high) the following scenario might arise in the intact brain: excitatory input from area CA1 and the entorhinal cortex excite both regular and burst firing subicular pyramidal cells, next, the burst firing cells excite each other via their recurrent excitatory connections, possibly aided by input from regular firing cells (however, we do not

have experimental evidence for this latter assumption). In contrast, regular firing cells do not receive any excitation from bursting cell as this is a unilateral connection. In addition, regular firing cells are more strongly involved in the recruitment of interneurons, which in turn are more densely connected to the regular firing cells, i.e., if regular firing cells are activated, this activity dies out quickly, whereas if bursting cells are activated, they excite each other and the reverberant activity among them might aid to depolarize their membrane potential during ripples.

Of note, the underlying mechanism of differential modulation of deep and superficial pyramidal cells in CA1 under anesthesia appear at least in part to be different from that in the subiculum: lack of excitation from CA2 to the deep pyramidal cells has been suggested to be involved in the different modulation (Valero et al., 2015). This is not the case in the subiculum as our in vitro repatch experiments identify inhibition as the only distinguishing parameter in the slice. Together with the proximo-distal organisation of excitatory connections from CA1 to the subiculum (Tamamaki et al., 1987; Witter et al., 2000) it seems unlikely that the different modulation of subicular pyramidal cells is 'inherited' from area CA1. Nevertheless the gradient of parvalbumin positive puncta from superficial to deep pyramidal cells identified in area CA1 is in line with our observation of different numbers of inhibitory connections onto regular and burst firing cells in the subiculum.

Furthermore, as pointed out in the introduction, various neuromodulators act to influence synaptic transmission and network dynamics and might also play a role in the modulation of pyramidal cells during ripples; the subiculum receives neuromodulatory input from various sources: noradrenaline from locus coeruleus (Loy et al., 1980), serotonine from the median raphe nucleus (McKenna and Vertes, 2001), acetylcholine from the nucleus of diagonal band (McKinney et al., 1983) and dopamine from the ventral tegmental area (Gasbarri et al., 1994).

4.1.3 Functional consequences of pyramidal subtype–specific modulation

Regarding extrahippocampal targets, the axon collateralization of subicular neurons is in contrast to the CA1 region very low: each subicular neuron tends to project to only one target region (Naber and Witter, 1998). Both the projection target and the proportion of regular versus burst firing neurons are topographically organized along the proximo-distal axis, implying a cell subtype specific pattern of innervation of extrahippocampal targets. Indeed, by means of retrograde tracers Kim et al. have shown that target regions of the proximal subiculum (amygdala, lateral entorhinal cortex, nucleus accumbens and medial/ventral orbitofrontal cortex) are innervated mostly by regular firing cells whereas target regions of the distal subiculum (medial entorhinal cortex, presubiculum, retrosplenial cortex and ventromedial hypothalamus) by bursting neurons (Kim and Spruston, 2012). I could show that burst firing and regular firing cells are differentially recruited during

ripples: burst firing cells are activated during ripples while regular firing cells are inhibited. Together with the anatomical details described above it is likely that mainly target regions of the burst firing cells receive input from the subiculum during SWRs. For the medial entorhinal cortex and the presubiculum, both target areas of the burst firing cells, it has already been been shown that there is hippocampal ripple locked input as indicated by a negative deflection (sharp wave) (Chrobak and Buzsáki, 1994). It would be interesting to see if the lateral entorhinal cortex receives less or no input during hippocampal ripples.

SWRs are especially suited for memory transfer because the time scale in which cortical neurons are activated with respect to hippocampal activity is within that of plasticity (Wierzynski et al., 2009). Furthermore the burst firing neurons appear to be an ideal bearer of memory related information because their output mode, bursting, is a highly reliable way of information transfer (Lisman, 1997) and is likely to be involved in the induction of long term plasticity (Sjöström and Nelson, 2002). This all points towards a central role of burst firing neurons in the transfer of memory contents to cortical and subcortical targets.

Subicular pyramidal cells have also been shown to be spatially modulated (Deadwyler and Hampson, 2004) and show robust theta phase precession (Kim et al., 2012). There is evidence that, unlike hippocampal neurons, subicular neurons do not remap in different environments (Sharp, 2006), while Kim et al found that a fraction of cells does remap in changing environments (Kim et al., 2012). Furthermore, 'boundary-vector cells', cells with firing patterns that depend on the distance and the allocentric direction vector to a delimitation of the environment have been described (Lever et al., 2009) and have been hypothesized to provide input to place cells (Hartley et al., 2000). In a recent study the properties of place cells with respect to proximo-distal position within the subiculum was investigated and it was found that in the proximal subiculum place cells had sharp and sparse place field firing similar to area CA1 whereas further distal place cells had a higher firing rate and more distributed spatial firing with multiple unitary fields (Kim et al., 2012), resembling those seen in grid cells in the medial entorhinal cortex on a linear track (Derdikman et al., 2009; Domnisoru et al., 2013). Therefore it seems likely that the different output modes of regular and burst firing cells described here are also reflected in the sparse versus distributed spatial coding of their place fields. Additionally, the more distal place cells, presumably burst firing cells, as they greatly outnumber regular firing cells in distal subiculum, have on average a higher information content (Kim et al., 2012), i.e. at most points in time it is more informative to estimate the animal's position from the firing pattern of a population of bursting cells than from regular firing cells, again stressing the beneficial use of burst firing neurons in information processing. Since the medial entorhinal cortex is one of the target areas of subicular burst firing cells in the distal part of the subiculum and also receives input from medial entorhinal cortex (Honda et al., 2012), it is tempting to speculate that the burst firing cells are providing and/or receiving input to the grid cells of the medial entorhinal cortex, which are, like subicular place cells, less sensitive to

environmental changes than place cells in other areas (Fyhn et al., 2007). Furthermore, during SWRs, the spatial information might be distributed to other target areas involved in processing of spatial information such as the presubiculum and the retrosplenial cortex (Kim and Spruston, 2012).

Considering the spatial properties of the main input region to the subiculum, area CA1, it has been shown that there is an analogous proximo-distal organization of spatial firing properties, with proximal CA1 pyramidal cells, i.e. the cells that project to distal subiculum, having more dispersed firing fields than distal CA1 pyramidal cells (Henriksen et al., 2010), suggesting functional organization along a proximo-distal axis represents a more general principle.

If the burst firing neurons are mainly concerned with the distribution and processing of spatial information, what might be the function of the regular firing cells? The lateral entorhinal cortex is believed to process non-spatial and object-related information (Hargreaves et al., 2005; Knierim et al., 2006; Tsao et al., 2013) and projects to the proximal portion of the subiculum, presumably mainly to regular firing cells and is itself one of the target regions of regular firing cells. Therefore it appears likely that the regular firing cells are more involved in the processing of non-spatial, contextual information and distribute this information to their target areas such as amygdala and nucleus accumbens. As I have shown here, the regular firing cells are largely silenced during ripples, therefore it is unlikely that they distribute this information during ripples. Yet it has been shown in a decision making task that reactivation of ensembles of neurons that have previously been active can also occur during non-SWR states such as theta and gamma oscillations (Johnson and Redish, 2007). While a recent study suggests that regular firing cells are not participating in gamma oscillations (Eller et al., 2015) it remains to be established whether they might be activated during theta oscillations or during specific task or task periods. Of note, the firing rate of the subicular principal cells is high compared to neighboring brain regions. The decrease of this firing rate during ripples is also a signal to the downstream target regions of the subiculum. The approximately 50 ms pause of excitatory inputs during a ripple is expected to alter network dynamics in the target regions, too.

4.1.4 Limitations

One possible limitation might be the differing recording position of our in vitro and in vivo experiments: the in vivo experiments have been conducted in the dorsal part of the subiculum, whereas the in vitro experiments were conducted in the ventral to medial part of the subiculum (from our lab's experience SWRs in vitro are more readily observed in these slices). As the different modulation of burst and regular firing cells could be observed in both sets of experiments, it is likely that the same mechanisms are at work. However, it is not known if the connectivity pattern in the dorsal part of the subiculum is similar to what

we have found in acute slices from the ventral to intermediate subiculum. Furthermore it would be interesting to investigate what the connectivity matrix looks like in the very proximal and very distal part of the subiculum. For example, we have shown that the connection probability between regular to bursting cells is higher than among regular firing cells. Does the number of recurrent connections remain the same in the very proximal part of the subiculum, where there are only regular firing cells? I.e. is the number of connections also determined by 'who is around', that is, the micro environment of a cell?

In the in vivo part I inserted two glass electrodes through two separate craniotomies. The LFP electrode was advanced to the distal CA1 region and the other electrode was used to record single cells in the subiculum in juxtacellular or whole-cell patch-clamp configuration. This approach increased the stability of the whole-cell recordings but had the disadvantage that the distance between the two electrodes might vary. Therefore the timing of the reference point, the peak of the ripple oscillations, relative to the intracellularly recorded membrane potential might vary. In addition, although, ripples are expected to occur largely simultaneous across the CA1 and the subiculum, it is still conceivable that some events do not have a concurrent counterpart in the subiculum and might make the detection of a modulation more difficult or variable. Possibly this might explain some of the variability in modulation, ranging from hyperpolarization to depolarization, and cells that did not show a clear modulation.

4.1.5 Outlook

The experimental findings in the subiculum described here could be advanced along at least two major lines: firstly, the functional impact of the cellular diversity could be further explored, and secondly our findings on the local network topology could be advanced to reveal how bursting and regular firing cells are embedded into a larger anatomical network of efferent and afferent projections. To proceed, a molecular marker for bursting and regular firing cells would be of great advantage. However, such a marker has not been identified, yet. One approach to achieve this could be by single-cell RNA sequencing methods (Zeisel et al., 2015; Fuzik et al., 2016), in which the nucleus is harvested into the recording pipette during patch-clamp recordings (which would allow the electrophysiological characterization as burst or regular firing), then the content could be analyzed for its gene expression patterns in the two cell subtypes. Once a marker was found, a genetically tagged mouse-line could be engineered. As an alternative approach, one could take advantage of the fact that bursting and regular firing cells have, at least in the furthest proximal and furthest distal parts of the subiculum, largely non-overlapping target regions. Retrograde viruses injected into the target regions could therefore be used to target almost exclusively one subtype of cells (a similar approach has been taken by Znamenskiy and Zador (Znamenskiy and Zador, 2013)). A disadvantage would be that not all, for example bursting cells would

be infected and it would not be entirely specific for the cell subtype the infection is targeted at. Once a sufficiently specific infection was achieved by one or the other method, it could be combined with optogenetical techniques to specifically modulate the activity of bursting or regular firing cells. Thereby one could analyze effects on network dynamics, by, for example, deactivating bursting cells whenever a ripple occurs. A fast feedback system could be implemented to detect ripples early on, see e.g. (Jadhav and Frank, 2009), and to trigger a light pulse from a light fiber implanted into the subiculum. Would replay events and/or spatial representation be disturbed? Furthermore, the impact of this perturbation on downstream targets such as the MEC could be investigated. Ultimately one could ask if burst or regular firing cells play a specific role in behavioral tasks, i. e. if behavioral performance can be impaired by specifically silencing one subtype of subicular pyramidal cells but not the other.

The second line mentioned above concerns the larger anatomical network in which bursting and regular firing cells are embedded. Beyond the known topography of projections from area CA1 to the subiculum (Amaral et al., 1991), it would be interesting to investigate if there is a systematic pattern of CA1 projections with respect to burst and regular firing cells. As discussed above, bursting cells are according to our results locally only connected to other bursting cells but not to regular firing cells - does this separation only occur in the subiculum or do CA1 pyramidal cells and possibly also inhibitory interneurons have preferential cell subtype targets in the subiculum? This question could be tackled in part by labeling cells with a retrograde rabies virus in vivo that 'jumps' exactly one synapse, i.e. it infects presynaptic neurons of the primarily infected cell. During the whole-cell current clamp recording biophysical and functional properties could be analyzed and after expression of a tag (usually a fluorescent protein) in the presynaptic cells, the local connectivity and also long range connections onto this cell could be studied (Rancz et al., 2011). Furthermore, although burst and regular firing cells have in part different long-range projection targets (Kim and Spruston, 2012), they still have common target areas and it remains to be determined if and how projections of burst firing cells intermingle with those of regular firing cells.

4.2 Extended discussion on 'Serotonin attenuates feedback excitation onto O-LM interneurons'

By means of whole-cell patch-clamp recordings of O-LM interneurons in combination with extracellular stimulation we could show that glutamatergic transmission onto O-LM interneurons in area CA1 is decreased by serotonin. Paired recordings of connected pyramidal-O-LM cells allowed us to identify a synapse that is modulated by 5-HT. The decrease in excitatory synaptic transmission is most likely mediated by a decrease in calcium influx

into presynaptic terminals and results, at least in part, from activation of the 5-HT_{1A} receptor subtype. This type of modulation is likely to be functionally important as action potentials evoked by theta train stimulation could readily be suppressed by release of endogenous serotonin. These experiments also show that the extremely low release probability, as demonstrated by the strong facilitation during consecutive stimuli as well as the high failure rate in the paired recordings, can be overcome by a theta stimulation protocol. This stimulation presumably leads to a high number of synchronously activated pyramidal cells that provide convergent glutamatergic input onto each O-LM interneuron allowing a sufficiently strong excitation to evoke action potential firing in O-LM interneurons despite the low release probability at this synapse. In the following paragraphs I will discuss (i) how pre- and post-synaptic modulatory effects of serotonin onto O-LM interneurons might add up, (ii) the expression of 5-HT receptor subtypes on axon terminals, and (iii) the state-dependent activity of serotonergic neurons. Finally I will consider some limitations of our approach and point to possible future directions.

4.2.1 What is the net effect of serotonin released onto O-LM interneurons?

In addition to the decrease in excitatory transmission upon 5-HT application, which we focused on in this study, 5-HT has also been shown to evoke an inward current in interneurons of the stratum oriens, mediated by 5-HT_2 receptors (Lee et al., 1999). This would depolarize O-LM interneurons, counterbalancing the reduction in excitatory transmission onto O-LM interneurons. However, while we did observe an inward current upon 5-HT application, we did not observe any prominent inward current after application of fenfluramine, an agent that triggers release of endogenous serotonin. The reason for this might be that the amount of active serotonin that is released upon fenfluramine application differs from that resulting from bath applied serotonin. This might lead to different effects if the receptors mediating the decrease in glutamatergic transmission and the one mediating the inward current have different affinities. Another explanation could be that the release of serotonin from stores in the slice is closer to the synapse and does not reach the respective postsynaptic somatic receptors responsible for the inward current. For both possibilities, in a more 'naturalistic' scenario in which serotonin is released upon raphe nuclei activity, the primary effect will be a reduction in the excitatory transmission onto O-LM cells. We conclude that the net effect of naturally released 5-HT onto O-LM interneurons will be a decrease in their activity, in line with our data from the evoked spike trains.

4.2.2 CA1 pyramidal cell axons express different 5-HT receptor subtypes

CCK positive interneurons, parvalbumin positive fast spiking basket cells, as well as O-LM interneurons are innervated mostly, if not exclusively by local CA1 pyramidal cells. For

CCK positive interneurons it has been shown that serotonin reduces synaptic excitation onto this cell type via presynaptic 5-HT_{1B} receptors, in contrast to parvalbumin expressing basket cells which are not modulated (Winterer et al., 2011). We have shown here that excitation onto O-LM interneurons is decreased by serotonin, albeit mediated by a different receptor subtype. From this it follows that there have to be CA1 pyramidal cell axons that express either exclusively 5-HT_{1B} - or 5-HT_{1A} receptors or none of them. In addition, they must then be selectively connected to the respective cell type. It remains to be investigated if pyramidal cells express different receptor configurations on different axonal branches or if a pyramidal cell with a certain configuration only targets specific cell types.

4.2.3 State–dependent activity of serotonergic neurons

As pointed out in the introduction, serotonergic signaling is involved in the regulation of various cognitive and behavioral functions. Serotonin is released upon action potential triggered vesicular release, therefore it should be feasible to infer timing and state dependence of serotonin action from activity patterns of the raphe nuclei. Several studies have been conducted in which extracellular recording methods have been employed to assess the activity of raphe nuclei neurons: the firing rate was found to be higher in the awake state than during sleep (McGinty and Harper, 1976; Trulson and Jacobs, 1979). However, the interpretation of these data is complicated by the vast diversity of raphe nuclei neurons, of which only a subset is serotonergic (Kirby et al., 2003). As a consequence the firing rate of raphe nuclein neurons is not always predictive of serotonin release. Another study in which putative serotonergic neurons were identified by their characteristic wave form, reported reciprocal activity during sleep/wake states among serotonergic neurons of the raphe nuclei (Urbain et al., 2006). Recently, recordings of identified serotonergic neurons became available by employing juxtacellular recordings and subsequent immunohistochemical analysis (Kocsis et al., 2006). This study demonstrated diverse correlations between firing rate and theta/non-theta states among serotonergic neurons in awake animals: one subpopulation of serotonergic neurons exhibited a clock-like activity that did not fire coherent with hippocampal theta oscillations. However, the firing rate in 3 out of 4 cells was decreased during theta states. Another subpopulation with confirmed serotonergic identity displayed phase-locked activity to hippocampal theta rhythm, although the firing rate was similarly high, both during theta and non-theta states (Kocsis et al., 2006). Earlier studies indicate that median raphe lesions lead to enhanced theta oscillations, independent of behavior (Maru et al., 1979). This phenotype could be attributed to 5-HT_{1A} receptor function as 5-HT_{1A} knock-out mice showed increased levels of theta oscillations as compared to wildtype littermates (Gordon et al., 2005) and increased levels of anxiety-related behavior (Ramboz et al., 1998; Heisler et al., 1998). These data indicate that under normal conditions, serotonin serves to inhibit excessive theta oscillations.

Previous studies have demonstrated that O-LM cells are active during theta oscillations. Interestingly, O-LM cells fire during the trough of theta oscillations (Varga et al., 2012; Katona et al., 2014), while a subset of serotonergic neurons elicits action potentials during the peak of theta oscillations (Kocsis et al., 2006). Possibly, rhythmic release of serotonin, i.e. phasic inhibition of glutamatergic transmission onto O-LM cells, might enable the phase-locked activity of O-LM interneurons during hippocampal theta under normal conditions. In the absence of serotonin action on 5-HT_{1A} receptors, as in the knock-out mice, the precise timing of O-LM cells with respect to theta oscillations might be lost, interfering with a normal regulation of theta-oscillations. However, manifold changes in synaptic transmission in different cell types and in different brain regions might contribute to the observed phenotype.

Moreover, it was found that during the inactive component of slow wave activity (i.e. in the absence of spindles, which in turn have been described to be associated with hippocampal ripples (Sirota et al., 2003)), firing of identified serotonergic neurons is increased compared to the active component (Schweimer et al., 2011). In this scenario glutamatergic transmission onto O-LM cells during SWRs is fully functional and active O-LM cells (Varga et al., 2012; Pangalos et al., 2013; Forro et al., 2015) might contribute to limit the influence of entorhinal cortex input (Leão et al., 2012) while at the same time facilitating intrahippocampal processing by counteracting Schaffer-collateral feedforward inhibition.

4.2.4 Limitations and outlook

With our methods we were not able to fully resolve which combination of receptor subtypes are responsible for the modulation by 5-HT. The commonly used 5-HT receptor subtype agonists and antagonists are not entirely specific and exhibit a variety of side-effects that might hinder the interpretation of the results yielded with those compounds. Moreover, it was found that O-LM cells can be divided into two subgroups based on their developmental origin and the expression of 5-HT_{3A}receptors (Chittajallu et al., 2013). In our study we did not distinguish between those two and it is not unlikely that the pyramidal cells targeting those two subtypes express different 5-HT receptor subtypes. This might be responsible for the only partial blockade of the reduction of glutamatergic transmission onto O-LM cells by the 5-HT_{1A} antagonist. Furthermore, the time course, concentration and spatial spread of serotonin bath application might differ from the natural conditions in vivo. In addition, the tissue penetration of the compounds could be inhomogenous throughout the slice and among different components. To partially overcome some of these limitations, one could use genetically modified mouse lines in which serotonergic projections can be specifically activated and in this way evoke serotonin release more naturally. In addition, new pharmacogenetic tools are being developed that will allow to target endogenously expressed receptors in specific cell types.

The observation that active O-LM cells can control incoming inputs from the EC and at the same time disinhibit Schaffer collateral input (Leão et al., 2012), led us to hypothesize that serotonin might act as a switch from predominant intra-hippocampal computation and the integration of inputs from the entorhinal cortex. This could be tested by comparing the efficiency of temperoammonic pathway and Schaffer collateral stimulation in control conditions and upon 5-HT application.

Understanding the action of serotonergic neuromodulation on a network level is of great interest, also because malfunctioning of the serotonergic system has been implicated in a number of psychiatric diseases. To fully understand how serotonergic neuromodulation is related to changes in brain state and hippocampal activity, it will be required to monitor the activity of identified serotonergic neurons and possibly manipulate them selectively. Furthermore, mouse models of psychiatric diseases could be employed to screen both for alterations in the serotonergic modulation of synaptic transmission, for example due to dysfunctional serotonin receptors, or altered activity of serotonergic neurons in the raphe nuclei.

4.3 Conclusions

The hippocampus, among other brain regions, is important for the formation, consolidation and retrieval of memory. These functions demand a network that is capable of reliable and yet flexible computation in a brain-state dependent manner. In addition, incoming intra- and extra-hippocampal signals need to be processed and integrated into existing activity patterns, possibly representing earlier memory traces. A defined network of local connections as well as long-range projecting neurons are finally necessary to appropriately route and distribute the results of intrahippocampal computation to its many target regions for further processing, such as evaluating possible behavioral responses and for long-term storage.

Various types of plasticity and activity modulation on different spatial and temporal scales are employed to fulfill these functions. This thesis presents examples of some of the principles that help to endow the hippocampus with its various functions: firstly, the modulation of O-LM interneurons by serotonin serves as an example for the action of neuromodulators, which can be spatially distributed and yet specific by means of selective receptor expression. The O-LM interneuron influences and even gates incoming inputs from both area CA3 and entorhinal cortex and is therefore in a strategically important position to integrate information from other brain areas. Secondly, oscillations are a mean to synchronize neuronal activity, which is important for the coordinated activity of groups of neurons and neuron types. In my thesis I focused on ripples, which occur in a particular brain state and play an important role in the consolidation of memory which in turn involves information transfer to other cortical and subcortical areas. As the subiculum is one of the

major output regions of the hippocampus I analyzed the sub- and suprathreshold modulation of subicular pyramidal cells during these network oscillations. These results suggest that the subiculum routes outgoing signals during ripples in a cell-subtype dependent fashion. The functional diversity of principal neurons, which is supported by the local network architecture, can be viewed as another path towards achieving the intricate computations fulfilled by the hippocampus, addressed in this thesis.

Appendix A

List of publications

- Claudia Böhm, Yangfan Peng, Nikolaus Maier, Jochen Winterer, James F.A. Poulet, Jörg R.P. Geiger and Dietmar Schmitz. Functional diversity of subicular principal cells during hippocampal ripples. *The Journal of Neuroscience*, 35(40):13608 —13618, Oct 2015
  http://dx.doi.org/10.1523/JNEUROSCI.5034-14.2015.

- Claudia Böhm, Maria Pangalos, Jochen Winterer and Dietmar Schmitz. Serotonin attenuates feedback excitation onto O-LM interneurons. *Cerebral Cortex*, 25(11):4572–4583, Nov 2015
  http://dx.doi.org/10.1093/cercor/bhv098.

- Prateep Beed, Anja Gundlfinger, Sophie Schneiderbauer, Jie Song, Claudia Böhm, Andrea Burgalossi, Michael Brecht, Imre Vida and Dietmar Schmitz. Inhibitory gradient along the dorsoventral axis in the medial entorhinal cortex. *Neuron*, 79(6):1197–1207, Sep 2013
  http://dx.doi.org/10.1016/j.neuron.2013.06.038.

- Nikolaus Maier, Genela Morris, Sebastian Schuchmann, Tatiana Korotkova, Alexey Ponomarenko, Claudia Böhm, Christian Wozny and Dietmar Schmitz. Cannabinoids disrupt hippocampal sharp wave-ripples via inhibition of glutamate release. *Hippocampus*, 22(6):1350–1362, June 2012
  http://dx.doi.org/10.1002/hipo.20971.

- Shota Zarnadze, Peter Bäuerle, Claudia Böhm, Dietmar Schmitz, Jörg R.P. Geiger, Tamar Dugladze and Tengis Gloveli. Cell-specific synaptic plasticity induced by network oscillations. *in revison.*

Bibliography

Ali AB, Thomson AM (1998) Facilitating pyramid to horizontal oriens-alveus interneurone inputs: dual intracellular recordings in slices of rat hippocampus. *J Physiol*, 507 (Pt 1):185–199.

Amaral DG, Dolorfo C, Alvarez-Royo P (1991) Organization of CA1 projections to the subiculum: a PHA-L analysis in the rat. *Hippocampus*, 1(4):415–435.

Andersen P, Morris R, Amaral D, Bliss T, O'Keefe J (2006) *The Hippocampus Book*. Oxford University Press.

Andrade R, Nicoll RA (1987) Pharmacologically distinct actions of serotonin on single pyramidal neurones of the rat hippocampus recorded in vitro. *J Physiol*, 394:99–124.

Bayley PJ, Hopkins RO, Squire LR (2006) The fate of old memories after medial temporal lobe damage. *J Neurosci*, 26(51):13311–13317.

Beck SG, Pan YZ, Akanwa AC, Kirby LG (2004) Median and dorsal raphe neurons are not electrophysiologically identical. *J Neurophysiol*, 91(2):994–1005.

Behr J, Wozny C, Fidzinski P, Schmitz D (2009) Synaptic plasticity in the subiculum. *Prog Neurobiol*, 89(4):334–342.

Bell CC, Han VZ, Sugawara Y, Grant K (1997) Synaptic plasticity in a cerebellum-like structure depends on temporal order. *Nature*, 387(6630):278–281.

Belluscio MA, Mizuseki K, Schmidt R, Kempter R, Buzsáki G (2012) Cross-frequency phase-phase coupling between theta and gamma oscillations in the hippocampus. *J Neurosci*, 32(2):423–435.

Bi GQ, Poo MM (1998) Synaptic modifications in cultured hippocampal neurons: dependence on spike timing, synaptic strength, and postsynaptic cell type. *J Neurosci*, 18(24):10464–10472.

Blasco-Ibáñez JM, Freund TF (1995) Synaptic input of horizontal interneurons in stratum oriens of the hippocampal CA1 subfield: structural basis of feed-back activation. *Eur J Neurosci*, 7(10):2170–2180.

Bliss TV, Lømo T (1973) Long-lasting potentiation of synaptic transmission in the dentate area of the anaesthetized rabbit following stimulation of the perforant path. *J Physiol*, 232(2):331–356.

Bragin A, Jandó G, Nádasdy Z, Hetke J, Wise K, Buzsáki G (1995) Gamma (40-100 Hz) oscillation in the hippocampus of the behaving rat. *J Neurosci*, 15(1 Pt 1):47–60.

Bunsey M, Eichenbaum H (1995) Selective damage to the hippocampal region blocks long-term retention of a natural and nonspatial stimulus-stimulus association. *Hippocampus*, 5(6):546–556.

Burton S, Murphy D, Qureshi U, Sutton P, O'Keefe J (2000) Combined lesions of hippocampus and subiculum do not produce deficits in a nonspatial social olfactory memory task. *J Neurosci*, 20(14):5468–5475.

Buzsáki G (1986) Hippocampal sharp waves: their origin and significance. *Brain Res*, 398(2):242–252.

Buzsáki G (1989) Two-stage model of memory trace formation: a role for "noisy" brain states. *Neuroscience*, 31(3):551–570.

Buzsáki G, Draguhn A (2004) Neuronal oscillations in cortical networks. *Science*, 304(5679):1926–1929.

Buzsáki G, Anastassiou CA, Koch C (2012) The origin of extracellular fields and currents–EEG, ECoG, LFP and spikes. *Nat Rev Neurosci*, 13(6):407–420.

Buzsáki G, Wang XJ (2012) Mechanisms of gamma oscillations. *Annu Rev Neurosci*, 35:203–225.

Bähner F, Weiss EK, Birke G, Maier N, Schmitz D, Rudolph U, Frotscher M, Traub RD, Both M, Draguhn A (2011) Cellular correlate of assembly formation in oscillating hippocampal networks in vitro. *Proc Natl Acad Sci U S A*, 108(35):E607–E616.

Böhm C, Pangalos M, Schmitz D, Winterer J (2015a) Serotonin attenuates feedback excitation onto O-LM interneurons. *Cereb Cortex*, 25(11):4572–4583.

Böhm C, Peng Y, Maier N, Winterer J, Poulet JFA, Geiger JRP, Schmitz D (2015b) Functional diversity of subicular principal cells during hippocampal ripples. *J Neurosci*, 35(40):13608–13618.

Cai X, Kallarackal AJ, Kvarta MD, Goluskin S, Gaylor K, Bailey AM, Lee HK, Huganir RL, Thompson SM (2013) Local potentiation of excitatory synapses by serotonin and its alteration in rodent models of depression. *Nat Neurosci*, 16(4):464–472.

Caporale N, Dan Y (2008) Spike timing-dependent plasticity: a hebbian learning rule. *Annu Rev Neurosci*, 31:25–46.

Chen JL, Carta S, Soldado-Magraner J, Schneider BL, Helmchen F (2013) Behaviour-dependent recruitment of long-range projection neurons in somatosensory cortex. *Nature*, 499(7458):336–340.

Chittajallu R, Craig MT, McFarland A, Yuan X, Gerfen S, Tricoire L, Erkkila B, Barron SC, Lopez CM, Liang BJ, Jeffries BW, Pelkey KA, McBain CJ (2013) Dual origins of functionally distinct O-LM interneurons revealed by differential 5-HT(3A)R expression. *Nat Neurosci*, 16(11):1598–1607.

Chrobak JJ, Buzsáki G (1994) Selective activation of deep layer (V-VI) retrohippocampal cortical neurons during hippocampal sharp waves in the behaving rat. *J Neurosci*, 14(10):6160–6170.

Cohen I, Navarro V, Clemenceau S, Baulac M, Miles R (2002) On the origin of interictal activity in human temporal lobe epilepsy in vitro. *Science*, 298(5597):1418–1421.

Dahlstroem A, Fuxe K (1964) Evidence for the existence of monoamine-containing neurons in the central nervous system. I. Demonstration of monoamines in the cell bodies of brain stem neurons. *Acta Physiol Scand Suppl*, pp. SUPPL 232:1–SUPPL 23255.

Davies DC, Wilmott AC, Mann DM (1988) Senile plaques are concentrated in the subicular region of the hippocampal formation in Alzheimer's disease. *Neurosci Lett*, 94(1-2):228–233.

Deadwyler SA, Hampson RE (2004) Differential but complementary mnemonic functions of the hippocampus and subiculum. *Neuron*, 42(3):465–476.

Deguchi Y, Donato F, Galimberti I, Cabuy E, Caroni P (2011) Temporally matched subpopulations of selectively interconnected principal neurons in the hippocampus. *Nat Neurosci*, 14(4):495–504.

Derdikman D, Whitlock JR, Tsao A, Fyhn M, Hafting T, Moser MB, Moser EI (2009) Fragmentation of grid cell maps in a multicompartment environment. *Nat Neurosci*, 12(10):1325–1332.

Deuchars J, Thomson AM (1996) CA1 pyramid-pyramid connections in rat hippocampus in vitro: dual intracellular recordings with biocytin filling. *Neuroscience*, 74(4):1009–1018.

Diekelmann S, Born J (2010) The memory function of sleep. *Nat Rev Neurosci*, 11(2):114–126.

Ding SL (2013) Comparative anatomy of the prosubiculum, subiculum, presubiculum, postsubiculum, and parasubiculum in human, monkey, and rodent. *J Comp Neurol*, 521(18):4145–4162.

Domnisoru C, Kinkhabwala AA, Tank DW (2013) Membrane potential dynamics of grid cells. *Nature*, 495(7440):199–204.

Draguhn A, Traub RD, Schmitz D, Jefferys JG (1998) Electrical coupling underlies high-frequency oscillations in the hippocampus in vitro. *Nature*, 394(6689):189–192.

Ego-Stengel V, Wilson MA (2010) Disruption of ripple-associated hippocampal activity during rest impairs spatial learning in the rat. *Hippocampus*, 20(1):1–10.

Eichenbaum H (2004) Hippocampus: cognitive processes and neural representations that underlie declarative memory. *Neuron*, 44(1):109–120.

Eller J, Zarnadze S, Bäuerle P, Dugladze T, Gloveli T (2015) Cell type-specific separation of subicular principal neurons during network activities. *PLoS One*, 10(4):e0123636.

English DF, Peyrache A, Stark E, Roux L, Vallentin D, Long MA, Buzsáki G (2014) Excitation and inhibition compete to control spiking during hippocampal ripples: intracellular study in behaving mice. *J Neurosci*, 34(49):16509–16517.

Epsztein J, Brecht M, Lee AK (2011) Intracellular determinants of hippocampal CA1 place and silent cell activity in a novel environment. *Neuron*, 70(1):109–120.

Feldmeyer D, Lübke J, Sakmann B (2006) Efficacy and connectivity of intracolumnar pairs of layer 2/3 pyramidal cells in the barrel cortex of juvenile rats. *J Physiol*, 575(Pt 2):583–602.

Fisahn A (2005) Kainate receptors and rhythmic activity in neuronal networks: hippocampal gamma oscillations as a tool. *J Physiol*, 562(Pt 1):65–72.

Fisahn A, Pike FG, Buhl EH, Paulsen O (1998) Cholinergic induction of network oscillations at 40 hz in the hippocampus in vitro. *Nature*, 394(6689):186–189.

Forro T, Valenti O, Lasztoczi B, Klausberger T (2015) Temporal organization of GABAergic interneurons in the intermediate CA1 hippocampus during network oscillations. *Cereb Cortex*, 25(5):1228–1240.

Fortin NJ, Agster KL, Eichenbaum HB (2002) Critical role of the hippocampus in memory for sequences of events. *Nat Neurosci*, 5(5):458–462.

Frank LM, Brown EN, Stanley GB (2006) Hippocampal and cortical place cell plasticity: implications for episodic memory. *Hippocampus*, 16(9):775–784.

Freund TF, Buzsáki G (1996) Interneurons of the hippocampus. *Hippocampus*, 6(4):347–470.

Fuhrmann F, Justus D, Sosulina L, Kaneko H, Beutel T, Friedrichs D, Schoch S, Schwarz MK, Fuhrmann M, Remy S (2015) Locomotion, theta oscillations, and the speed-correlated firing of hippocampal neurons are controlled by a medial septal glutamatergic circuit. *Neuron*, 86(5):1253–1264.

Fuzik J, Zeisel A, Máté Z, Calvigioni D, Yanagawa Y, Szabó G, Linnarsson S, Harkany T (2016) Integration of electrophysiological recordings with single-cell RNA-seq data identifies neuronal subtypes. *Nat Biotechnol*, 34(2):175–183.

Fyhn M, Hafting T, Treves A, Moser MB, Moser EI (2007) Hippocampal remapping and grid realignment in entorhinal cortex. *Nature*, 446(7132):190–194.

Gasbarri A, Verney C, Innocenzi R, Campana E, Pacitti C (1994) Mesolimbic dopaminergic neurons innervating the hippocampal formation in the rat: a combined retrograde tracing and immunohistochemical study. *Brain Res*, 668(1-2):71–79.

Girardeau G, Benchenane K, Wiener SI, Buzsáki G, Zugaro MB (2009) Selective suppression of hippocampal ripples impairs spatial memory. *Nat Neurosci*, 12(10):1222–1223.

Gloveli T, Dugladze T, Rotstein HG, Traub RD, Monyer H, Heinemann U, Whittington MA, Kopell NJ (2005) Orthogonal arrangement of rhythm-generating microcircuits in the hippocampus. *Proc Natl Acad Sci U S A*, 102(37):13295–13300.

Goldin M, Epsztein J, Jorquera I, Represa A, Ben-Ari Y, Crépel V, Cossart R (2007) Synaptic kainate receptors tune oriens-lacunosum moleculare interneurons to operate at theta frequency. *J Neurosci*, 27(36):9560–9572.

Gordon JA, Lacefield CO, Kentros CG, Hen R (2005) State-dependent alterations in hippocampal oscillations in serotonin 1A receptor-deficient mice. *J Neurosci*, 25(28):6509–6519.

Goutagny R, Jackson J, Williams S (2009) Self-generated theta oscillations in the hippocampus. *Nat Neurosci*, 12(12):1491–1493.

Graves AR, Moore SJ, Bloss EB, Mensh BD, Kath WL, Spruston N (2012) Hippocampal pyramidal neurons comprise two distinct cell types that are countermodulated by metabotropic receptors. *Neuron*, 76(4):776–789.

Greene JR, Mason A (1996) Neuronal diversity in the subiculum: correlations with the effects of somatostatin on intrinsic properties and on GABA-mediated IPSPs in vitro. *J Neurophysiol*, 76(3):1657–1666.

Griguoli M, Maul A, Nguyen C, Giorgetti A, Carloni P, Cherubini E (2010) Nicotine blocks the hyperpolarization-activated current Ih and severely impairs the oscillatory behavior of oriens-lacunosum moleculare interneurons. *J Neurosci*, 30(32):10773–10783.

Hampson RE, Deadwyler SA (2003) Temporal firing characteristics and the strategic role of subicular neurons in short-term memory. *Hippocampus*, 13(4):529–541.

Hannon J, Hoyer D (2008) Molecular biology of 5-HT receptors. *Behav Brain Res*, 195(1):198–213.

Hargreaves EL, Rao G, Lee I, Knierim JJ (2005) Major dissociation between medial and lateral entorhinal input to dorsal hippocampus. *Science*, 308(5729):1792–1794.

Harris KD, Hirase H, Leinekugel X, Henze DA, Buzsáki G (2001) Temporal interaction between single spikes and complex spike bursts in hippocampal pyramidal cells. *Neuron*, 32(1):141–149.

Harrison PJ, Eastwood SL (2001) Neuropathological studies of synaptic connectivity in the hippocampal formation in schizophrenia. *Hippocampus*, 11(5):508–519.

Hartley T, Burgess N, Lever C, Cacucci F, O'Keefe J (2000) Modeling place fields in terms of the cortical inputs to the hippocampus. *Hippocampus*, 10(4):369–379.

Hasselmo ME (1995) Neuromodulation and cortical function: modeling the physiological basis of behavior. *Behav Brain Res*, 67(1):1–27.

Hebb DO (1949) *The organization of behavior: A neuropsychological theory.* New York: Wiley.

Heisler LK, Chu HM, Brennan TJ, Danao JA, Bajwa P, Parsons LH, Tecott LH (1998) Elevated anxiety and antidepressant-like responses in serotonin 5-HT1A receptor mutant mice. *Proc Natl Acad Sci U S A*, 95(25):15049–15054.

Henriksen EJ, Colgin LL, Barnes CA, Witter MP, Moser MB, Moser EI (2010) Spatial representation along the proximodistal axis of CA1. *Neuron*, 68(1):127–137.

Honda Y, Sasaki H, Umitsu Y, Ishizuka N (2012) Zonal distribution of perforant path cells in layer III of the entorhinal area projecting to CA1 and subiculum in the rat. *Neurosci Res*, 74(3-4):200–209.

Huxter JR, Zinyuk LE, v L Roloff E, Clarke VRJ, Dolman NP, More JCA, Jane DE, Collingridge GL, Muller RU (2007) Inhibition of kainate receptors reduces the frequency of hippocampal theta oscillations. *J Neurosci*, 27(9):2212–2223.

Hyman BT, Hoesen GWV, Damasio AR, Barnes CL (1984) Alzheimer's disease: cell-specific pathology isolates the hippocampal formation. *Science*, 225(4667):1168–1170.

Inostroza M, Born J (2013) Sleep for preserving and transforming episodic memory. *Annu Rev Neurosci*.

Jackson J, Amilhon B, Goutagny R, Bott JB, Manseau F, Kortleven C, Bressler SL, Williams S (2014) Reversal of theta rhythm flow through intact hippocampal circuits. *Nat Neurosci*, 17(10):1362–1370.

Jadhav SP, Frank LM (2009) Reactivating memories for consolidation. *Neuron*, 62(6):745–746.

Jadhav SP, Kemere C, German PW, Frank LM (2012) Awake hippocampal sharp-wave ripples support spatial memory. *Science*, 336(6087):1454–1458.

Jarrard LE, Feldon J, Rawlins JN, Sinden JD, Gray JA (1986) The effects of intrahippocampal ibotenate on resistance to extinction after continuous or partial reinforcement. *Exp Brain Res*, 61(3):519–530.

Jensen O, Lisman JE (2000) Position reconstruction from an ensemble of hippocampal place cells: contribution of theta phase coding. *J Neurophysiol*, 83(5):2602–2609.

Johnson A, Redish AD (2007) Neural ensembles in CA3 transiently encode paths forward of the animal at a decision point. *J Neurosci*, 27(45):12176–12189.

Jung HY, Staff NP, Spruston N (2001) Action potential bursting in subicular pyramidal neurons is driven by a calcium tail current. *J Neurosci*, 21(10):3312–3321.

Jung MW, McNaughton BL (1993) Spatial selectivity of unit activity in the hippocampal granular layer. *Hippocampus*, 3(2):165–182.

Kamondi A, Acsády L, Wang XJ, Buzsáki G (1998) Theta oscillations in somata and dendrites of hippocampal pyramidal cells in vivo: activity-dependent phase-precession of action potentials. *Hippocampus*, 8(3):244–261.

Karlsson MP, Frank LM (2008) Network dynamics underlying the formation of sparse, informative representations in the hippocampus. *J Neurosci*, 28(52):14271–14281.

Katona L, Lapray D, Viney TJ, Oulhaj A, Borhegyi Z, Micklem BR, Klausberger T, Somogyi P (2014) Sleep and movement differentiates actions of two types of somatostatin-expressing GABAergic interneuron in rat hippocampus. *Neuron*, 82(4):872–886.

Katzner S, Nauhaus I, Benucci A, Bonin V, Ringach DL, Carandini M (2009) Local origin of field potentials in visual cortex. *Neuron*, 61(1):35–41.

Kim SM, Frank LM (2009) Hippocampal lesions impair rapid learning of a continuous spatial alternation task. *PLoS One*, 4(5):e5494.

Kim SM, Ganguli S, Frank LM (2012) Spatial information outflow from the hippocampal circuit: distributed spatial coding and phase precession in the subiculum. *J Neurosci*, 32(34):11539–11558.

Kim Y, Spruston N (2012) Target-specific output patterns are predicted by the distribution of regular-spiking and bursting pyramidal neurons in the subiculum. *Hippocampus*, 22(4):693–706.

Kintscher M, Breustedt J, Miceli S, Schmitz D, Wozny C (2012) Group II metabotropic glutamate receptors depress synaptic transmission onto subicular burst firing neurons. *PLoS One*, 7(9):e45039.

Kirby LG, Pernar L, Valentino RJ, Beck SG (2003) Distinguishing characteristics of serotonin and non-serotonin-containing cells in the dorsal raphe nucleus: electrophysiological and immunohistochemical studies. *Neuroscience*, 116(3):669–683.

Kispersky TJ, Fernandez FR, Economo MN, White JA (2012) Spike resonance properties in hippocampal O-LM cells are dependent on refractory dynamics. *J Neurosci*, 32(11):3637–3651.

Klausberger T, Magill PJ, Márton LF, Roberts JDB, Cobden PM, Buzsáki G, Somogyi P (2003) Brain-state- and cell-type-specific firing of hippocampal interneurons in vivo. *Nature*, 421(6925):844–848.

Klausberger T, Somogyi P (2008) Neuronal diversity and temporal dynamics: the unity of hippocampal circuit operations. *Science*, 321(5885):53–57.

Knierim JJ, Lee I, Hargreaves EL (2006) Hippocampal place cells: parallel input streams, subregional processing, and implications for episodic memory. *Hippocampus*, 16(9):755–764.

Ko H, Hofer SB, Pichler B, Buchanan KA, Sjöström PJ, Mrsic-Flogel TD (2011) Functional specificity of local synaptic connections in neocortical networks. *Nature*, 473(7345):87–91.

Kocsis B, Varga V, Dahan L, Sik A (2006) Serotonergic neuron diversity: identification of raphe neurons with discharges time-locked to the hippocampal theta rhythm. *Proc Natl Acad Sci U S A*, 103(4):1059–1064.

Kosaka T, Wu JY, Benoit R (1988) GABAergic neurons containing somatostatin-like immunoreactivity in the rat hippocampus and dentate gyrus. *Exp Brain Res*, 71(2):388–398.

Kosofsky BE, Molliver ME (1987) The serotoninergic innervation of cerebral cortex: different classes of axon terminals arise from dorsal and median raphe nuclei. *Synapse*, 1(2):153–168.

Kroeze WK, Kristiansen K, Roth BL (2002) Molecular biology of serotonin receptors structure and function at the molecular level. *Curr Top Med Chem*, 2(6):507–528.

Kropff E, Carmichael JE, Moser MB, Moser EI (2015) Speed cells in the medial entorhinal cortex. *Nature*, 523(7561):419–424.

Lacaille JC, Mueller AL, Kunkel DD, Schwartzkroin PA (1987) Local circuit interactions between oriens/alveus interneurons and CA1 pyramidal cells in hippocampal slices: electrophysiology and morphology. *J Neurosci*, 7(7):1979–1993.

Latuske P, Toader O, Allen K (2015) Interspike intervals reveal functionally distinct cell populations in the medial entorhinal cortex. *J Neurosci*, 35(31):10963–10976.

Lee AK, Wilson MA (2004) A combinatorial method for analyzing sequential firing patterns involving an arbitrary number of neurons based on relative time order. *J Neurophysiol*, 92(4):2555–2573.

Lee K, Dixon AK, Pinnock RD (1999) Serotonin depolarizes hippocampal interneurones in the rat stratum oriens by interaction with 5HT2 receptors. *Neurosci Lett*, 270(1):56–58.

Lee SH, Marchionni I, Bezaire M, Varga C, Danielson N, Lovett-Barron M, Losonczy A, Soltesz I (2014) Parvalbumin-positive basket cells differentiate among hippocampal pyramidal cells. *Neuron*, 82(5):1129–1144.

Lever C, Burton S, Jeewajee A, O'Keefe J, Burgess N (2009) Boundary vector cells in the subiculum of the hippocampal formation. *J Neurosci*, 29(31):9771–9777.

Levy WB, Steward O (1983) Temporal contiguity requirements for long-term associative potentiation/depression in the hippocampus. *Neuroscience*, 8(4):791–797.

Leão RN, Mikulovic S, Leão KE, Munguba H, Gezelius H, Enjin A, Patra K, Eriksson A, Loew LM, Tort ABL, Kullander K (2012) OLM interneurons differentially modulate CA3 and entorhinal inputs to hippocampal CA1 neurons. *Nat Neurosci*, 15(11):1524–1530.

Lisman JE (1997) Bursts as a unit of neural information: making unreliable synapses reliable. *Trends Neurosci*, 20(1):38–43.

Lisman JE, Jensen O (2013) The theta-gamma neural code. *Neuron*, 77(6):1002–1016.

Liu X, Ramirez S, Pang PT, Puryear CB, Govindarajan A, Deisseroth K, Tonegawa S (2012) Optogenetic stimulation of a hippocampal engram activates fear memory recall. *Nature*, 484(7394):381–385.

Loy R, Koziell DA, Lindsey JD, Moore RY (1980) Noradrenergic innervation of the adult rat hippocampal formation. *J Comp Neurol*, 189(4):699–710.

Maccaferri G, Dingledine R (2002) Control of feedforward dendritic inhibition by NMDA receptor-dependent spike timing in hippocampal interneurons. *J Neurosci*, 22(13):5462–5472.

Maccaferri G, McBain CJ (1995) Passive propagation of LTD to stratum oriens-alveus inhibitory neurons modulates the temporoammonic input to the hippocampal CA1 region. *Neuron*, 15(1):137–145.

Maccaferri G, McBain CJ (1996) The hyperpolarization-activated current (Ih) and its contribution to pacemaker activity in rat CA1 hippocampal stratum oriens-alveus interneurones. *J Physiol*, 497 (Pt 1):119–130.

Mamounas LA, Mullen CA, O'Hearn E, Molliver ME (1991) Dual serotoninergic projections to forebrain in the rat: morphologically distinct 5-HT axon terminals exhibit differential vulnerability to neurotoxic amphetamine derivatives. *J Comp Neurol*, 314(3):558–586.

Markram H, Lübke J, Frotscher M, Sakmann B (1997) Regulation of synaptic efficacy by coincidence of postsynaptic APs and EPSPs. *Science*, 275(5297):213–215.

Markram H, Toledo-Rodriguez M, Wang Y, Gupta A, Silberberg G, Wu C (2004) Interneurons of the neocortical inhibitory system. *Nat Rev Neurosci*, 5(10):793–807.

Marshall L, Helgadóttir H, Mölle M, Born J (2006) Boosting slow oscillations during sleep potentiates memory. *Nature*, 444(7119):610–613.

Martina M, Vida I, Jonas P (2000) Distal initiation and active propagation of action potentials in interneuron dendrites. *Science*, 287(5451):295–300.

Maru E, Takahashi LK, Iwahara S (1979) Effects of median raphe nucleus lesions on hippocampal EEG in the freely moving rat. *Brain Res*, 163(2):223–234.

McBain CJ, DiChiara TJ, Kauer JA (1994) Activation of metabotropic glutamate receptors differentially affects two classes of hippocampal interneurons and potentiates excitatory synaptic transmission. *J Neurosci*, 14(7):4433–4445.

McGinty DJ, Harper RM (1976) Dorsal raphe neurons: depression of firing during sleep in cats. *Brain Res*, 101(3):569–575.

McKenna JT, Vertes RP (2001) Collateral projections from the median raphe nucleus to the medial septum and hippocampus. *Brain Res Bull*, 54(6):619–630.

McKinney M, Coyle JT, Hedreen JC (1983) Topographic analysis of the innervation of the rat neocortex and hippocampus by the basal forebrain cholinergic system. *J Comp Neurol*, 217(1):103–121.

Melzer S, Michael M, Caputi A, Eliava M, Fuchs EC, Whittington MA, Monyer H (2012) Long-range-projecting GABAergic neurons modulate inhibition in hippocampus and entorhinal cortex. *Science*, 335(6075):1506–1510.

Molliver ME (1987) Serotonergic neuronal systems: what their anatomic organization tells us about function. *J Clin Psychopharmacol*, 7(6 Suppl):3S–23S.

Montgomery SM, Sirota A, Buzsáki G (2008) Theta and gamma coordination of hippocampal networks during waking and rapid eye movement sleep. *J Neurosci*, 28(26):6731–6741.

Morris RG, Anderson E, Lynch GS, Baudry M (1986) Selective impairment of learning and blockade of long-term potentiation by an N-methyl-D-aspartate receptor antagonist, AP5. *Nature*, 319(6056):774–776.

Morris RGM, Schenk F, Tweedie F, Jarrard LE (1990) Ibotenate lesions of hippocampus and/or subiculum: Dissociating components of allocentric spatial learning. *Eur J Neurosci*, 2(12):1016–1028.

Moser EI, Kropff E, Moser MB (2008) Place cells, grid cells, and the brain's spatial representation system. *Annu Rev Neurosci*, 31:69–89.

Muller RU, Kubie JL (1987) The effects of changes in the environment on the spatial firing of hippocampal complex-spike cells. *J Neurosci*, 7(7):1951–1968.

Murphy KP, Reid GP, Trentham DR, Bliss TV (1997) Activation of NMDA receptors is necessary for the induction of associative long-term potentiation in area CA1 of the rat hippocampal slice. *J Physiol*, 504 (Pt 2):379–385.

Nabavi S, Fox R, Proulx CD, Lin JY, Tsien RY, Malinow R (2014) Engineering a memory with LTD and LTP. *Nature*, 511(7509):348–352.

Naber PA, Witter MP (1998) Subicular efferents are organized mostly as parallel projections: a double-labeling, retrograde-tracing study in the rat. *J Comp Neurol*, 393(3):284–297.

Nakashiba T, Buhl DL, McHugh TJ, Tonegawa S (2009) Hippocampal CA3 output is crucial for ripple-associated reactivation and consolidation of memory. *Neuron*, 62(6):781–787.

Nakazawa K, Quirk MC, Chitwood RA, Watanabe M, Yeckel MF, Sun LD, Kato A, Carr CA, Johnston D, Wilson MA, Tonegawa S (2002) Requirement for hippocampal CA3 NMDA receptors in associative memory recall. *Science*, 297(5579):211–218.

O'Keefe J, Dostrovsky J (1971) The hippocampus as a spatial map. preliminary evidence from unit activity in the freely-moving rat. *Brain Res*, 34(1):171–175.

O'Keefe J, Nadel L (1978) *The Hippocampus as a Cognitive Map*. Oxford University Press.

O'Keefe J, Recce ML (1993) Phase relationship between hippocampal place units and the EEG theta rhythm. *Hippocampus*, 3(3):317–330.

O'Mara S (2006) Controlling hippocampal output: the central role of subiculum in hippocampal information processing. *Behav Brain Res*, 174(2):304–312.

Pandey A, Sikdar SK (2014) Depression biased non-hebbian spike-timing-dependent synaptic plasticity in the rat subiculum. *J Physiol*.

Pangalos M, Donoso JR, Winterer J, Zivkovic AR, Kempter R, Maier N, Schmitz D (2013) Recruitment of oriens-lacunosum-moleculare interneurons during hippocampal ripples. *Proc Natl Acad Sci U S A*, 110(11):4398–4403.

Patel J, Schomburg EW, Berényi A, Fujisawa S, Buzsáki G (2013) Local generation and propagation of ripples along the septotemporal axis of the hippocampus. *J Neurosci*, 33(43):17029–17041.

Ramboz S, Oosting R, Amara DA, Kung HF, Blier P, Mendelsohn M, Mann JJ, Brunner D, Hen R (1998) Serotonin receptor 1A knockout: an animal model of anxiety-related disorder. *Proc Natl Acad Sci U S A*, 95(24):14476–14481.

Rancz EA, Franks KM, Schwarz MK, Pichler B, Schaefer AT, Margrie TW (2011) Transfection via whole-cell recording in vivo: bridging single-cell physiology, genetics and connectomics. *Nat Neurosci*, 14(4):527–532.

Rich PD, Liaw HP, Lee AK (2014) Place cells. large environments reveal the statistical structure governing hippocampal representations. *Science*, 345(6198):814–817.

Royer S, Zemelman BV, Losonczy A, Kim J, Chance F, Magee JC, Buzsáki G (2012) Control of timing, rate and bursts of hippocampal place cells by dendritic and somatic inhibition. *Nat Neurosci*, 15(5):769–775.

Ryan TJ, Roy DS, Pignatelli M, Arons A, Tonegawa S (2015) Memory. Engram cells retain memory under retrograde amnesia. *Science*, 348(6238):1007–1013.

Savelli F, Yoganarasimha D, Knierim JJ (2008) Influence of boundary removal on the spatial representations of the medial entorhinal cortex. *Hippocampus*, 18(12):1270–1282.

Schlingloff D, Káli S, Freund TF, Hájos N, Gulyás AI (2014) Mechanisms of sharp wave initiation and ripple generation. *J Neurosci*, 34(34):11385–11398.

Schweimer JV, Mallet N, Sharp T, Ungless MA (2011) Spike-timing relationship of neurochemically-identified dorsal raphe neurons during cortical slow oscillations. *Neuroscience*, 196:115–123.

Scoville WB, Millner B (1957) Loss of recent memory after bilateral hippocampal lesions. *J Neurol Neurosurg Psychiatry*, 20(1):11–21.

Segal M (1975) Physiological and pharmacological evidence for a serotonergic projection to the hippocampus. *Brain Res*, 94(1):115–131.

Segal M (1980) The action of serotonin in the rat hippocampal slice preparation. *J Physiol*, 303:423–439.

Sharp PE (2006) Subicular place cells generate the same "map" for different environments: comparison with hippocampal cells. *Behav Brain Res*, 174(2):206–214.

Sharp PE, Green C (1994) Spatial correlates of firing patterns of single cells in the subiculum of the freely moving rat. *J Neurosci*, 14(4):2339–2356.

Sik A, Penttonen M, Ylinen A, Buzsáki G (1995) Hippocampal ca1 interneurons: an in vivo intracellular labeling study. *J Neurosci*, 15(10):6651–6665.

Sirota A, Csicsvari J, Buhl D, Buzsáki G (2003) Communication between neocortex and hippocampus during sleep in rodents. *Proc Natl Acad Sci U S A*, 100(4):2065–2069.

Sjöström PJ, Nelson SB (2002) Spike timing, calcium signals and synaptic plasticity. *Curr Opin Neurobiol*, 12(3):305–314.

Solstad T, Boccara CN, Kropff E, Moser MB, Moser EI (2008) Representation of geometric borders in the entorhinal cortex. *Science*, 322(5909):1865–1868.

Staff NP, Jung HY, Thiagarajan T, Yao M, Spruston N (2000) Resting and active properties of pyramidal neurons in subiculum and CA1 of rat hippocampus. *J Neurophysiol*, 84(5):2398–2408.

Stafstrom CE (2005) The role of the subiculum in epilepsy and epileptogenesis. *Epilepsy Curr*, 5(4):121–129.

Steinvorth S, Levine B, Corkin S (2005) Medial temporal lobe structures are needed to re-experience remote autobiographical memories: evidence from H.M. and W.R. *Neuropsychologia*, 43(4):479–496.

Stewart M (1997) Antidromic and orthodromic responses by subicular neurons in rat brain slices. *Brain Res*, 769(1):71–85.

Sun C, Kitamura T, Yamamoto J, Martin J, Pignatelli M, Kitch LJ, Schnitzer MJ, Tonegawa S (2015) Distinct speed dependence of entorhinal island and ocean cells, including respective grid cells. *Proc Natl Acad Sci U S A*.

Sławińska U, Kasicki S (1998) The frequency of rat's hippocampal theta rhythm is related to the speed of locomotion. *Brain Res*, 796(1-2):327–331.

Tamamaki N, Abe K, Nojyo Y (1987) Columnar organization in the subiculum formed by axon branches originating from single CA1 pyramidal neurons in the rat hippocampus. *Brain Res*, 412(1):156–160.

Thompson LT, Best PJ (1989) Place cells and silent cells in the hippocampus of freely-behaving rats. *J Neurosci*, 9(7):2382–2390.

Tort ABL, Komorowski RW, Manns JR, Kopell NJ, Eichenbaum H (2009) Theta-gamma coupling increases during the learning of item-context associations. *Proc Natl Acad Sci U S A*, 106(49):20942–20947.

Tort ABL, Rotstein HG, Dugladze T, Gloveli T, Kopell NJ (2007) On the formation of gamma-coherent cell assemblies by oriens lacunosum-moleculare interneurons in the hippocampus. *Proc Natl Acad Sci U S A*, 104(33):13490–13495.

Traub RD, Bibbig A (2000) A model of high-frequency ripples in the hippocampus based on synaptic coupling plus axon-axon gap junctions between pyramidal neurons. *J Neurosci*, 20(6):2086–2093.

Trulson ME, Jacobs BL (1979) Raphe unit activity in freely moving cats: correlation with level of behavioral arousal. *Brain Res*, 163(1):135–150.

Tsao A, Moser MB, Moser EI (2013) Traces of experience in the lateral entorhinal cortex. *Curr Biol*, 23(5):399–405.

Urbain N, Creamer K, Debonnel G (2006) Electrophysiological diversity of the dorsal raphe cells across the sleep-wake cycle of the rat. *J Physiol*, 573(Pt 3):679–695.

Valero M, Cid E, Averkin RG, Aguilar J, Sanchez-Aguilera A, Viney TJ, Gomez-Dominguez D, Bellistri E, de la Prida LM (2015) Determinants of different deep and superficial CA1 pyramidal cell dynamics during sharp-wave ripples. *Nat Neurosci*, 18(9):1281–1290.

Vandecasteele M, Varga V, Berényi A, Papp E, Barthó P, Venance L, Freund TF, Buzsáki G (2014) Optogenetic activation of septal cholinergic neurons suppresses sharp wave ripples and enhances theta oscillations in the hippocampus. *Proc Natl Acad Sci U S A*, 111(37):13535–13540.

Varga C, Golshani P, Soltesz I (2012) Frequency-invariant temporal ordering of interneuronal discharges during hippocampal oscillations in awake mice. *Proc Natl Acad Sci U S A*, 109(40):E2726–E2734.

Villani F, Johnston D (1993) Serotonin inhibits induction of long-term potentiation at commissural synapses in hippocampus. *Brain Res*, 606(2):304–308.

Vitalis T, Ansorge MS, Dayer AG (2013) Serotonin homeostasis and serotonin receptors as actors of cortical construction: special attention to the 5-HT3A and 5-HT6 receptor subtypes. *Front Cell Neurosci*, 7:93.

Vorel SR, Liu X, Hayes RJ, Spector JA, Gardner EL (2001) Relapse to cocaine-seeking after hippocampal theta burst stimulation. *Science*, 292(5519):1175–1178.

Vélez-Fort M, Rousseau CV, Niedworok CJ, Wickersham IR, Rancz EA, Brown APY, Strom M, Margrie TW (2014) The stimulus selectivity and connectivity of layer six principal cells reveals cortical microcircuits underlying visual processing. *Neuron*, 83(6):1431–1443.

Whittington MA, Traub RD, Jefferys JG (1995) Synchronized oscillations in interneuron networks driven by metabotropic glutamate receptor activation. *Nature*, 373(6515):612–615.

Wierzynski CM, Lubenov EV, Gu M, Siapas AG (2009) State-dependent spike-timing relationships between hippocampal and prefrontal circuits during sleep. *Neuron*, 61(4):587–596.

Wilhelm I, Rose M, Imhof KI, Rasch B, Büchel C, Born J (2013) The sleeping child outplays the adult's capacity to convert implicit into explicit knowledge. *Nat Neurosci*, 16(4):391–393.

Wilson MA, McNaughton BL (1994) Reactivation of hippocampal ensemble memories during sleep. *Science*, 265(5172):676–679.

Winterer J, Stempel AV, Dugladze T, Földy C, Maziashvili N, Zivkovic AR, Priller J, Soltesz I, Gloveli T, Schmitz D (2011) Cell-type-specific modulation of feedback inhibition by serotonin in the hippocampus. *J Neurosci*, 31(23):8464–8475.

Witter MP, Naber PA, van Haeften T, Machielsen WC, Rombouts SA, Barkhof F, Scheltens P, da Silva FHL (2000) Cortico-hippocampal communication by way of parallel parahippocampal-subicular pathways. *Hippocampus*, 10(4):398–410.

Wozny C, Maier N, Fidzinski P, Breustedt J, Behr J, Schmitz D (2008a) Differential cAMP signaling at hippocampal output synapses. *J Neurosci*, 28(53):14358–14362.

Wozny C, Maier N, Schmitz D, Behr J (2008b) Two different forms of long-term potentiation at CA1-subiculum synapses. *J Physiol*, 586(Pt 11):2725–2734.

Xu HT, Han Z, Gao P, He S, Li Z, Shi W, Kodish O, Shao W, Brown KN, Huang K, Shi SH (2014) Distinct lineage-dependent structural and functional organization of the hippocampus. *Cell*, 157(7):1552–1564.

Yartsev MM, Witter MP, Ulanovsky N (2011) Grid cells without theta oscillations in the entorhinal cortex of bats. *Nature*, 479(7371):103–107.

Yassin L, Benedetti BL, Jouhanneau JS, Wen JA, Poulet JFA, Barth AL (2010) An embedded subnetwork of highly active neurons in the neocortex. *Neuron*, 68(6):1043–1050.

Ylinen A, Bragin A, Nádasdy Z, Jandó G, Szabó I, Sik A, Buzsáki G (1995a) Sharp wave-associated high-frequency oscillation (200 Hz) in the intact hippocampus: network and intracellular mechanisms. *J Neurosci*, 15(1 Pt 1):30–46.

Ylinen A, Soltész I, Bragin A, Penttonen M, Sik A, Buzsáki G (1995b) Intracellular correlates of hippocampal theta rhythm in identified pyramidal cells, granule cells, and basket cells. *Hippocampus*, 5(1):78–90.

Zeisel A, Muñoz-Manchado AB, Codeluppi S, Lönnerberg P, Manno GL, Juréus A, Marques S, Munguba H, He L, Betsholtz C, Rolny C, Castelo-Branco G, Hjerling-Leffler J, Linnarsson S (2015) Brain structure. Cell types in the mouse cortex and hippocampus revealed by single-cell RNA-seq. *Science*, 347(6226):1138–1142.

Zhang H, Lin SC, Nicolelis MAL (2010) Spatiotemporal coupling between hippocampal acetylcholine release and theta oscillations in vivo. *J Neurosci*, 30(40):13431–13440.

Znamenskiy P, Zador AM (2013) Corticostriatal neurons in auditory cortex drive decisions during auditory discrimination. *Nature*, 497(7450):482–485.